AUTONOMOUS UNIVERSITY OF NUEVO LEON

SCHOOL OF CHEMICAL SCIENCES

THE RECOMBINANT HYBRID PEPTIDE LL-37_RENALEXIN EXHIBITS ANTIMICROBIAL ACTIVITY AT LOWER MICS THAN ITS COUNTERPART SINGLE PEPTIDES

By

JULIUS KWESI NARH

A dissertation submitted to the Faculty of Chemical Sciences. In partial fulfillment of the requirement to obtain the MASTER OF SCIENCE degree with Orientation in APPLIED MICROBIOLOGY

December 2023

DECLARATION

THE RECOMBINANT HYBRID PEPTIDE LL-37_RENALEXIN EXHIBITS ANTIMICROBIAL ACTIVITY AT LOWER MICS THAN ITS COUNTERPART SINGLE PEPTIDES

Thesis Approval:

DR. XRISTO ZÁRATE KALFÓPULOS

(Thesis Advisor)

DR. JOSÉ RUBEN MORONES RAMÍREZ

(Committee member)

DR. JESÚS ALBERTO GÓMEZ TREVIÑO

(Committee member)

DRA. MELISSA MARLENE RODRIGUEZ

(Committee member)

DR. MARÍA ELENA CANTÚ CÁRDENAS

(Graduate Sub-Director)

THE RECOMBINANT HYBRID PEPTIDE LL-37_RENALEXIN EXHIBITS ANTIMICROBIAL ACTIVITY AT LOWER MICS THAN ITS COUNTERPART SINGLE PEPTIDES

Thesis Review:

DR. JOSÉ RUBEN MORONES RAMÍREZ

(Committee member)

DR. JESÚS ALBERTO GÓMEZ TREVIÑO

(Committee member)

DRA. MELISSA MARLENE RODRIGUEZ

(Committee member)

DR. MARÍA ELENA CANTÚ CÁRDENAS

(Graduate Sub-Director)

DEDICATION

I dedicate this thesis dissertation to the family of Mr. Braimah Alhassan and his wife Mercy Offeibea. To my mother (Gifty Narkwor Kofi-Wayo), My siblings (Gladys, Abigail, and Agnes), My niece (Isabella), My nephew (Gideon), My stepmother (Maa Esther), and stepsiblings (Vivian, Michael, and Caleb) and to all family and friends for their supports and encouragements.

ACKNOWLEDGMENT

My greatest acknowledgment goes to God Almighty for the knowledge, wisdom, health, and mercy bestowed onto me to pursue my academic career to this level. I thank the Autonomous University of Nuevo Leon (UANL), the university body for believing in me and appreciating my potential as well as academic qualifications to be admitted into one of its internationally recognized postgraduate studies programs as an international student from Ghana (West Africa). I am very much grateful to the Mexican National Council for Humanities, Science, and Technology (CONAHCYT) for the financial support offered to me to buttress my postgraduate studies. My sincere appreciation goes to my postgraduate thesis advisor Dr. Xristo Zárate Kalfópulos for giving me an opportunity to join his vibrant research group where cutting-edge research is a hallmark. I also appreciate his teachings, supervision, time, and care for me as a student. I am grateful to all the teaching and non-teaching staff of the Department of Applied Microbiology for their professional assistance during my stay at the university. My gratitude also goes to my thesis committee members Dr. José Ruben Morones Ramírez, Dr. Jesús Alberto Gómez Treviño, and Dra. Melissa Marlene Rodriguez, thank you for your professional guidance, corrections, and suggestions that ensure the success of my project work. Lastly, my endless appreciation goes to my colleagues (MSc. Applied Microbiology, 2022 batch), laboratory teammates, and senior colleagues for their assistance, tuition, encouragement, and acceptance to work with an African student.

ABSTRACT

An alarming global public health and economic peril has been the emergence of antibiotic resistance resulting from clinically relevant bacteria pathogens, including *Enterococcus faecium, Staphylococcus aureus, Klebsiella pneumonia, Acinetobacter baumannii, Pseudomonas aeruginosa,* and *Enterobacter* species constantly exhibiting intrinsic and extrinsic resistance mechanisms against last-resort antibiotics like gentamycin, ciprofloxacin, tetracycline, colistin, and standard ampicillin prescription in clinical practices. The discovery and applications of antimicrobial peptides (AMPs) with antibacterial properties have been considered and proven as alternative antimicrobial agents to antibiotics. In this study, we have designed, produced, and purified a recombinant novel multifunctional hybrid antimicrobial peptide LL-37_Renalexin for the first time via the application of newly designed flexible GS peptide linker coupled with the use of our previously characterized small metal binding proteins SmbP and CusF3H+ as carrier proteins that allow for an enhanced bacterial expression, using BL21(DE3) and SHuffle T7(DE3) *E. coli* strains, and purification of the hybrid peptide via immobilized metal affinity chromatography. The purified tag-free LL-37_Renalexin hybrid peptide exhibited above 80% reduction in bacteria colony-forming units and broad-spectrum antimicrobial effects against *Staphylococcus aureus*, *Escherichia coli*, Methicillin-resistant *Staphylococcus aureus* (MRSA), and *Klebsiella pneumoniae* bacteria clinical isolates at a lower minimum inhibition concentration level (10 – 33 μM) as compared to its counterpart single AMPs LL-37 and Renalexin (50 – 100 μM).

TABLE OF CONTENT

LIST OF TABLES

LIST OF FIGURES

LIST OF ABBREVIATIONS

µl	Microliter
µM	Micromolar
6xHis	Hexahistidine
ABP	Antibacterial Peptide
bp	Base pair
BSA	Bovine Serum Albumin
bw	Body Weight
℃	Degree Celsius
CCR	C-Chemokine Receptors
DNA	Deoxyribonucleic Acid
CFU	Colony Forming Unit
CMC	Cellular Machinery of Choice
CV	Column volume
E. coli	Escherichia coli
FDA	Food and Drug Administration
FPLC	Fast Protein Liquid Chromatography
g	Gram
GDP	Gross Domestic Production
GFP	Green Fluorescence protein
GMMES	Genetically Modified Microbial Expression System
GMPES System	Genetically Modified Prokaryotic and Eukaryotic
GST	Glutathione S-transferase
h	Hour
HC50	Half Hemolytic Dose
hCAP	Human Cathelicidin Antimicrobial Peptide
HVP	High Valine Protein

IF	Insoluble Fraction
IMAC	Immobilized Metal Affinity Chromatography
kDa	Kilo-Dalton
LD50	Half Lethal Dose
m	Minute
MBC	Microbicidal Concentration
MBP	Maltose Binding Protein
MDR	Multi-Drug Resistant
MHA	Mueller Hinton Agar
MIC	Minimum Inhibition Concentration
mM	Milimolar
ml	Millimeter
mRNA	Messenger Ribonucleic Acid
MRSA	Methicillin Resistant *staphylococcus aureus*
Msch	Mechanosensitive Channel Protein
NCCLS Standard	National Committee for Clinical Laboratory
ng	Nanogram
NP	Nanoparticles
PBS	Phosphate Buffered Saline
PCR	Polymerase Chain Reaction
pH	Hydrogen Potential
pI	Isoelectric Point
PLR	Peptide to Lipid Ratio
pr-AMP	Proline-rich antimicrobial Peptide
R&D	Research and Development
rAMP	Recombinant Antimicrobial Peptide
RBS	Ribosome Binding sites
rDNA	Recombinant DNA Technology

rDPT	Recombinant Dermatopontin
RFP	Red Fluorescence Protein
RL	Reduction Level
RNA	Ribonucleic Acid
rpm	Rotation per minute
RT	Room Temperature
s	Second
SDS-PAGE Electrophoresis	Sodium Dodecyl Sulfate Polyacrylamide Gel
SF	Soluble Fraction
S. aureus	Staphylococcus aureus
SUMO	Small Ubiquitin-like Modifiers
TLR	Toll-like Receptors
TrP	Thioredoxin Protein
TSA	Tryptic Soy Agar
TSB	Tryptic Soy Broth
TZP	Piperacillin-tazobactam
UMPS	Unique Membrane Protein Structures
WHO	World Health Organization

SUMMARY

Julius Kwesi, Narh

Autonomous University of Nuevo Leon

Faculty of Chemical Science

Graduation Date: December 2023.

Thesis Title: **The recombinant hybrid peptide LL-37_Renalexin exhibits antimicrobial activity at lower MICs than its counterpart single peptides**

Page Number: 149

Candidate for the Degree: Master of Science with Orientation in Applied Microbiology

Study Area: Molecular Microbiology

Study Purpose and Method: The objective of this study is the development of a strategy and methodology for the design and production of novel hybrid peptides of biopharmaceutical significance via the application of CusF3H+ and SmbP as carrier proteins, and strains of *Escherichia coli* as microbial expression systems. To achieve this goal, advanced molecular biology and microbiology techniques were employed to design of a hybrid peptide, recombinant plasmid construction, and expression of the recombinant fusion protein in the expression host. Affinity chromatographic techniques were used as reliable and well characterized bioanalytical technique for the purification of the expressed recombinant fusion protein, and subsequently, the antimicrobial pharmacological activity of the hybrid peptide was evaluated via NCCLS methods.

Contribution and Conclusion: In this study, two recombinant plasmid constructs DNA were designed as vectors for the expression of a novel hybrid antimicrobial peptide LL-37_Renalexin. The carrier proteins show a significant advantage in the production, secretion, and purification of the hybrid peptide. The affinity chromatographic purification technique used yielded a highly purified recombinant peptide with intact bioactivity and purity comparable to commercially available therapeutic peptides. Antimicrobial bioactivity results indicate that the novel hybrid peptide exhibited a broad-spectrum antibacterial potency at a lower minimum inhibition concentration as compared to its counterpart single peptides LL-37 and Renalexin reported. Generally, this project describes a cost-effective, simple, reliable, and advanced molecular microbiology strategy for the production and purification of recombinant peptides of biopharmaceutical relevance.

DR. XRISTO ZÁRATE KALFÓPULOS

(Thesis Advisor)

CHAPTER ONE

1.0 INTRODUCTION

1.1 Background

An alarming worldwide health crisis in human settings is the global spread of bacterial infections with *Enterococcus faecium*, *Staphylococcus aureus*, *Klebsiella pneumonia*, *Acinetobacter baumannii*, *Pseudomonas aeruginosa*, and *Enterobacter* species commonly referred to as critical pathogens as the prevailing causal agents (Deng *et al*., 2017). The pandemic of critical pathogens like *Staphylococcus aureus* and *Escherichia coli* in both temperate and tropical countries has been reported by several infectious disease surveillance and prevention agencies reports including World Health Organization (WHO), Center for Disease Dynamics Economic and Policy (CDDEP), and the Center for Disease Control and Prevention (CDC) (Sriram *et al*., 2021). The use of antibiotics such as kanamycin, tetracycline, gentamycin, and ciprofloxacin has marked a sovereign achievement in the management and control of infectious diseases prevalence in developed and developing countries, providing relevant improvement in clinical outcomes and the reduction in bacterial infection mortality and morbidity (WHO, 2015).

Antibiotic resistance, the second globalized public health peril in this new era of modern medicine, prevailed from pathogenic development of novel resistance mechanisms of genetic and epigenetic origins against the available antibiotics by circumventing the therapeutic actions of these drugs, leading to the failure of drugs to curb the menace of infection (Dar *et al*., 2017; Soares *et al*., 2021). The international recognition of antibiotic resistance threat to public health and the treatment of bacterial infections has increased

with a profligate economic loss of about 5.8% of the Gross Domestic product (GDP) in developing countries in particular (Jit *et al*., 2020; WHO, 2019).

The United States, CDC antibiotics resistance threats reported in 2019 showed the following data on mortality and pathogen: 18% deaths from antibiotic resistance overall, 28% deaths from antibiotic resistance in hospitals, 41% Vancomycin-resistant *Enterococcus*, 29% Multidrug-resistant *Pseudomonas aeruginosa*, 21% Methicillin-resistant *Staphylococcus aureus* (MRSA), 25% drug-resistant *Candida* and 33% Carbapenem-resistant *Acinetobacter*. The WHO (2019) antibiotic drug report indicated an increasing ineffectiveness of 32 new antimicrobial drugs in clinical phase trials and has identified two antimicrobial resistance (AMR) indicators in Methicillin-resistance *Staphylococcus aureus* (MRSA) and *Escherichia coli* conventional in 25 temperate and tropical countries including Mexico and recommended multisectoral actions to achieve a sustainable control.

In recent years untwining the bactericidal and bacteriostatic potencies of antimicrobial peptides (AMPs) such as defensins, cathelicidin, LL-37, gramicidin D, histatins and renalexin expressed via recombinant systems as the toolbox for engineering and production has provided the platforms for large-scale production and applications of AMPs to aviate the ill effects antibiotic resistance threats posed on public health and economics conditions (Perez-Perez *et al*., 2021; Zhang *et al*., 2021). AMPs are peptide modules constituting 10 – 100 amino acids long in most cases, positively charged with a net charge of around +2 to +9, amphipathic with a natural membrane destructive activity towards gram-negative and gram-positive bacteria (Nooranian *et al*., 2021). Often considered as immune modulators found as crucial components of the innate immune

system of both vertebrates and invertebrates with known antibacterial, antiviral, antifungal, and anti-inflammatory biological activities (Gulluce, Karadayi and Baris, 2015; Deng *et al*., 2017; Nuti *et al*., 2017; Perez-Perez *et al*., 2021). Antimicrobial peptides, the preferred biological agents alternative to antibiotics, actively curb the ill effects of antibiotic resistance mainly by disrupting the cell wall, plasma membrane, inducing pore formation, inhibiting DNA replication and protein synthesis in their target pathogens, showing a broad spectrum of therapeutic activities (Jindal *et al*., 2015; Ołdak and Zielińska, 2017). In a study by Perez-Perez *et al*. (2021), the antimicrobial peptide LL-37, a subgroup in the cathelicidin family, was successfully produced and purified via immobilized metal affinity chromatography with the protein tag SmbP. Tag-free LL-37 peptide was obtained upon enterokinase cleavage of SmbP_LL-37. After IMAC purification, protein gel electrophoresis and ImageJ analysis showed 90% purity of the recombinant peptide with a recovery level of 3.6mg (SmbP_LL-37) per liter LB culture medium. The antimicrobial activity of tag free LL-37 showed promising results against *Staphylococcus aureus* (69% sensitivity) and *Escherichia coli* (64% sensitivity) at 50 μM peptide concentration. The bactericidal effects of AMPs like Renalexin, LL-37, Cecropin and others have been evaluated against *Staphylococcus aureus, Klebsiella pneumoniae*, MRSA, and *Escherichia coli* biofilms at different peptide concentration levels, killing kinetic studies also revealed a rapid elimination of target pathogens with their respective biofilms within 24 h (Kang *et al*., 2019; Scott *et al*., 2015).

To further our ongoing research into novel antimicrobial agents that can be used as alternatively to antibiotics, this present study seeks to design, express, and purify a novel recombinant hybrid AMP LL−37_Renalexin, and to evaluate the biological activity of the

hybrid peptide against selected gram-positive and gram-negative bacteria pathogens of clinical importance. The molecular biology techniques and technologies employed in the present study could serve as a reliable protocol of production and purification of novel recombinant protein-based therapeutic agents against antibiotic-resistant pathogens.

1.2 Problem statement

Over the years studies have reported the devastating economic and public health threats associated with the global spread of antibiotic-resistant critical bacteria pathogens including *Staphylococcus aureus* and *Escherichia coli*. An estimates 2.8 million antibiotic-resistant infection cases are being reported each year in the United State which contributes to more than 35, 000 deaths. Concerning *Clostridium difficile* 223,900 cases documented led to at least 12,800 deaths. Elsewhere in Canada, 26% *Staphylococcus aureus* and *Escherichia coli* resistance to first-line antimicrobial drugs coupled with the number of deaths directly mounted to 5,400 in 2018 were indicated (WHO, 2020; CDDEP, 2021; Sriram *et al*., 2021). The economic losses associated with antibiotic resistance and the spread of antibiotic-resistant bacteria pathogens are on the rise globally with 5.3% in 2017 and 5.8% in 2019 regarding losses in the Gross Domestic Production (GDP) (WHO, 2017; WHO, 2019).

Of particular concern in Mexico, clinically prevalent multiplex bacteria pathogens like *Staphylococcus aureus, E. coli, Klebsiella* spp., *Acinetobacter baumannii,* and *Pseudomonas aeruginosa* shows resistance to commonly prescribed and most potent antibiotics like Erythromycin, Oxacillin, Trimethoprim, Sulfamethoxazole, Gentamycin, Tobramycin, and Carbapenem used in the country (Garza-Gonzalez *et al*., 2020).

Antibiotic usage coupled with its bioequivalence has dropped significantly from 13 to 7 in daily doses per 1000 Mexican inhabitants. Although this improvement sounds encouraging, the regulatory strategies are incomplete and less monitored, availing the worrisome spread of deadly resistance determinates like *blaNDM-1 and mcr-1* in the country (Amábile-cuevas, 2020). The antibiotic resistance threat issues reported from specific areas such as Guadalajara, Mexico City, and Monterrey within the country are indicative of an overwhelming public health peril associated with the emergence of antibiotic resistant bacteria pathogens coupled with the indiscriminate usage and prescription of antimicrobial therapeutics and this update has to spur the Mexican government to set up a compulsory nature of the National Strategy of Action Against Resistance to Antimicrobials (NSAARM) in order to mitigate antimicrobial resistance prevalence and to improve upon the usage of antibiotics in the country *(*Garza-González *et al.*, 2019*;* Mukherjee *et al*., 2021). A recent study by Garza-González *et al*. (2019) revealed alarming antibiotic-resistant challenges in about 22,943 clinical bacteria isolates across 20 Mexican States. Among these isolates were gram-negative and gram-positive bacteria pathogens reported show consistent resistance against some last-resort antimicrobial agents including vancomycin, ciprofloxacin, carbapenem, piperacillin-tazobactam (TZP), cefepime, meropenem, and methicillin commonly prescribed in both public and private hospitals in Mexico. 21.4% Methicillin-resistance in *Staphylococcus aureus*, 21% Vancomycin resistance in *Enterococcus* spp., 19.4% Ciprofloxacin resistance in *Escherichia coli*, 19.1% TZP resistance in *Acinetobacter* spp., and multidrug resistance (MDR) in *Pseudomonas aeruginosa* and *Klebsiella* spp. being 40% and 22.6% respectively were revealed (Garza-González *et al*., 2019; Llanes *et al*., 2012; Mukherjee *et al*., 2021). The state of the world antibiotic resistance report (2021), as published by the

Center for Disease Dynamic, Economic and Policy (CDDEP) indicated the following distressing public health threat in Mexico, 35% Methicillin resistant *Staphylococcus aureus*, 20% Carbapenem resistant *Enterobacter* spp., 60% beta lactamase resistant *Enterococcus* spp., 100% Colistin resistant *Escherichia coli,* 75% Tetracycline resistant *Acinetobacter* spp., and 90% Ampicillin and 50% Ciprofloxacin resistant critical pathogens.

1.3 Justification

In the search for new antibacterial agents against drug-resistant bacteria, AMPs referred to as host defense peptides have been tested and shown novel therapeutic activities against resistant-bacteria pathogens like *Staphylococcus aureus, Streptococcus pneumonia*, *Escherichia coli,* and *Pseudomonas aeruginosa* displaying bacteriostatic, and microbicidal properties against these pathogens. Antimicrobial peptides (AMPs) including both single and hybrid peptides have been reported to exhibit a broad arena of biological activities in cell membrane disruption through non-specific interactions between cationic AMPs and the negatively charged bacterial membrane surface resulting in almost negligible or limited pathogen resistance to AMPs. Although only a few AMPs are in clinical use due to the difficulties encountered in the isolation and purification of AMPs from their natural biological sources coupled with the unavailability of synthetic AMPs as compared to their endogenous counterparts (Montfort-Gardeazabal *et al.,* 2021; Kaprou *et al.,* 2021). The application of recombinantly purified antimicrobial peptides as an alternative to antibiotics to fight prevailing antibiotic-resistant pathogens has yielded promising and prudent results with relevant minimum inhibition concentrations (MIC),

(15.62 −31.25µg/ml) for indolicidins, (62.5µg/ml) for renalexin, (31.25 – 62.5 µg/ml) for indolicidins analogs IN1 and IN2 and (250µg/ml) for renalexin analog RN1 (Jindal *et al*., 2015). Although the single antimicrobial peptide showed promising results with significant MIC, the hybrid peptides such as RN7– IN7, RN7 – IN8, and RN6 – IN6 revealed a broad spectrum of bactericidal potentials at minimum concentrations in their target pathogens as compared to their counterpart single peptides, *E. coli* ATCC 25922 (7.81µg/ml), *S. aureus* ATCC 25923 (7.81µg/ml), methicillin-resistant *S. aureus* (MRSA) (7.81µg/ml) and *P. aeruginosa* ATCC 15442 (15.62µg/ml), with no hemolytic effect on human red blood cells (RBCs) (Jindal *et al*., 2015; Shang *et al*., 2020).

Few research studies have reported the production of hybrid AMPs, of which most of these studies are based on in-silico modeling with few studies on AMPs derived from human and amphibian origins not considering their broad-spectrum antibacterial potencies (Jindal *et al*., 2015; Ghosh, 2020). In this study, we propose to design, express, and purify a novel hybrid antimicrobial peptide LL-37_Renalexin of human and Sea Bullfrog (amphibian) origin using a newly designed GS flexible peptide linker, and SmbP and CusF3H+ as a carrier protein and ascertain its antimicrobial activity against clinical isolates of *Staphylococcus aureus*, *Escherichia coli*, Methicillin-resistant *Staphylococcus aureus* (MRSA), and *Klebsiella pneumoniae*.

1.4 Hypothesis

The hybrid peptide LL-37_Renalexin can be produced in *Escherichia coli* strains using SmbP and CusF3H+, showing antibacterial activity against clinical isolates of *Staphylococcus aureus* and *Escherichia coli* at a lower concentration as compared to its counterpart single peptide LL-37 itself.

1.5 Objective

1.5.1 Main objective

To produce recombinant hybrid peptide AMP LL-37_Renalexin using SmbP and CusF3H+ as protein tags, with antibacterial activity against *Staphylococcus aureus*, *Escherichia coli*, Methicillin-resistant *Staphylococcus aureus* (MRSA), and *Klebsiella pneumoniae* clinical isolates.

1.5.2 Specific objectives

1. Construct a plasmid DNA expression vector that encodes the recombinant hybrid peptide LL-37_Renalexin tagged with SmbP and CusF3H+ respectively.
2. Express, purify, and characterize the recombinant hybrid peptide LL-37_Renalexin in *E. coli* BL21(DE3) and *E. coli* SHuffle T7(DE3).
3. Evaluate the antibacterial activity of purified hybrid peptide LL-37_Renalexin against clinical isolates of *Staphylococcus aureus*, *Escherichia coli*, Methicillin-resistant *Staphylococcus aureus* (MRSA), and *Klebsiella pneumoniae*.

CHAPTER TWO

2.0 LITERATURE REVIEW

2. 1 Bacterial infection and antibiotics resistance

Infectious diseases like pneumonia, osteomyelitis**,** meningitis, endocarditis, toxic shock syndrome, bacteremia, and sepsis caused by common bacterial pathogens, including *Staphylococcus aureus* and *Escherichia coli* have been a global dilemma and a peril to human health as well as animal production with pathogens like *Salmonella species, Campylobacter species, L. monocytogenes, and E. coli* reported in many countries. In Mexico alone, bacterial infection cases reported over the years are on the rise with severity in humans, as well as in veterinary production (Garza-González *et al*., 2019; Llanes *et al*., 2012). Reportedly over 30.6% *Staphylococcus aureus* infections, 57.8% *Escherichia coli* infections, and 13.8% of infections are caused by other pathogens including *Klebsiella pneumonia, Pseudomonas aeruginosa, Clostridium perfringens*, and *Burkholderia* and *Pseudomallei* spp. as revealed in the state of the world antibiotics report by the Center for Disease Dynamic, Economic and Policy (CDDEP, 2020; Sriram *et al*., 2021)**.** The co-existence of two or more bacterial strains in infection could result in genetic mutations coupled with horizontal gene transfer favoring the transmission of antimicrobial resistance (AMR) among antibiotic-resistant gene-producing strains to non-antibiotic-resistant gene-producing strains harnessing the natural phenomenon of the spread of antibiotic resistance among related and non-related pathogens (Garza-González *et al*., 2019; Mukherjee *et al*., 2021). Cases of infection from previously known antibiotic-sensitive bacterial pathogens developing resistance have become an endemic challenge in many temperate and tropical countries including Australia, the United States, Canada, Mexico, Brazil, and Africa

responsible for the rise in antibiotic resistance globally (CDC, 2019: Mukherjee *et al*., 2021).

Of particular concern in Mexico, bacterial pathogens like *Staphylococcus aureus, Escherichia coli, Acinetobacter* sp., *Klebsiella* sp., and others including *Mycobacterium tuberculosis* known as critical pathogens by the WHO have been the predominant antimicrobial-resistant (AMR) pathogens escalated from the indiscriminate and prescribed misuse of antibiotics in the country. The excessive use of antibiotics in veterinary practice has also contributed to the emergence of resistant bacteria pathogens commonly referred to as ESKAPE (Mukherjee *et al*., 2021). The associated AMR public health threats in the country include 68.7% drug resistance index (DRI) in human diseases, 66.2% drug resistance index (DRI) in animal diseases, 12.2% infant mortality, 28% under-five deaths from pneumococcal diseases, 23% deaths from tuberculosis and 1246 under-five deaths from diarrheal diseases coupled with an economic loss of 5.37% of gross domestic production (GDP) as at 2018 (Amábile-cuevas, 2020; Sriram et al., 2021; WHO, 2020).

The prevalence of clinically relevant multiplex bacteria pathogens including but not limited to *Staphylococcus aureus, Enterobacter* sp., *Klebsiella* sp., *Acinetobacter baumannii,* and *Pseudomonas aeruginosa* have shown drug-resistance against the most potent antimicrobial drug classes like beta-lactams, penicillin, macrolides, and quinolones considered as last resort antimicrobial agents like Erythromycin, Oxacillin, Trimethoprim, Sulfamethoxazole, Gentamycin, Tobramycin, Ciprofloxacin, and Carbapenem (Table 2.1) used in the country (Garza-Gonzalez *et al*., 2020). 41% Vancomycin-resistant *Enterococcus*, 29% Multidrug-resistant *Pseudomonas aeruginosa*, 21% Methicillin-

resistant *Staphylococcus aureus* (MRSA), 25% drug-resistant *Candida* and 33% Carbapenem-resistant *Acinetobacter* pathogens have been identified in many Northern American countries including Mexico (CDC, 2019; Sriram *et al*., 2021). A recent study by the World Health Organization indicated the ineffectiveness of 32 new antimicrobial drugs in clinical phase trials, and identified two antimicrobial resistance (AMR) indicators in Methicillin-resistance *Staphylococcus aureus* (MRSA) and *Escherichia coli* conventional in 25-temperate and tropical countries and recommended multisectoral actions to achieve a sustainable control and management of AMR infections (David and Karl, 2018; WHO, 2020; Zhang and Yang, 2022).

Table 2. 1: Antibiotics, killing mechanism, target bacteria, and resistance mechanisms.

Antibiotics/Classes	Mode of Action	Bacteria	Mechanism of Resistance
Penicillin and carbapenem (beta-lactam)	Inhibiting bacterial cell wall synthesis	*Escherichia coli* and *Klebsiella pneumoniae*	Producing beta-lactamase and carbapenemase and porin alteration
Macrolides	Inhibiting protein synthesis by binding to the 50S ribosomal subunit	*K. pneumoniae*	Producing erythromycin esterases (Eres) such as EreA and EreC
Ticarcillin (beta-lactam) and ciprofloxacin (quinolone)	Inhibiting bacterial cell wall and protein synthesis	*Pseudomonas aeruginosa*	Resistance-nodulation-division (RND) efflux pumps
Macrolides	Inhibiting protein synthesis	*Streptococcus pneumoniae*	Ribosomal demethylation, expelling by efflux pump, and target site mutation
Quinolones	Inhibiting nucleic acid synthesis	*K. pneumoniae* and *Clostridium perfringens*	Mutations in the genes that encode gyrase and topoisomerase IV
Trimethoprim-sulfamethoxazole	Inhibiting folate synthesis	*Burkholderia pseudomallei*	Structural modification of dihydrofolate reductase (DHFR) or dihydropteroic acid synthase (DHPS)

Source: Adapted from (Zhang and Yang, 2022).

2.2 Antimicrobial peptides (AMPs) as an alternative to conventional antibiotics

The recent applications of AMPs as disease control therapeutics coupled with the growing interest in the area of AMPs research and development as antibacterial, anticancer, and anti-inflammatory therapeutic agents produced via the exploration of biotechnological and recombinant expression systems have provided promising and safer platforms for the expression and applications of AMPs as antimicrobial drugs (Jindal *et al*., 2015; Montfort-Gardeazabal *et al*., 2021; Nuti *et al*., 2017). The isolation, characterization, and therapeutic use of the first commercially manufactured antimicrobial peptide (AMPs) gramicidin, an isolate from the bacterium *Bacillus brevis* has been recognized since 1939. AMPs of eukaryotic and prokaryotic origin have exhibited potential biological activity in vivo and in vitro against gram-negative and gram-positive bacterial pathogens of clinical importance (Dar *et al*., 2017). The increasing trends in antibiotic resistance across the globe aligned with the rise in the ineffectiveness of new antimicrobial drugs against resistant-bacterial infections elicited by pathogens like *Staphylococcus aureus*, *Escherichia coli*, and *Pseudomonas aeruginosa* has culminated in the need for novel infection therapeutics (Dar *et al*., 2017). The discovery and use of AMPs like LL-37, Indolicidins, Renalexin, Histatins, and Defensin with therapeutic potencies against multi-drug resistant pathogens have been elucidated in several studies at an optimistic therapeutic concentration (Malmsten, 2014; Dar *et al*., 2017; Cheng *et al*., 2021; Perez-Perez *et al*., 2021). Antimicrobial peptides constitute about 20 – 100 amino acid residues, positively charged, amphipathic biomolecules, and contain substantial hydrophilic and hydrophobic domains with either helical, loop, and sheet structural motifs (Figure 2.1) and are considered as one of the main protein-based components of the immune system in humans, insects, amphibians, and plants that (Moulahoum *et al*., 2020). This class of

therapeutic peptides is considered simple proteins that evolved years ago however, they still confer strong therapeutic actions in recent applications at respective concentration levels in vitro and in animal study models (Pasupuleti *et al*., 2011; Soltani *et al*., 2021). Many AMPs are amphipathic and cationic in structure with a net charge of +2 to +9, confirming strong polarity to bacterial cell surface structures thereby conceding antibacterial activity against bacterial pathogens that possess public health threats globally (Wei and Zhang, 2022). In mammals, AMPs like LL-37, α, β−defensins and renalexin are known as immune modulators, produced and prevalent in immune cells such as neutrophils, granulocytes, and keratinocytes stimulated upon by bacterial infection, and have strong antimicrobial effects on broad spectrum bacterial infections. AMPs from mammalian domains have been well studied and known for their striking similarities regardless of cellular concentration, structure, and functionality (Dar *et al*., 2017; Nuti *et al*., 2017).

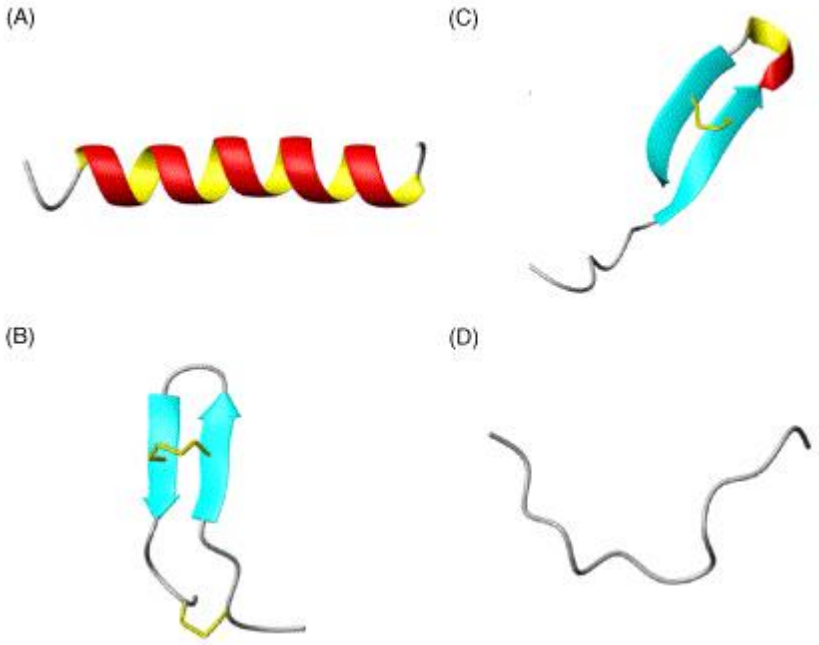

Figure 2. 1: Structural classes of AMPs, a) Alpha helical, Magainin, b) Beta sheet, Tachyplesin, c) Loop, Tigerinin, d) Extended structure, Indolicidins. Disulfide linkage indicated in yellow, blue arrow indicate β-sheet structure, α-helix coil indicated in red. Source: (Powers and Hancock, 2013; Zhou, 2019).

2.3 Origin of antimicrobial peptides (AMPs) of therapeutic importance

AMPs are naturally small bioactive peptides produced by all class of living organisms such as microorganisms, plants, insects, human, and animal (Huan *et al*., 2020). AMPs are known for modulation, orchestration, and as indispensable components of the innate immune system as the first-line of defense against bacterial attack in eukaryotes and are often synthesized as a competition strategy in prokaryotes to limit and outcompete the cellular growth of competitive microbes (Seyedjavadi *et al*., 2021a). Upon the early discovery of AMPs in the 1939s, microbiologist Rene Dubos first isolated gramicidin from a soil *Bacillus brevis* strain, which demonstrated antibacterial potencies against *Pneumococcal* infections in mice. Posterior to gramicidin isolation, several AMPs have been discovered from both eukaryotic and prokaryotic kingdoms with many of these peptides acting as active immunity components. Defensins were the first animal-originated AMPs isolated from rabbit leukocytes, lactoferrin from cow milk, LL-37 from human leukocyte, Renalexin from skin of bullfrog *Rana catesbeiana*, tyrocidine from *bacillus*, purothionine from *Triticum aestivum* (plant), and cancrin from *Rana cancrivora* (Moretta *et al*., 2021; Nuti *et al*., 2017). The growing interest in AMPs applications over the years has encouraged researchers to investigate their structural, functional, and biodiversity as potential new therapeutics (Figure 2.2). To date, over 3,569 AMPs isolated from six life forms including bacteria (380), archaea (5), fungi (25), animal (2600), plants

(371) and finally protists (8) have been discovered, with over 3,245 AMPs structurally characterized and deposited in the antimicrobial peptide database (APD3) updated on January 07, 2023 (Table 2.2). The broad spectrum bioactivity of the well-known and characterized AMPs has allowed researchers to investigate their potencies against other pathogenic microbes like fungi, viruses and parasites with many serving as a reservoir of naturally occurring AMPs (Huan *et al*., 2020; Moretta *et al*., 2021; Wang *et al*., 2016).

Table 2. 2: Structural statistics of 3,425 AMPs in the APD3

Structural class	**Peptide number**	**Percentage (%)**
Helix	490	14.31
Beta structure	89	2.60
Helix and beta unpacked	4	0.12
Combine helix and beta packed	117	3.42
Neither helix nor beta structure	22	0.64
Rich in unusual amino acid	113	3.30
Disulfide bridge (but no 3D)	521	15.21
Unknown 3D structure	2069	60.41
Total	**3,425**	**100**

Source: https://aps.unmc.edu/APD3/

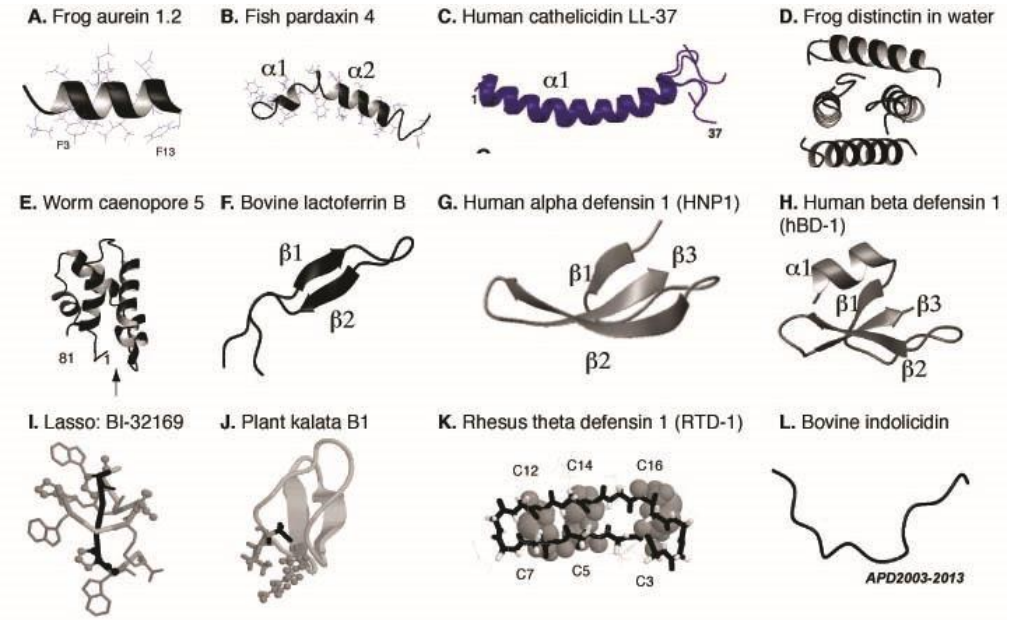

Figure 2. 2: Structural diversity of various AMPs isolates of different life forms. Adapted from (Wang *et al*., 2016).

2.4 Therapeutic classification of AMPs

The therapeutic bioactivities of antimicrobial peptides are tremendous and have been categorized based on their pharmacological potencies against specific microbial pathogens and targeted diseases. According to the Antimicrobial Peptide Database 3 (APD3), these categories include antibacterial, antiviral, antiparasitic, anti-tumor, and anti-human immunodeficiency virus (HIV) (Figure 2.3). The most widely exploited categories among these class of antimicrobial peptides are the antibacterial peptides and antifungal peptides, as this can be attributed to the glowing interest of scientific research in antimicrobial agents and the global emergence of drug-tolerant microbial pathogens like *Staphylococcus aureus, Pseudomonas aeruginosa, Candida albicans,* and *Escherichia coli* (De J. Sosa *et al*., 2010; Mukherjee *et al*., 2021). Antibiotic resistance load in human and veterinary medicine has been regarded as a secret pandemic and a

global public health threat as reported by the World Health Organization (WHO, 2019) and Antimicrobial Resistance Surveillance System of the United Kingdom and that of Canada (De J. Sosa *et al*., 2010).

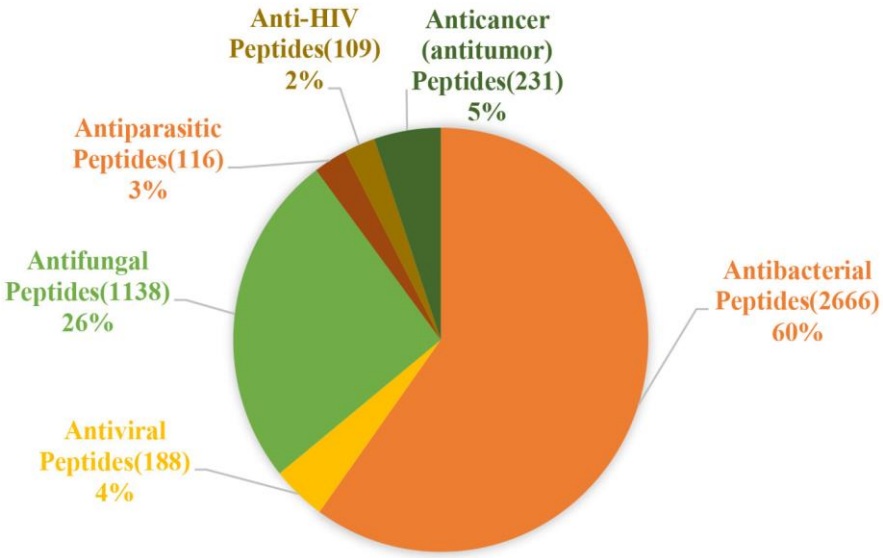

Figure 2. 3: Statistical distribution of AMPs based on function. Adapted from APD3 database (https://aps.unmc/APD3/).

2.4.1 Antibacterial peptides (ABPs)

This category of AMPs account for the largest portion (60%) of the total AMPs deposited in the APD3 and is known to possess vast inhibitory pharmaco-potencies against pathogenic bacteria like *Escherichia coli*, *Staphylococcus aureus*, *Listeria monocytogenes*, MRSA, and *Pseudomonas aeruginosa* that withhold a severe threat to human and veterinary medicine (Huan *et al*., 2020). Both natural and synthetically derived antibacterial peptides have shown bioactivity against gram-negative and gram-positive bacteria pathogens affiliating economic and public health threats in human settings (Zhang and Yang, 2022). Current studies accessing the therapeutic actions of novel ABPs like

LL-37, indolicidins, Renalexin, and IN1 have revealed a promising minimum inhibitory concentrations (MIC) coupled with very no significant cytotoxicity against the immune cells of human and model organisms (Huan *et al*., 2020; Perez-Perez *et al*., 2021; Soltani *et al*., 2021). Perez-Perez *et al*. (2021) reported, recombinant antibacterial peptide LL-37 shown a promising therapeutic actions at 50 µM against *Escherichia coli* and *Staphylococcus aureus*. Kang *et al*. (2019) indicated the therapeutic actions of antibacterial peptide LL-37 at 100 µM against bacteria *Staphylococcus aureus* biofilms within a 24 h exposure. Kang and colleagues also reported that the conjugation of LL-37 with silver nanoparticles (AgNP) enhances the killing efficacy of the peptide and revealed a broad spectrum of bioactivity against other bacterial pathogens (Kang *et al*., 2019). Jindal *et al*. (2015) study shows that two antibacterial peptides indolicidins and Renalexin exhibited novel therapeutic actions against *Escherichia coli, Staphylococcus,* and *Pseudomonas aeruginosa* at MIC of 7.81µg/ml with no hemolytic activities in model animal.

2.5 AMPS mechanism of action

The mechanisms of therapeutic action of AMPs including antibacterial peptides have been extensively exploited over the years (Erdem Büyükkiraz and Kesmen, 2022). Studies in both in vitro, in vivo, and model plasma membranes have confirmed novel and distinct modes of action compared to clinically prescribed antibiotics by extensively provoking plasma membrane incision and permeability leading to membrane disruption and cell death (Erdem Büyükkiraz and Kesmen, 2022; Wei and Zhang, 2022). Other studies have also indicated the biochemical interactions of AMPs with numerous intracellular targets like ribosomes, nuclei acids and some cellular enzymes attributed to the ability of these

drug candidates to permeate the plasma membrane of target microbial pathogens (Huan *et al*., 2020; Scott *et al*., 2015). Considering their interaction with intracellular targets, antimicrobial peptides have to traverse the cell membrane of its target microbial pathogens to elicit therapeutic actions intracellularly (Zhang and Yang, 2022). By knowledge it is generally accepted that binding interaction of AMPs to the cell membrane of a target pathogen is driven by the electrostatic force of attraction between the positively charged AMPs with the negatively charged head of the phospholipids, teichoic acids, and other polarized membrane biomolecules without the need for cell-specific surface receptors thereby traversing the membrane of respective target pathogens (Erdem Büyükkiraz and Kesmen, 2022). This molecular interaction is omitted in eukaryotic membranes due to neutral biomolecules like phosphatidylcholine and sphingomyelins, rendering ABPs more potent against microbial pathogens (Kang *et al*., 2019). Upon binding to anionic bacterial membrane biomolecules, the peptide undergoes structural conformational changes and becomes converted into an amphiphilic α-helical and helical-like structures in aqueous solution thereby promoting molecular interactions with the membrane. However, for β-sheet based AMPs no major conformational changes occur upon binding the membrane of target pathogens instead the presence of a stable disulfide bridge structure (s) within the peptide facilitates membrane traversion (Nuti *et al*., 2017; Peters *et al*., 2010; Wei and Zhang, 2022). A major factor that compromises the cellular and molecular binding of AMPs to the membrane of target bacterial pathogens is the peptide to lipid ratio (PLR). At lower peptide to lipid ratio, the cationic AMP remains unbound however arranged parallel to the membrane plane inserted at the interface of the lipid hydrophobic acyl chains and the hydrophilic heads. As the peptide to lipid ratio increases, the AMP aggregates on the membrane surface and undergoes reorientation required for reliable

molecular interaction leading to membrane traversion, pore formation, and disruption of membrane integrity resulting in cell death via release of bacteria intracellular components (Erdem Büyükkiraz and Kesmen, 2022; Wei and Zhang, 2022).

Despite diverse studies on the application and proposed theories of mode of action of AMPs, the precise and detailed mechanism of peptide-membrane interaction and cell-killing action of many antimicrobial peptides have not been well elucidated and firmly established, with the exception of the Food and Drug Administration (FDA) approved AMPs like Daptomycin, vancomycin, colistin, dalbavancin, Teicoplanin, and Bacitracin (Wei and Zhang, 2022). Although, well-established models are being proposed for membrane-active peptides including the barrel-stave model, the carpet model, and the toroidal pores models (Figure 2.4) considered as the three main proposed models of mechanisms of action for membrane-active peptides *(Dar et al., 2017;* Nuti *et al*., 2017).

2.5.1 The Barrel-stave model

This model of peptide-membrane interaction proposed the self-association and insertion of the peptide into the phospholipid structure on the microbial cell surface, resulting in the formation of water-sac pores. The hydrophobic regions of the amphipathic AMP interact with the cell membrane phospholipid acyl groups and the hydrophilic regions forms the lining of the water-sac pore, whiles the membrane lipid head phase remains localized at the membrane-water interface. The pore conductance channel disrupts transmembrane potentials and ion gradients leading to a loss of cellular components and cell lysis. The peptide length cascade in this model plays a significant functionality in the peptide traverse action through the hydrophilic core in the lipid bilayer. AMPs like LL-37 and

alamethicin with at least 20 amino acids in length are known to indulge in barrel-starve model in eliciting cell lysis bioactivity (Reinhardt and Neundorf, 2016; Scott *et al*., 2015).

2.5.2 The carpet model

This mechanism of action of AMPs was initially described based on the mode of action of Dermaseptins. Dermaseptins are peptide isolates from the skin of frogs and were the first vertebrate peptide to elicit lethal effects on filamentous pathogenic fungi of clinic importance. These peptides are composed of 27 − 34 amino acids long with lysine residues, cationic and possess an amphipathic helix structure in an aqueous environment or when integrated with the phospholipid bilayer of bacterial membrane. This model does not observe peptides insertion into the hydrophobic core or assembly with hydrophobic surfaces facing each other. Instead, the hydrophilic regions of the peptide face the headgroups of the lipid bilayer membrane, facilitating the reorientation of the hydrophobic region towards the lipid bilayer core forming a localized carpet (Figure. 2.4). At some high peptide concentrations, the local threshold capacity of the lipid membrane is lost eventually, and the peptide permeates the phospholipid membrane forming a transient pore in the membrane. Antimicrobial peptides like LL−37 and Cecropin are known for their disruption of intracellular pathways like DNA replication and protein synthesis often employs this model in the elicitation of therapeutic actions by pore formation in target pathogen (Dar *et al*., 2017; Nuti *et al*., 2017).

2.5.3 The toroidal pore model

Toroidal pore formation in target pathogens as a novel mechanism of bioactivity has been carried out by short chain, positively charged AMPs like renalexin, mellitins, protegrins, and the magainins. This action model differs from that of barrel−stave model in that the

peptide mainly associates with the phospholipid acyl head in both horizontal and perpendicular orientations. Insertion of the peptide helices induces a continuous bending of the monolayer lipids through the pore so that the water core becomes aligned with the lipid membrane and the inserted peptide. Transient pore formation by the peptide leads to leaflets associations with the lipid bilayer, which result in elicitation of lethal effects similar to that of barrel−stave pores (Dar *et al*., 2017; Nuti *et al*., 2017).

2.5.4 Other proposed modes of actions of AMPs

Several research studies have reported other interesting models of action of AMPs with indications of favorable views on the interaction between the lipid membrane and the peptide. A study proposed that the pore formation in the lipid bilayer by peptides is due to electroporation effects that is highly influenced by the polarity of the peptide (Huan *et al*., 2020). Another study has stipulated that the binding of peptides to the cell membrane of target pathogens causes an imbalance and localized membrane curvature which facilitates the sinking of the peptide leading to transient pore formation within the membrane of bacteria pathogens (Erdem Büyükkiraz and Kesmen, 2022). Furthermore, the therapeutic activity of antimicrobial peptides with intracellular biomolecules such as DNA, RNA and some cellular polypeptides could be attributed with the electrostatic interactions between the positively charged AMPs and the negative regions of these biomolecules. Recent studies proposed that AMPs like indolicidins and LL−37 are capable of inhibition of membrane and DNA synthesis in bacterial and fungi at promising MIC levels via electroporation effect and imbalance membrane curvature (Bolívar Parra *et al*., 2020; Kang *et al*., 2019; Perez-Perez *et al*., 2021).

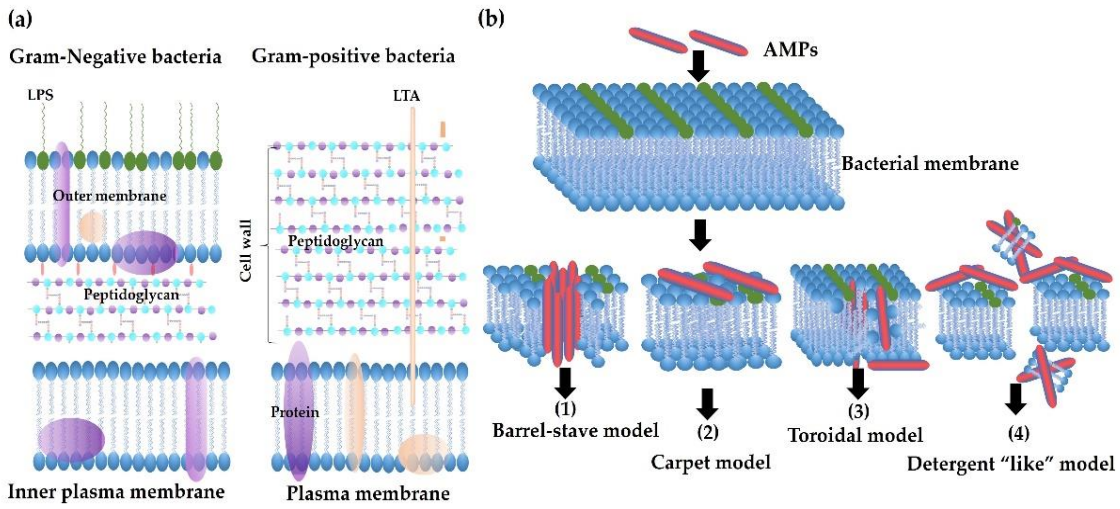

Figure 2. 4: Bacterial membrane topology and mechanisms of action of antimicrobial peptides (AMPs). (a) Schematic of lipid bilayer membrane structure in Gram-positive and Gram-negative bacteria. (b) Mechanisms of action of AMPs. Membrane-active AMPs interrupt the integrity of the membrane by forming different pores via the following models: (1) Barrel-Stave model: AMPs perpendicularly insert into the lipid bilayer membrane and form a channel. (2) Carpet model: AMPs shield the lipid membrane surface of the bacteria without forming specific pores. (3) Toroidal pore model: AMPs are inserted perpendicularly in the lipid bilayer membrane without specific peptide–peptide interactions to form a channel. (4) Detergent-like mode: AMPs function like a chemical detergent to lyse bacteria membranes into small molecular fragments *(*Rodríguez-Rojas *et al*., 2021; Zhang and Yang, 2022).

2.6 Immunomodulatory function of AMPs

Many of the characterized AMPs including LL-37, gramicidin, β-defensins, Renalexin, and cathelicidin-based AMPs like hCAP-18 are known for both bactericidal and immunomodulatory functionalities in microbial infections by recruiting phagocytes,

neutrophils, and other immune cells for pathogen engulfment and phagocytosis (Erdem Büyükkiraz and Kesmen, 2022). In ensuring their immunomodulatory therapeutic actions, AMPs first exhibit chemokine-like bioactivity via chemokine receptors like CCR2 and CCR6 by recruiting and migrating leucocytes such as dendritic cells, monocytes, and macrophages to infection sites (Gan *et al*., 2021; Zhang and Yang, 2022). Secondly, AMPs such as LL-37 and hBD3 can modulate host immunity via pro-inflammatory activity by the activation of Toll-like receptors (TLR4) leading to mediation of an inflammatory responses through cytokine expression on activated leukocytes. For example, the human-defensin DEFB126 have been reported to have strong neutralizing and binding abilities towards lipopolysaccharides (LPS), as a result could exhibit LPS-induced inflammatory through cytokines like IL-1β, IL-6, and TNF-α on macrophages release during localize and systemic bacterial infection (Büyükkiraz and Kesmen, 2022; Li *et al.*, 2015). A study by Scott *et al*. (2002), indicated that various AMPs have intracellular interactions with nucleic acid DNA and RNA, with a capability of consistent molecular regulation of 29 (up) and 20 (down) genes including chemokines and chemokine-receptors on macrophages, monocytes and the human A549 epithelial cells. This study reported that upon infection, the host immune responses lead to high cellular levels of antimicrobial peptides including the human cathelicidin hCAP-18, and LL-37 produced in the granules of leukocytes.

2.7 Intracellular therapeutic action of AMPs

There is reliable research evidence reporting that highly cationic antimicrobial peptide can traverse the lipid membrane of target microbial pathogens without causing rupture and disruption of the membrane integrity rather, they target intracellular biomolecules such as

DNA, RNA, and proteins of cellular and metabolic importance thereby resulting in the release of lytic enzymes like hydrolases or inhibiting the metabolic enzymes necessary for microbial growth (Gan *et al*., 2021; Wei and Zhang, 2022). Wei and Zhang (2022) indicated the molecular binding of AMP CF-14 to bacterial DNA gyrase by blocking microbial DNA replication and transcription leading to the inhibition of cell growth. Also a 21 amino acid antimicrobial peptide buforin II with a partial sequence similarity to eukaryotic Histone H2A protein has been reported to have direct interaction with nucleic acid and can penetrate lipid vesicles of target pathogens without compromising the permeability of the membrane and ultimately exhibit bactericidal properties inhibiting microbial growth and cellular metabolisms (Klubthawee *et al*., 2020). Several studies revealed that generally AMPs like Cecropin, LL-37, defensins, Renalexin and buforin II interfere with microbial protein synthesis at various levels including initiation of translation, transition of translation complex to elongation stage, premature termination of translation as well as inhibition of protein folding. Proline-rich AMPs are usually found to be bounded to prokaryotic ribosomes and the protein complex required to initiate protein translation. Wei and Zhang (2022) again confirm that the AMP apidecin has therapeutic property of binding to the microbial 70S ribosomes and can block the cellular assembly of the 50S ribosomal large subunit. A proline-rich AMP (pr-AMP) Bac5 can bind and associate strongly to bacteria ribosomal tunnel complex leading to the prevention of protein synthesis from the initiation right to the elongation phase. Pyrrhocoricin a proline-rich polypeptide have been reported to exhibit bactericidal actions by binding and inhibiting the cellular function of relevant bacterial biomolecules such as significant heat shock protein-like DnaK and bacterial chaperone GroEL thereby interfering with proper protein folding (Nuti *et al*., 2017). The inhibition of cellular biosynthesis of cell wall

components in targeted microbial pathogens of clinical importance has been indicated as one of the novel therapeutic potencies of some AMPs that binds to lipid II to ensure the failure in the polymerization of peptidoglycan-membrane subunits for complete cell wall synthesis. Teixobactin is an example, that shows strong affinity to cell wall teichoic acids lipid II and III conserved motifs thereby inhibiting bacteria cell wall biosynthesis (Nuti *et al*., 2017; Wei and Zhang, 2022).

2.8 Cellular toxicity of AMPs

Irrespective of the multi-functional and broad spectrum of antimicrobial functionality of AMPs (Figure 2.5) in addressing pressing human health issues, there is the need combat significant and urgent challenges associated with the toxicity, peptide instability and short half-life which compromise the duration and extent of therapeutic actions of most AMPs (Erdem Büyükkiraz and Kesmen, 2022). The evaluation of toxicity of both in-vivo and in-vitro ensures an essential step in the research and development of novel AMPs as an alternative to conventional antibiotics, anticancer and anti-inflammatory agents. A standard index employed to ascertain acute and chronic toxicity in-vivo and in-vitro includes but is not limited to the half lethal dose (LD50) and half hemolytic activity (HC50). The subacute in-vivo toxicity of the AMPs S-thanatin was evaluated in ICR mice via continual intravenous injection at variable doses of 125, 50, and 20 mg/kg of mice body weight for 14 days with results demonstrating little to no significant cellular changes in serum biochemistry and hematology (Wei and Zhang, 2022). Wei and Zhang (2022) ascertain and evaluate the toxicity and immunogenicity of the AMP P34 at different dosage levels in-vivo with results suggesting no hypersensitivity cellular reaction during the immunogenicity experiment, coupled with no death in the animal model used at an

LD50 of less than 330 mg/kg. *Heterometrus petersii* derived AMP HP1404 showed a very low toxicity effects against mammalian cells (HC50 = 226.7 µg/ml) and no toxicity in BALB/c mice via intraperitoneal injection (80 mg/kg) and LD50 at 89.8 mg/kg by intravenous injection (Gong *et al*., 2021).

A novel hemoglobin-derived AMP JH-3 an isolate from bovine erythrocytes has been reported to show high LD50 of 180 mg/kg in mice when administered via intraperitoneal injection and subcutaneous injection with no observable evidence of cellular death even at dosage as high as 240 mg/kg body weight (bw) (Erdem Büyükkiraz and Kesmen, 2022; Leite *et al*., 2019). A study by Wei and Zhang (2022) also indicated that anoplin-based antimicrobial peptide J-RR and J-AR as peptide dimer analogs exhibited a 16-fold increment in antimicrobial bioactivity with no relevant cellular toxicity in adult mice at LD50 of 53.6 mg/kg. Several studies have indicated and shown that generally AMPs have significantly lower LD50 in animals when administered via intravenous and intraperitoneal injection (Erdem Büyükkiraz and Kesmen, 2022; Gan *et al*., 2021; Leite *et al*., 2019; Wei and Zhang, 2022).

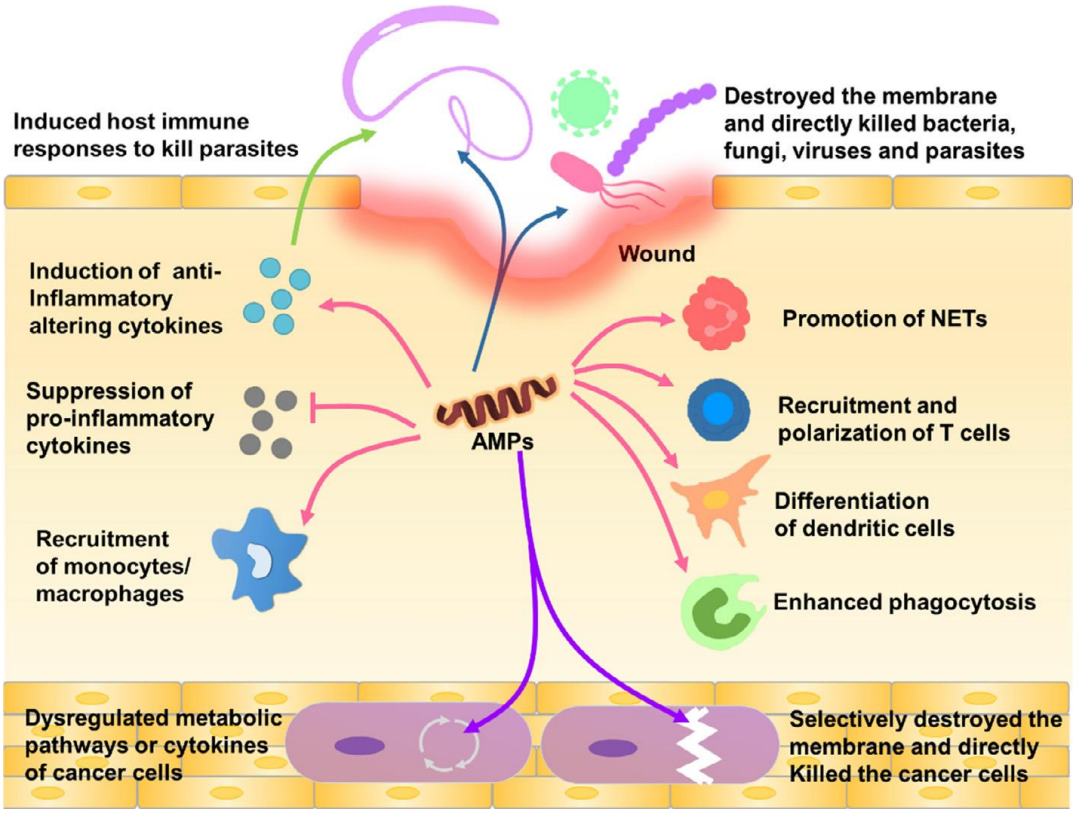

Figure 2. 5: Multi–functional bioactivity of antimicrobial peptide. Adapted from (Wei and Zhang, 2022).

2.9 Strategies to improve bioactivity and reduce biotoxicity of AMPs

Many antimicrobial peptides including the natural, synthetic and recombinantly produced have been reported of exhibit a broad spectrum of bioactivity and biotoxicity attributed to their hydrophobic, amphipathic and strong cationic nature (net positive charge), which ensures a challenge in balancing the desirable bioactivities to patient safety (Erdem Büyükkiraz and Kesmen, 2022). However, the adjustment of amino acid residues and structural motifs (Figure 2.6) has demonstrated in recent studies an excellent maintenance of antibacterial properties and reducing cellular toxicity (Wei and Zhang, 2022).

Temporin-1CEa a natural AMP isolated from the brown skin Chinese frog *Rana chensinensis* has been reported to exhibit potent anticancer activities against human cancer cell lines including breast cancer cell line MCF-7. Although this peptide shows hemolytic actions against normal human cells at half lethal dose (LD) of 99.08M. Six chemical derivatives of temporin-1CEa developed by molecular modification and replacement of acidic and neutral amino acid residues on the hydrophobic phase of the α-helix structure with lysine resulted in a peptide with much lower biotoxicity as compared to the natural temporin-1CEa (Cremet *et al*., 2022). Furthermore, structural and composition modifications involving the conjugation of novel AMPs with biomaterials such as chitosan indicated a reduced toxicity effects of the AMPs at their therapeutic doses via the adjustment of excessive electrostatic actions thereby prolonging its half-life. The grafting of anoplin AMP with chitosan biopolymers gave birth to a control strategy in the hemolytic propensity of AMPs like LL-37, Cecropin, Defensin, and Renalexin. Conjugated anoplin-chitosan biopolymers are said to remain completely non-hemolytic at a maximum concentration at 2048 µg/ml as compared to pure anoplin peptide (HC50 of 512µg/ml) (Erdem Büyükkiraz and Kesmen, 2022; Shang *et al*., 2020). Other grafted conjugates of AMPs with improved therapeutic actions and reduced cellular toxicity have been designed and tested such as AuNP-PEG with AMP BP100, hyaluronic acid (HA) grafted with AMP nisin, hyaluronic acid and collagen grafted with AMP Tet213, and polylactic acid (PLA) and poly(lactic-co-glycolic) acid nanoparticle mixed with AMP GIBIM-P5S9 (Wei and Zhang, 2022).

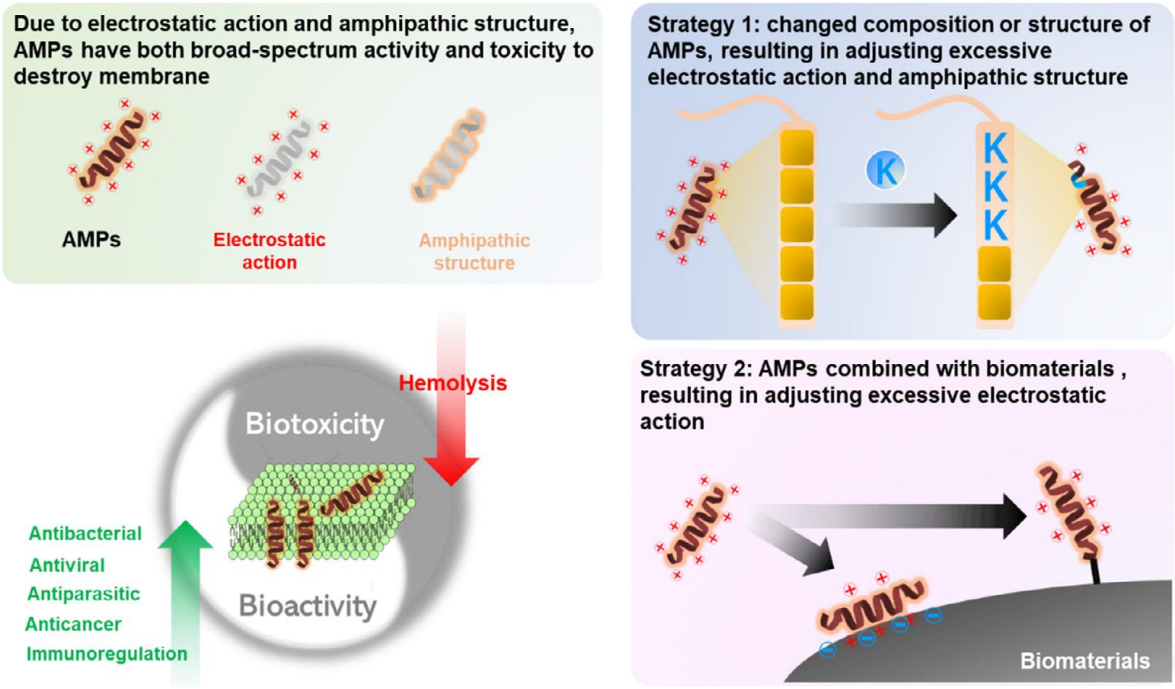

Figure 2. 6: Strategies for improving the bioactivities and reducing cellular toxicity of AMPs. Adapted from (Wei and Zhang, 2022).

2.10 Antimicrobial peptide: LL-37

Among the various peptides of the innate immune system in human, LL−37 is the only α-helix (Figure 2.7) cathelicidin-based antimicrobial peptide with antimicrobial therapeutic action against bacterial, viral and fungi infections (Kang *et al*., 2019). The biosynthesis of LL−37 occurs in most immune cells including the mast cell, neutrophils, mucosal epithelial cell, keratinocytes, adipocytes and the T and B lymphocytes. LL−37 cellular expression dwells under the regulations of endogenous factors like growth factors, vitamins and cytokines activation upon microbial infections (Kang *et al*., 2019). Cathelicidin (hCAP18) a distinct mammalian immune-protein that is functionally similar but structurally different to defensins and acts as a precursor molecule that undergoes proteolytic cleavage at the C-terminal to release short peptides with antimicrobial and

immune modulatory activity commonly known as LL-37. The isolation of the bovine neutrophil antimicrobial peptide Bac5 has led to the discovery of cathelicidin and unveiling the elucidation that these peptides are release via cleavage from inactive precursors (Dürr *et al*., 2016; Pasupuleti *et al*., 2017). LL-37 is a cathelicidin-derived peptide isolated from the human antibacterial cathelicidin peptide (hCAP18/LL-37) owes its name to the 37 amino acid residues and the first two leading leucine (LL) in the peptide sequence. This peptide is biochemically amphipathic with highly conversed N−terminal and C−terminal regions. The hCAP18/LL-37 has a molecular size of about 18 kDa, which after proteolytic cleavage produces LL−37 of molecular weight 4.7 kDa with a net positive charge of +6. The release of LL−37 from the white blood cells (WBCs) during microbial infection increases the production of reactive oxygen species coupled with delayed cellular apoptosis thereby modulating the immune cells for the efficient killing of an intruding pathogen (Moretta *et al*., 2021). Aside the immunomodulation by LL−37, it is also known to interact with cellular membrane as well as intracellular molecules in target pathogens resulting in membrane traversion and pore formation in the target pathogen leading to cell lysis (Montfort-Gardeazabal *et al*., 2021; Seyedjavadi *et al*., 2021). The antibacterial activity of naturally and recombinantly purified LL−37 against multi-drug resistant (MDR) bacteria pathogens has been reported over the years in many publications. A study by Cheng *et al*. (2021), reported a minimum inhibition concentration (MIC) of LL−37 at 32 µg/ml against *P. aeruginosa*, 32 µg/ml against *S. aureus*, and 16 µg/ml against Enterotoxigenic *Escherichia coli* K88 (ETEC K88). Perez-Perez *et al*. (2021), reported that microbial recombinantly purified LL−37 (both protein tagged and free LL−37) with 90% purity exhibited remarkable inhibition at an MIC of 50 µM against antibiotic-resistant *S. aureus,* and *E. coli* clinical isolates, with an estimated percentage of

zonal inhibition (PZI) of 69% against *Staphylococcus aureus* and 64% against *Escherichia coli*. A minimum inhibition concentration of 32 µM of LL−37 was also reported as compared to synthetic antibiotics like Rifampin (100 µM), and Gentamycin (100 µM) considering the dosage level and the kinetics of antimicrobial activity. LL−37 has been reported to exhibit biofilm disruption of a 24 h and 48 h old *S. aureus* biofilm (Kang *et al*., 2019).

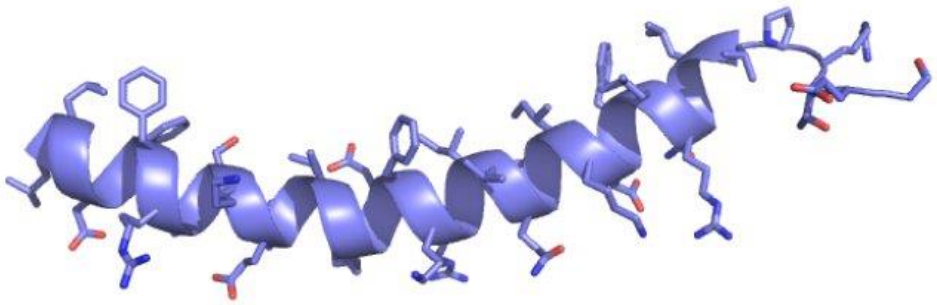

Figure 2. 7: 3D molecular Riben secondary structure of AMP: LL-37. Adapted from (Liscano *et al*., 2020; Mohan, 2016).

2.11 Antimicrobial peptide: Renalexin

Following the emergence drug-tolerant microbial pathogens in the early 90 s has propel researchers to seek for biologics as therapeutics against resistant-pathogens (Amábile-cuevas, 2020; De J. Sosa *et al*., 2010). A study by Douglas Clark and colleagues in the early 1994 has led to the discovery of a novel antimicrobial peptide isolated from the skin of the American Amphibian *Rana catesbeiana* commonly known as Bullfrog, recently considered as a novel biological source for diverse AMPs of reliable therapeutic applications. These peptides with 20 amino acid residues termed Renalexin (*Ranalexin), with a molecular weight of 2.2 kDa, and a net charge of +3. Renalexin has a unique

3D−structure (Fig. 2.8) similar to the well−known antibiotic Polymyxin and has the amino acid sequence NH_2-Phe-Leu-Gly-Gly-Leu-Ile-Lys-Ile-Val-Pro-Ala-Met-Ile-Cys-Ala-Val-Thr-Lys-Lys-Cys-COOH (Nuti *et al*., 2017). It contains a single intramolecular disulfide bond between two cysteine amino acids at position 14 and 20 which forms a heptapeptide ring within the molecule like that seen in the antibiotic Polymyxin. Renalexin is initially synthesized as a precursor peptide with a putative signals sequence and an acidic amino acid-rich region at its N−terminal. Interestingly the putative signal sequence of Renalexin is like that of opioid peptides in other related amphibians like *Phyllomedusa sauvagei* and *Phyllomedusa bicolor*. Detailed analysis including northern blotting and in−situ hybridization revealed that the mRNA of Renalexin is express right from metamorphosis to adulthood (Bolívar Parra *et al*., 2020; Nuti *et al*., 2017). A study by Jindal *et al*. (2015), indicated that synthetic renalexin shows novel antibacterial pharmacological actions against 30 *Pneumococcal* clinical isolates, *Staphylococcus aureus* and MRSA at an MIC of 7.81- 15.62 µg/ml. Renalexin has therapeutic actions against both gram−positive and gram−negative bacteria by interacting with phospholipid membrane via electrostatic binding, in cases where the peptide traverses the membrane it inhibits protein expression which leads to cell death (Dar *et al*., 2017; Nuti *et al*., 2017).

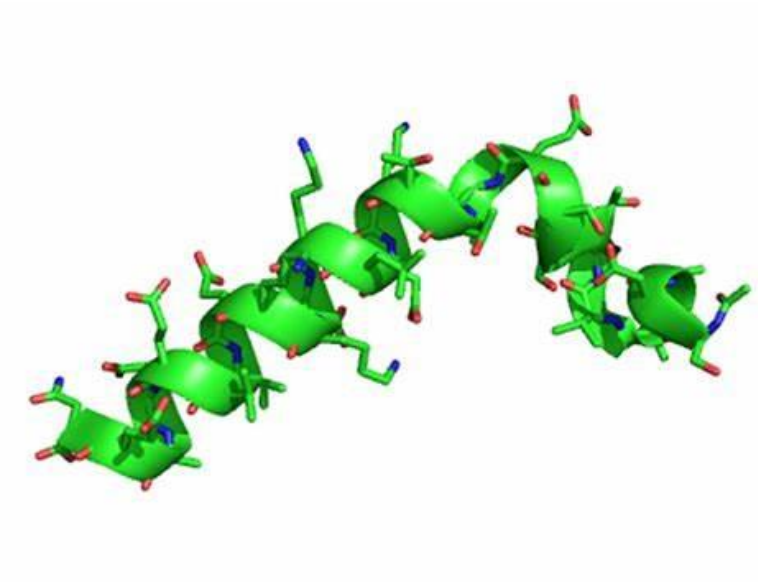

Figure 2. 8: 3D molecular Riben secondary structure of AMP renalexin. Adapted from (Liscano *et al*., 2020; Mohan, 2016).

2.12 Hybrid AMP

A promising avenue in the design of novel antimicrobial peptides with high potency of antibacterial therapeutic properties involves the combination of two or more antimicrobial peptides of known bioactivity via the use of protein linkers such as the flexible linkers GPDGSGPDESGPDES, EAAAK, and ALEA. The first application of this expression strategy considered the hybridization of the AMP Cecropin A and mellitin into a single hybrid peptide with extremely novel antibacterial activity against gram-negative and gram-positive bacteria including MRSA and *Pseudomonas aeruginosa*. Following the design and expression of the first hybrid peptide which exhibited higher bioactivity as compared to its parental peptides has led to the development of several hybrid peptides including the bovine lactoferricins, microcins, Cecropin A and B with LL-37, and LL-37 with rat neutrophil peptide 1 (Kruchinin and Bolshakova, 2022; Wade *et al*., 2019). The bactericidal concentrations of hybrid AMPs reported in several studies indicate the

emergence of new antimicrobial agents of therapeutic importance including MCh-AMP1 (3.33 – 6.67 µM), DiMCh-AMP1 (1.67 – 6.72 µM) (Seyedjavadi *et al*., 2021). Jindal *et al*. (2015), reported that the four distinct hybrid AMPs RN7-RN10, RN7-IN9, RN7-IN8 and RN7-IN6 developed from renalexin and indolicidins possess a potential antibacterial activity against 30 different *Pneumococcal* clinical isolates, *E. coli*, *S. aureus*, and MRSA with a minimum inhibitory concentration (MIC) of (7.81-15.62 µg/ml) as compared to their single parental peptides showing an MIC of (32.5 – 62.29 µg/ml) and also shows therapeutic killing kinetic time within less than an hour which is far less than most standard antibiotics such as erythromycin, ceftriaxone, and colistin. The analysis of Jindal and colleagues further indicated that these hybrid AMPs exhibited no cytotoxic or hemolytic effects on human erythrocytes and NL-20 normal lung cell lines at their respective MIC. A study by Wade *et al*. (2019) revealed that AMPs mixture constituting two single peptides (hybrid peptide) and three single peptides (tripeptides) exhibited strong antibacterial activity against MRSA and *pseudomonas* at an MIC higher than the hybrid peptides which is considered of having roughly twice the concentration of individual amino acids at same molar concentrations as compared to single normal peptide counterparts. The hybrid AMPs often possess strong positive net charges (+6 to +9) which elicits good electrostatic binding activity for the membrane permeating peptides like LL-37, and indolicidins. Their amphipathic and solubility properties are enhanced through the hybridization and as well turn to lower the killing time of these peptides. Many hybrid peptides reported in literature are designed from two peptides with the same bioactivities such as membrane permeability or membrane translocation (Kravchenko *et al*., 2022; Shang *et al*., 2020; M. Zhang *et al*., 2018). However, in this recent study we seek to design a novel hybrid AMP LL-37_Renalexin of both membrane permeability and translocation

properties with strong cationic charge with help of GS flexible peptide linker and carrier proteins SmbP and CusF3H+.

2.13 Novel hybrid AMP: LL-37_Renalexin

The hybrid AMP LL-37_Renalexin is a novel peptide that consists of a membrane-permeating peptide LL-37 and a membrane translocation and permeating peptide Renalexin; both peptides are known for their extracellular and intracellular antibacterial activities and have the sequence indicated in (Table 2.3). The AMP LL-37 has a sequence of 37 amino acid residues, Renalexin is composed of 20 amino acids long, and a simple protein linker (GS). The entire peptide has a molecular weight of 6.740 kDa (theoretically predicted) and a net positive charge of +9 which suggests a strong electrostatic binding potential of the peptide. It has a helical structure, one disulfide bond at the tail end with multiple thioether bonds as in lantibiotics and polymycin (see Figure 2.9). LL-37_Renalexin shows a total hydrophobic ratio of 44% and hydrophilic ratio of 66% coupled with protein binding potential (PBP) of 1.46 Kcal/mol (Boman index) as described by the AMP calculator and predictor APD3 (http://aps.unmc.edu/AP/prediction/).

Table 2. 3: Amino sequences of the components of the hybrid AMP LL-37_Renalexin.

AMP	Sequence (aa)
LL-37: Renalexin: Peptide linker:	LLGDFFRKSKEKIGKEFKRIVQRIKDFLRNLVPRTES FLGGLIKIVPAMICAVTKKC GS
LL-37_Renalexin:	LLGDFFRKSKEKIGKEFKRIVQRIKDFLRNLVPRTESGSFLGGLI KIVPAMICAVTKKC

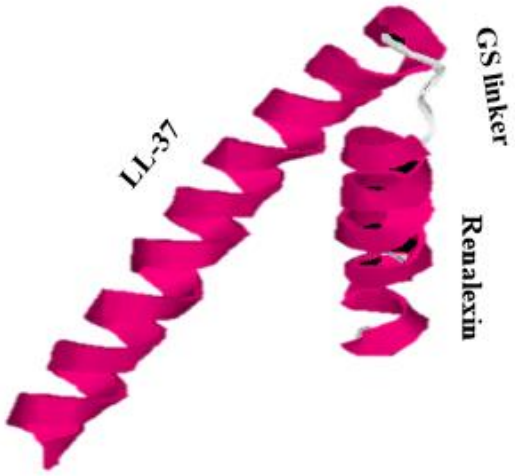

Figure 2. 9: 3D helical molecular secondary Riben structure of LL-37_ Renalexin predicted in I-TASSER: Protein Structure and Function Prediction (https://zhanggroup.org/I-TASSER-MTD/).

2.14 Recombinant production of AMPs

2.14.1 Recombinant membrane protein production in microbial systems

Biologically, few membrane proteins of therapeutic importance are naturally abundant in their native forms as well as the natural sources. As such, for biophysical and biochemical characterization and production require the recombination of gene or gene clusters with relatively efficient molecular regulators and promoters into plasmid vectors for expression as a recombinant protein (Fazaeli *et al*., 2018; Kesidis *et al*., 2020). Dated back in the 1998, the first recombinant membrane proteins were published including the microbial proteins *MscL* (Mechanosensitive channel protein) and *KcsA* (Potassium channel sensitive protein) all expressed in *Escherichia coli* with *SERCA1a* and Ca^{2+}*-ATPase* produced in

Saccharomycess cerevisiae (Kesidis *et al*., 2020). Considering the unique membrane protein structures (UMPS) in microbial expression systems like *E. coli*, over 521 UMPS were recombinantly produced and their amino acid sequences deposited in the protein database (PDB), with over 468 recombinant proteins isolated from *E. coli*, generally considered as cellular machinery of choice (CMC), 31 protein isolated from the yeast *Pichia pastoris*, and 22 proteins from *S. cerevisiae* (Montfort-Gardeazabal *et al*., 2021).

2.14.2 Recombinant AMPs as alternative to conventional antibiotics

The therapeutic potencies of AMPs as a recombinant protein expressed in microbial expressions systems have been elucidated and tested against bacterial pathogens. Although, the initial exploration of AMPs relied on extraction from their natural biological sources which comes with a major setbacks considering the application of large amounts of biological raw materials *(Nuti et al*., 2017). Typical example would be the extraction of the AMP Dermaseptins from the skin of *Phyllomedusa sauvigii* frog might cause the extinction of an entire frog ecosystem particularly when required for therapeutic and research purposes where large amount of the peptide is required. In addition, natural AMPs are being translated as precursor proteins that undergo proteolytic cleavage into an active and matured peptide. The human cathelicidin AMP (hCAP18) predominately synthesized as pre-protein that undergoes proteolytic cleavage to release the active peptide LL-37 is a typical example (Scott *et al*., 2002). Interestingly, most released peptides may be exposed to protease degradation into an alternative active form at other sites. This posttranslational processing of AMPs makes the purification from the natural sources extremely sophisticated as the desired peptide may not be present in a unique and active form (Soltani *et al*., 2021). Fortunately, the application of genetic engineering and

molecular cloning techniques facilitates the overexpression of AMPs as heterogeneous recombinant proteins in genetically modified microbial expression systems (GMMES) such as *E. coli* BL21(DE3), *E. coli* C41(DE3), *E. coli* SHuffle T7, and *E. coli* K12. Because most therapeutic peptides can exhibit pharmacological actions at their secondary domains which permits production in microbial systems, it allows for the efficient and fast production of numerous therapeutic peptides as heterogeneous proteins. A study by Perez-Perez *et al*. (2021), reported the successful production of LL-37 as a recombinant AMP (rAMP) in *E. coli* BL21(DE3) with a final percentage purity of 95%. The recombinant LL-37 (rLL-37) exhibited therapeutic actions at a final concentration of 50 µM against antibiotic resistant clinical bacteria isolates like *Staphylococcus aureus* and *Escherichia coli*. It has been revealed that rLL-37 could control *Staphylococcus aureus* infections and biofilm formation by 4–fold reduction in log phase of bacteria growth within a 24 hour incubation, at a final concentration of 128 µM susceptible against $1x10^6$ colony forming units (CFU/ml) of intracellular target pathogens *Staphylococcus aureus* and *E. coli* (Kang *et al*., 2019). About 80% closure in wound infection was observed in 926 endothelial cells after treatment with recombinant dermatopontin (rDPT), an extracellular matrix protein, at a final concentration of 20 ng/ml. The rDPT peptide was expressed in *E. coli* GJ1158 via molecular cloning and transformation with the recombinant expression vector pRSETA_DPT (Madom *et al*., 2020). Recent advances in recombinant DNA technologies and the expression of novel therapeutics as recombinant proteins in microbial systems has propel the design and production of hybrid AMPs with striking pharmacological actions against multi-drug resistant bacteria pathogens (MDR-BP) in genetically modified prokaryotic and eukaryotic systems (GMPES) such as *E. coli* BL21(DE3), *E. coli* C41(DE3), *Pichia pastoris*, *Spodoptera frugiperda* (Sf 9, Sf 21), and the Chinese Hamster

Ovary cell (CHO) (Kesidis *et al*., 2020). Research by Madom *et al*.(2020), reported the successful expression of the hybrid AMP Cecropin A_Thanatin as a recombinant peptide in *P. pastoris* X-33 which harbors the expression vector pPICZa_CA plasmid encoding the recombinant peptide (rCecA_T). The purified rCecA_T exhibited antibacterial activity at a promising minimum inhibition concentration (MICs) 6.25 µM against *Staphylococcus aureus* and *epidermidis,* 12.50 µM against *Escherichia coli* and *Klebsiella oxytoca,* and 25 µM against *Pseudomonas aeruginosa*. A recombinant hybrid AMP S2 composed of species-specific targeting and broad-spectrum domains was successfully designed and expressed in *Escherichia coli*. S2 showed specific killing therapeutic activity against *Escherichia coli* ATCC 25922, *Pseudomonas aeruginosa* ATCC 27853, *Escherichia coli* UB1005, *Salmonella typhimurium* 14028, *Salmonella pullorum* C7913, and *Staphylococcus aureus* ATCC 29213, with no traces of resistance induced upon exposure to concentrations of the purified S2 peptide as compared to the conventional antibiotic penicillin (Shang *et al*., 2020).

2.14.3 *E. coli* expression system

Many *E. coli* cell strains serve as a reliable expression system not only considering the production of soluble proteins but also as an attractive cellular system for expressing eukaryotic membrane proteins. Owing to their high potential expression efficiency and the possible genetic manipulations coupled with their high growth rate (Figure 2.10) (Vargas-Cortez *et al*., 2016). *E. coli* ensures many relevant possibilities for the expression of eukaryotic heterogeneous proteins, although this cellular expression machinery may provide some undesirability as a host system owing to the differences in the biochemical compositions in the microbial and the eukaryotic membrane and cellular structures (Mesa-

Pereira *et al*., *2018*; Soares *et al*., 2021). Due to the lack of post-translational modifications of an expressed polypeptide and the absence of molecular chaperones in bacteria that plays significant role in protein folding and processing can lead to the non-functionality and as well incorrectly folded protein. *E. coli* cells including but not limited *E. coli* BL21(DE3), *E. coli* K12, *E. coli* C41(DE3), *E. coli* C43(DE3), *E. coli* C44(DE3), and *E. coli* Shuffle(DE3) are known for an efficient and fast growth rate as this could lead to overexpression of the target recombinant protein and by the knowledge we understand that the accumulation of those recombinant proteins could be toxic to the microbial cell (Kesidis *et al*., 2020; Moulahoum *et al*., 2020). The appropriate selection of *E. coli* expression strain in combination with the reliable promoter and regulator system (Table 2.4) is essential for efficient expression and protein yield. The commonly exploited *E. coli* expression systems to produce recombinantly homologous and heterogeneous protein are the *E. coli* BL21(DE3), *E. coli* K12, *E. coli* C41(DE3), *E. coli* C43(DE3), and *E. coli* C44(DE3), and Rosetta. The majority of heterogeneous recombinant proteins are been expressed under the influence of the T7 promoter, ara promoter, T5 promoter and the tet promoter (Kesidis *et al*., 2020; Santos *et al*., 2019; Vargas-Cortez *et al*., 2016). One essential and crucial target in the expression of heterogeneous proteins in *E. coli* involves the combination of a reliable promoter, plasmid vector, and an expression strain. Several studies have reported substantial efficiency in the expression of many heterogeneous eukaryotic proteins in *E. coli* BL21(DE3) strain harboring the DE3 gene from T7 bacteriophage that encodes the T7RNA-based polymerase (Fazaeli *et al*., 2018; Santos *et al*., 2019; Vargas-Cortez *et al*., 2016). Although studies have revealed that the T5 promoter system is eight times slower in expression compared to the T7 promoter system, however it does reduce the pressure posed on the microbial expression machinery via

protein overexpression, and as well the toxic effects resulting from protein accumulation (Fazaeli *et al*., 2018; Kesidis *et al*., 2020).

Table 2. 4: Commonly used bacterial plasmid expression vectors and promoters.

Plasmid Series	Promoter	Inducer	Repressor System	Tag	Selection Marker	Source
pET	T7/lac, T7	IPTG	LacI	None	Ampicillin (AmpR)	Invitrogen
pBAD	araBAD	Arabinose	araC	None	Ampicillin (AmpR)	Invitrogen
pRSET	T7/lac	IPTG	LacI	6xHis	Ampicillin (AmpR)	Invitrogen
pASK-IBA	tet	Anhydrotetracycline (AHT)	Tet-repressor	Various	Chloramphenicol (CamR)	IBA Life Sciences
pMAL	tac	IPTG	LacI	MBP	Ampicillin (AmpR)	NEB
pQE	T5	IPTG	LacI	8xHis	Ampicillin (AmpR)	Qiagen

Source: Adapted from (Kesidis *et al*., 2020).

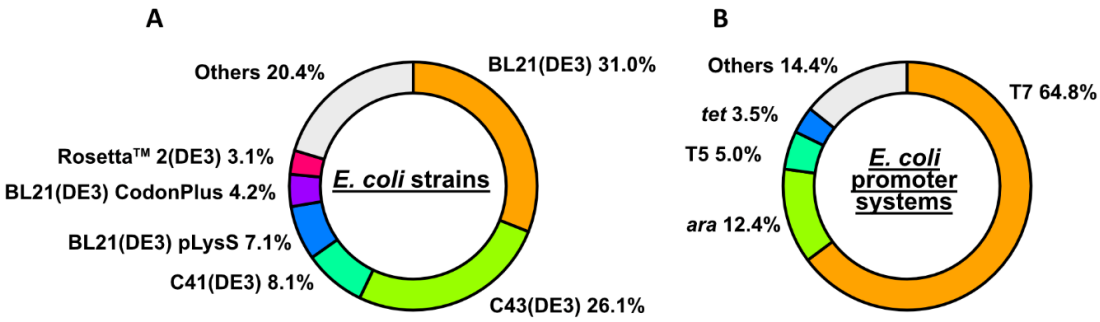

Figure 2. 10: Most used *E. coli* strains (A) and (B) promoter systems for efficient protein expression. Source: (Kesidis *et al*., 2020).

2.14.4 Plasmid construct design

Selecting an appropriate expression host system alone is inefficient for successful protein production and yield. However, the essential design of plasmid expression construct is crucial and serves as a critical element in the production of recombinant proteins. An optimal plasmid construct design plays an essential role role in the overall stages of recombinant protein production from cloned gene transcription, translation, and translocation-insertion into membrane space for proper protein folding. In addition, downstream purification and processing of the expressed protein also depends on a reliable construct such that some genes are constructed into plasmid vectors with a signal sequence, cleavage site, and sometimes a promoter region (Figure 2.11) that enhance the expression and purification through simple laboratory techniques like immobilized metal affinity chromatography, and as well minimizes or inhibits the bioactivity of the expressed protein as described in our previous publications (Santos *et al*., 2019; Vargas-Cortez *et al*., 2017). The design of plasmid vector constructs can be generated via molecular biology techniques such as Gibson Assembly, topoisomerase-based cloning, gateway recombination cloning, and restriction enzyme cloning as one of the most widely used methods. However, these traditional gene cloning methods have increasingly been replaced with new technology like *de novo* synthesis of DNA. This new method provides reliable efficient in the cloning process, the nucleotide sequence of the gene (DNA insert) needs to carefully assessed (Montfort-Gardeazabal *et al*., 2021). A study by Perez-Perez *et al*. (2021), indicated that the accuracy and rate of recombinant protein translation is directly aligned with the base sequence in the mRNA and the presence of signal proteins can significantly enhance the expression level. Efficient codon optimization is crucial for using of expression machineries in a microbial expression system coupled with the

addition of ribosomal binding sites (RBS), ATG (methionine) initiation site and a TAA termination site. Furthermore, modifying of the coding sequence often facilitates structural studies analysis of recombinant proteins by ensuring high and pure level of recombinant protein expressed (Deng *et al*., 2017).

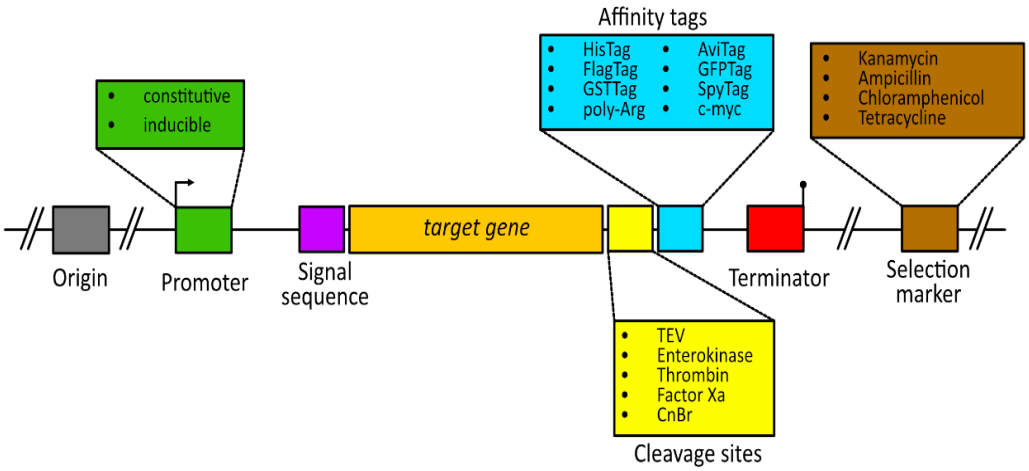

Figure 2. 11: Design of synthetic DNA (coding gene) insert cloned into plasmid expression vector construct. A signal sequence is inserted upstream into the target gene. Tags can be clone at the 5´ or 3´ end of target gene for significant purification, a proteolytic cleavage site exist between the target gene and the tag for reliable removal of a tag protein. The entire gene insert is flank with a constitutive or inducible promoter and a terminator sequence (Kesidis *et al*., 2020).

2.14.5 Protein tags

Fusion protein plays a significant role in the production of soluble biopharmaceuticals protein-based products like insulin, interleukins, and antimicrobial peptides as well as enhancing the downstream processes in purification of these products by the applications of technologies like affinity chromatography. The crucial role fusion proteins commonly

referred to as protein tags exhibit in the expression and purification of recombinant proteins in expression systems including bacteria, yeast, fungi, and mammalian cells is not limited to the prevention of the formation of inclusion bodies however, protein tags also ensures the secretion and localization of expressed proteins (Hanafiah *et al*., 2020; Kang *et al*., 2019; Santos *et al*., 2019). These classes of proteins are known for their unique and short amino acid sequences coupled with their approximately low molecular weight. It has a reliable signal sequence at the N-terminal which directs the localization of expressed recombinant proteins into the cytoplasmic or periplasmic membrane via the Sec or the Tat pathways as we previously described. Many fusion proteins including the green fluorescence protein (GFP), the maltose binding protein (MBP), and the glutathione S-transferase (GST) have been employed in the purification of recombinant proteins. However, some of these protein tags require sophisticated purification techniques and more cost-related methodologies (Cheng *et al.*, 2021; Mesa-Pereira *et al*., 2018). In our previous studies we have described the discovery and the experimental flexibilities associated with the expression and the purification of recombinant proteins using novel protein tags like the SmbP and the CusF3H+. This recent study seeks to employ these two-fusion proteins to produce an unprecedented hybrid antimicrobial peptide.

2.14.6 Small metal binding protein (SmbP)

The small metal binding protein SmbP is a microbial periplasmic protein isolated from the bacterium *Nitrosomonas europaea*. SmbP is a small molecular weight protein of size 10.3 kDa and it is constituted of 94 amino acid sequences. This protein is characterized by the unusually high level of histidine amino acid residues coupled with the presence of 10 repeats of seven amino acid motifs which ensures efficiency in the protein bio-

functionality. The expulsion of divalent metallic ions like Ni(II), Cu(II), and Zn(II) from the cytoplasmic and periplasmic regions is a function commonly referred to as metal scavenger is initiated by SmbP via the secondary secretory pathway due to the presence of a signal peptide at the N-terminal of the protein. Our previous studies have indicated the recombinant applications of SmbP as a protein tag. We have also reported the capability of SmbP to facilitate the solubility of heterogeneous recombinant proteins expressed in the cytoplasmic and periplasmic membrane region of *E. coli* (Perez-Perez *et al*., 2021; Santos *et al*., 2019). The signal sequence in SmbP is reliable and ensures efficient localization of expressed recombinant proteins and as well modulates the transport of proteins to microbial membrane regions where disulfide bond formation could be initiated for proper protein folding (Gomez-Lugo *et al*., 2014; Perez-Perez *et al*., 2021; Santos *et al*., 2019).

2.14.7 CusF3H+

The fusion protein CusF3H+ was the second protein tag characterized from our previous studies. This protein is an enhanced version of the wild type of *Escherichia coli* periplasmic membrane protein named CusF, which constituted the bacterium CusCFBA system that allows the eruption of toxic metal Cu(I) ion and resistance to Ag(I) ions from the cytoplasmic and periplasmic membrane of bacteria cell. The enhanced version CusF3H+ has a modified N-terminal sequence which harbors three more histidine (3H+) amino acid residues constituting a molecular size of 9.9 kDa as compared to the wild type of size 9.57 kDa. The applications of CusF3H+ as fusion protein for the purification of recombinant proteins of therapeutic importance have been reported in our numerous

research publications (Gomez-Lugo *et al*., 2014; Mesa-Pereira *et al*., 2018; Perez-Perez *et al*., 2021; Santos *et al*., 2019).

2.15 Production of recombinant proteins like AMPs and others

Bacterial strains are highly considered the first-choice microorganisms for recombinant protein production owing to their fast growth kinetics with doubling time about 20 min, large periplasmic space, simple but reliable protein secretion mechanisms and the presence of molecular chaperones within the periplasmic space which allows for efficient protein folding into native secondary structures without proteolytic degradation thereby retaining the bioactivity of expressed proteins even in crude cell lysates (Mohammed and Yousuf, 2018). Although other microorganisms including *Saccharomyces cerevisiae*, *Pichia pastoris* and other filamentous fungi considered as excellent protein secretors have been extensively exploited in the production of heterogeneous recombinant high-value protein (HVP). The quest and high demand for recombinant AMP of antibacterial properties has spur the use of bacteria cells as expression system extensively exploited in both research and development purposes coupled with the use of less sophisticated techniques and chemical reagents for purification and the ease of bacteria transformation with recombinant plasmid vectors harboring the gene(s) encoding the target protein. The application of genetically modified microbial expression systems like *Escherichia coli* BL21(DE3), *E. coli* C41(DE3), *E. coli* K12, *E. coli* SHuffle T7(DE3), *E. coli* Rosettae facilitated the intracellular and extracellular secretion of rAMPs, reduction microbial bioprocess complexity and improved the product quality (Rosano and Ceccarelli, 2014). A study by Collins *et al*. (2013) reported the recombinant production of silk-elastin-like proteins (SELPs) in *E. coli* BL21(DE3) microbial system yielding a 500 mg/L of final

purified SELP under the following expression conditions of 4 hour incubation at 37°C with 200 rpm rotation and 0.5 mM IPTG for expression induction after transformation with pET (ampicillin selective marker). AMP like LL-37 has been successfully expressed in *E. coli* BL21(DE3) after transformation with pET30a (kanamycin selective marker) at a 4 h incubation at 37°C, 220 rpm with a 0.1 mM final IPTG concentration. A 95% purity of the target peptide was obtained showing a promising bioactivity against antibiotic-resistance *Staphylococcus aureus* and *Escherichia coli* suggesting that the chosen microbial expression system has produced the peptide in its native form (Perez-Perez *et al*., 2021). It was revealed that the replacement of fusion tag SmbP with three different tags like CusF and PelB for secretion and transport via the sec pathway and Tor A for transportation via the tat pathway has facilitated an increase in red fluorescence protein (RFP) level and quality as compared to SmbP tag as expressed in the *E. coli* BL21(DE3). Cholesterol oxidase has been expressed in *E. coli* microbial system as recombinant protein with maintained bioactivity after series of expression protocol optimization like host strain from *Streptomyces* spp. to *E. coli*, culture media, and IPTG induction concentration. The optimized recombinant production protocol showed an increase of yield from 3.2 to 158 U/L after column nickel affinity chromatographic purification (Fazaeli *et al*., 2018).

2.16 Purification of recombinant AMPs by Immobilized Metal Affinity Chromatography (IMAC)

IMAC is a reliable protein purification technique that is extensively employed in research and development (R&D) laboratories to purify synthetic and recombinant proteins associated with protein tags. This technique relies on the strong affinity of fusion proteins commonly referred to as protein tags such as small metal binding proteins SmbP, CusF, CusF3H+, Glutathione S-transferases (GST), Maltose binding protein (MBP), FLAG

peptide, and the Hexa-histidine peptide (6X His tag) genetically engineered at the N or C-terminal with the amino acid residues of the target protein thereby allowing target recombinant proteins to be expressed as recombinant fusion proteins with respective tags (Adamíková *et al*., 2019; Riguero *et al*., 2020). Although, chromatographic technique comes with some purification challenges which might compromise the purity and yield of proteins considering the type of column resin and the metal chelators employed, the method is highly reliable coupled with efficient protein purity and yield as reported by several studies (Adamíková *et al*., 2019; Afzal *et al*., 2021; Riguero *et al*., 2020). Recently new IMAC techniques are being developed and used to address chromatographic purification impacts on recombinant proteins of therapeutic applications. This includes the use of column resins coated with prominent metal chelators like iminodiacetic acid (IDA) and nitrilotriacetic acid (NTA) permitting the conjugation of resins with affinity metal ions such as Cu(II), Zn(II), and Ni(II). The affinity of protein tags to the metal ions on the column resins allows for the chromatographic separation of expressed recombinant proteins associated with above mentioned fusion proteins (Santos *et al*., 2019). Riguero *et al*. (2020), reported that the use of IDA charged with Cu(II) yielded a higher purity and quantity of His-tagged AMP recombinant proteins with maintained bioactivity properties as compared to other metal chelators. It was revealed that IDA chelators ensure the diversified usage of different sorbent chemicals including HiTrap chelating HP, TSK chelate-5WP, and the Poros 20MC. The HiTrap chelating HP columns charged with Zn(II) or Ni(II) ions have been extensively use in the purification of rAMPs (recombinant AMPs) like LL-37 and Bin1b via IMAC with a promising 95% protein purity (Perez-Perez *et al*., 2021). SmbP, a fusion protein isolated from the bacterium *Nitosomonas europapaea* has been used in the IMAC purification of green fluorescence protein (GFP) expressed in

Escherichia coli as SmbP-GFP. It has been reported that IMAC column resin charged with Ni(II) ions ensure efficient affinity to SmbP (9.9 kDa) facilitating the Chromatographic purification of SmbP-GFP with a higher yield and purity (Vargas-Cortez *et al*., 2016). The protein tags like CusF3H+, SmbP, PelB_SmbP, and the TorA_SmbP have allowed for reliable purification of recombinant GFP (rGFP) via IMAC with the application of HiTrap column resins charges with Ni(II). It was revealed that these protein tags facilitated the expression of rGFP as soluble fractions without formation of inclusion bodies known to be misfolded proteins (Gomez-Lugo *et al*., 2014). Mo *et al*. (2018), demonstrated a successful IMAC purification of AMP AP2 expressed as recombinant protein (smt3AP2) using the SUMO (small ubiquitin-like modifier) fusion technology with hexa-histidine (6X His) modification at the N-terminal which permitted the purification of AP2 in its native form thereby retaining the antibacterial bioactivity of the peptide after cleavage of the SUMO-tag via endopeptidase specific SUMO proteases and yielded 2.7 mg/L of purified AP2. In the process the soluble lysate of cells expressing smt3AP2 were passed through HiTrap columns conjugated with affinity metal ions allowing the recombinant smt3AP2 to bind HiTrap-charged columns thereby allowing unbounded protein counterparts without protein tags to be eluted as column flow-through. The bounded smt3AP2 were eluted as purified peptide with imidazole at varying concentrations as reported. Studies has it that for an IMAC purification the cellular processing buffers such as lysing buffer must be devoid of chemical metal chelators like Ethylenediaminetetraacetic acid (EDTA) which are known as metal ion scavengers leading to poor and low yield in IMAC purification (Kesidis *et al*., 2020; Lee *et al*., 2011; Perez-Perez *et al*., 2021; Seyedjavadi *et al*., 2021a).

CHAPTER THREE

3.0 MATERIALS AND METHODS

3.1 Study Area

This research study was conducted at the Protein Expression and Purification Laboratory of the Postgraduate Faculty of Chemical Sciences, Autonomous University of Nuevo Leon (UANL), Mexico. All experimental methods right from gene design, propagation, molecular cloning, plasmid construct design and transformation, protein expression, purification, and finally bioactivity assays were carried out in the Protein Expression and Purification Laboratory, except for synthesis of synthetic DNA fragments encoding the target recombinant hybrid peptide. All wet laboratory experiments were conducted under aseptic conditions with standard laboratory protocols and practice supervised by the principal investigator. Laboratory wastes generated were disposed according to the guidelines described by the Postgraduate Faculty of Chemical Sciences (FCQ, UANL, MX).

3.2 Design and synthesis of LL-37_Renalexin gene (Hybrid AMP)

The amino acid sequence of the hybrid antimicrobial peptide LL-37_Renalexin was designed according to the mature primary amino acid sequences of LL-37 and Renalexin retrieved from AMP database (https://APD3.unmc.edu/structure) with the accession numbers AP0030/2K60 for LL-37 and AP00513/P39084 for Renalexin. The sequences were modified based on preferential codon usage in *E. coli* expression systems (http://genomes.urv.es/CAIcal). The entire amino acid sequence was flanked at respective sites on the designed sequence with the amino acid sequences of the following: protein tags SmbP and CusF3H+, enterokinase, GS peptide linker, *Nde*1, *Kpn*1, and *Xho*1

restriction enzyme sites. The complete amino acid sequence of the hybrid peptide LL-37_Renalexin with its flanking regions was sent to GenScript Biotech (Piscataway, USA) for the synthesis of a synthetic DNA (492 bp) fragment. The synthetic DNA was synthesized as a clone into the plasmid pUC57 (pUC57_SmbP_LL37-Renalexin) and a lyophilized sample at a concentration of 4 µg was transported to the Protein Expression and Purification Laboratory, UANL.

3.3 Plasmid propagation and purification

A stock solution of plasmid pUC57_SmbP_LL37-Renalexin at a concentration of 144.1 ng/µl was prepared by dissolving the lyophilized sample in 50 µl of DNase-free molecular grade water. A 10 ng/µl working solution of plasmids pUC57_SmbP_LL-37_Renalexin, pET30a+_SmbP, and pET30a+_CusF3H+ were separately transformed into *E. coli* DH5α calcium competent cells for in vivo propagation. 30 µl *E. coli* DH5α cells were mixed with 2 µl of the respective plasmids pUC57_LL-37_Renalexin, pET30a_SmbP, and pET30a_CusF3H+ in a separate new 1.5 ml Eppendorf tubes and incubated on ice for 30min, after incubation cells were heat shocked for transformation at 42°C in a water bath for 45 s followed by 3 min incubation on ice. A negative transformation control reaction contained 30 µl *E. coli* DH5α competent cells plus 2 µl deionized MQ water. Transformants cells were re-energized in 800 µl Luria-Bertani (LB) broth by incubation at 37°C, 200 rpm for an hour. A 50 µl concentrated cell suspensions were collected after centrifugation at 13,000 rpm for 5 min at 4°C and spread on LB agar with ampicillin (50 µg/ml) for pUC57_SmbP_LL-37_Renalexin Transformants and LB agar with kanamycin (50 µg/ml) for pET30a+_SmbP and pET30a+_CusF3H+ Transformants. Inoculated LB agar plates were incubated at 37°C for 16 h. The overnight cultured plates with colonies

of transformed *E. coli* DH5α cells were selected for plasmid propagation. Single colonies were picked and inoculated into 5 ml LB/kanamycin and LB/ampicillin (30 µg/ml) broth respectively and incubated at 37°C, 200 rpm, for 16 h. Cell pellets were collected from overnight culture by centrifugation (Legend Microcentrifuge 17R, Thermo Scientific) at 13,000 rpm for 1 min and lysed. The cell lysate was employed for plasmid purification using the DNA-spin^{TM} plasmid purification kit (*iNtRON* Biotechnology, Boston, USA) with the following reagent solutions; cell resuspension buffer, lysing buffer, neutralization buffer, washing buffer, and elution buffer supplied by the manufacturer. The purity and concentration of the eluted plasmids was analyzed using the Nanodrop 2000 spectrophotometer (Thermo Scientific) (Gomez-Lugo *et al*., 2014; Perez-Perez *et al*., 2021).

3.4 Restriction digestion of the purified plasmids

Restriction enzyme digestion of purified plasmid DNA; pUC57_SmbP_LL-37_Renalexin, pET30a+_SmbP, and pET30a+_CusF3H+ was carried out to cleave the circular plasmids into linear DNA molecules using restriction enzymes *Nde*1 (**5'-CATATG-3'**), *Kpn1* (**5'-GGTACC-3'**), and *Xho*1 (**5'CTCGAG-3'**) yielding a 5' sticky ends after cleavage. A 50 µl restriction reaction volume was performed with the following components: 10 Units of each restriction enzyme *Nde*1, *Kpn1* and *Xho*1 (New England Biolabs, Ipswich, USA), 2 µg of each plasmid DNA (DNA template), 10X NEB buffer, and molecular grade water (Table 3.1, 3.2 and 3.3). Reaction tubes with the first restriction enzyme *Nde*1 were incubated at 37°C for one and half hours, followed by the addition of the second enzyme *Xho*1/*Kpn1* with subsequent incubation under the same

conditions. Restriction enzyme inactivation was achieved following the manufacturer's protocol by incubation of reaction tubes in a water bath at 65°C for 20 min.

Table 3. 1: Restriction enzyme digestion of pUC57_SmbP_LL-37_Renalexin plasmid DNA.

Components	**Reaction volume (50 µl)**	**Final concentration**
DNase-free water	37.4 µl	-
10X NEB buffer	5 µl	1 X
*Nde*1	1 µl	10 Units
*Xho*1	1 µl	10 Units
pUC57_SmbP_LL-37_Renalexin	5.6 µl	40 ng/ µl

Table 3. 2: Restriction enzyme digestion of pET30a +_SmbP plasmid DNA.

Component	**Reaction volume (50 µl)**	**Final concentration**
DNase-free water	24.4 µl	-
10X NEB buffer	5 µl	1 X
*Nde*1	1 µl	10 Units
*Xho*1	1 µl	10 Units
pET30a_SmbP	18.6 µl	40 ng/ µl

Table 3. 3: Restriction enzyme digestion of pET30a +_CusF3H+ plasmid DNA.

Component	**Reaction volume (50 µl)**	**Final concentration**
DNase-free water	22.6 µl	-
10X NEB buffer	5 µl	1 X
Kpn1	1 µl	10 Units
*Xho*1	1 µl	10 Units
pET30a_CusF3H+	20.4 µl	40 ng/ µl

3.5 Electrophoresis and visualization of restriction digestion products

The restriction digestion products were analyzed on a 1% agarose gel stained with Ethidium bromide (EtBr). The agarose gel was prepared as follows; 0.3 g agarose powder (Molecular grade) was dissolved in 30 ml of 1X Tris-acetate−EDTA (TAE) buffer under microwave (RIVAL^{TM} Microwave) heat for 90 s. The dissolved gel was mixed with 5 µl Ethidium bromide at a final concentration 1 µg/ml (for DNA nucleotides intercalation and visualization). The mixture was gently cast into a gel casting tray with the appropriate well comb fixed. The gel was allowed to solidify at room temperature for 25 min. Casted agarose gel was then used for electrophoresis analysis of digested plasmid DNAs under 70 V for 5 min followed by 110 V for 25 min and visualized under UV light (UVP White/UV Transilluminator). All the 50 µl reaction volumes were loaded into the wells of the gel with a ten-kilo base (10 kb) DNA molecular ladder (New England Biolabs) used as marker for fragment size estimation.

3.6 Digested DNA fragment purifications and quantification

For purification of the target DNA fragments cut from the agarose gel, the MEGAquick-spin fragment DNA purification kit (iNtRON Biotechnology) with its reaction reagents was employed following the manufacturer's protocol with slight modifications that suit the goal of this study. A 300 – 400 mg of target DNA gel fragments (LL-37_Renalexin, pET30a+_SmbP, and pET30a+_CusF3H+) with a 5'overhangs were cut from the agarose gel into separate new 1.5 ml Eppendorf tubes with 600 µl BNL buffer, and dissolved at 55°C for 10 – 15 min. Dissolved samples were transferred into a 1 ml fragment DNA purification column and centrifuged at 13,000 rpm for 1 min, column flow-through was discarded and columns were washed with 700 µl washing buffer by centrifugation at 13,000 rpm for 1 min, column flow-through was discarded. Columns were dried by centrifugation under the same conditions to remove the access washing buffer. Elution of respective DNA fragments (LL-37_Renalexin, pET30a+_SmbP, and pET30a+_CusF3H+) was performed with 30 – 50 µl DNase-free water into sterilized 1.5 ml Eppendorf tubes. The concentration of the purified DNA fragments was quantified using the Nanodrop 2000 spectrophotometer (Thermofisher scientific) and samples were stored at – 20°C until required.

3.7 Recombinant expression plasmid DNA construct design

3.7.1 In-silico ligation simulation

Prior to performing wet laboratory experiment for the molecular ligation of purified digested plasmid with the gene construct that encodes for the target peptide, an in-silico simulation was analyzed using the SnapGene molecular cloning tool (www.SnapGene6.2.com). The DNA nucleotide sequence map of the plasmid vector

pET30a+ was retrieved and downloaded from the Novagen Sigma Aldrich webpage (www.Novagen.com) and imported into SnapGene tool for analysis. The restriction enzyme digestion simulation was performed with the enzymes *Nde*1 and *Xho*1 which yielded a sticky end with a 5' overhang. The synthetic DNA nucleotide sequence of the gene that encodes the peptide SmbP_LL-37_Renalexin and CusF3H+_LL-37_Renalexin were respectively imported into the SnapGene tool as the DNA inserts. The same restriction enzymes were employed to cleave the DNA inserts which also resulted in a sticky end with 5' overhangs on both ends of the synthetic DNA strands. The insertion of the synthetic DNA insert into the linearized plasmid vectors was simulated producing a complete circular plasmid construct with the synthetic DNA insert at the expected position on the plasmid.

3.7.2 Molecular DNA ligation

Molecular ligation reactions were carried out for the design of two recombinant plasmid DNA constructs that harbor the synthetic DNA insert which encodes the hybrid antimicrobial peptide LL-37_Renalexin. The restriction digested DNA insert fragment was cloned into the digested plasmid vectors pET30a+_CusF3H+, and pET30a+_SmbP via molecular ligation reaction using the T4 DNA ligase (New England Biolabs), with pET30a+ acting as the plasmid vector, CusF3H+ and SmbP acting as fusion tags. pET30a+_CusF3H+_LL-37_Renalexin, and pET30a+_SmbP_LL-37_Renalexin were the designed recombinant expression plasmid vectors, respectively. A 20 µl reaction volume of ligation was carried out in a 1.5 ml Eppendorf tubes with the following reaction components; LL-37_Renalexin DNA template (DNA insert), plasmid vector pET30a+_CusF3H+ and pET30a+_SmbP, 10X buffer, T4 DNA ligase, and DNase free

water (Table 3.4, and 3.5). A master premix was prepared of which 17 µl was pipetted into four different 1.5 ml Eppendorf tubes followed by the addition of DNA template and water to a 20 µl final volume. The reaction tubes were incubated at room temperature (25°C) for 2 h and subsequently incubated at 4°C for 16 h overnight.

Table 3. 4: Molecular ligation of pET30a+_CusF3H+_LL-37_Renalexin expression vector.

Components	**Tube 1**	**Tube 2**	**Tube 3**	**Tube 4**
DNase-free water	15 µl	14 µl	13 µl	12 µl
10 X Buffer	2 µl	2 µl	2 µl	2 µl
T4 DNA ligase	1 µl	1 µl	1 µl	1 µl
pET30a+_CusF3H+	2 µl	2 µl	2 µl	2 µl
LL-37_Renalexin	0 µl	1 µl	2 µl	3 µl

Table 3. 5: Molecular ligation of pET30a+_SmbP_LL-37_Renalexin expression vector.

Components	**Tube 1**	**Tube 2**	**Tube 3**	**Tube 4**
DNase-free water	15 µl	14 µl	13 µl	12 µl
10 X Buffer	2 µl	2 µl	2 µl	2 µl
T4 DNA ligase	1 µl	1 µl	1 µl	1 µl
pET30a+_SmbP	2 µl	2 µl	2 µl	2 µl
LL-37_Renalexin	0 µl	1 µl	2 µl	3 µl

3.8 Propagation and purification of designed recombinant plasmid constructs

In vivo propagation of the designed plasmid constructs was performed in transformed *E. coli* DH5α by heat shock method as described above. Briefly, a 5 µl of each plasmid construct was incubated on ice with 30 µl of *E. coli* DH5α competent cells in 1.5 ml Eppendorf tubes respectively. Transformed *E. coli* DH5α competent cells were re-energized in 800 µl LB broth by incubation at 37°C for 1 h. A 50 µl of cell pellet suspensions were aseptically spread on LB/kanamycin (30 µg/ml) agar plates and cultured at 37°C for overnight. The culture plates showing the higher population of transformed *E. coli* DH5α colonies were selected as isolates harboring the most efficiently cloned recombinant plasmid constructs pET30a+_CusF3H+_LL-37_Renalexin, and pET30a+_SmbP_LL-37_Renalexin respectively. Single colonies were picked from each selected plate with respective plasmid construct, sub-cultured in 5 ml LB broth with kanamycin (30 µg/ml), and incubated at 37°C, 220 rpm for 16 h. After overnight culture cell pellets were collected by centrifugation at 13, 000 rpm for 10 min. The harvested cell pellets were lysed, and the lysate was used as a source for plasmid purification using the DNA-spin^{TM} plasmid purification kit (*iNtRON* Biotechnology), following the manufacturer's procedures. Purified plasmid constructs were quantified using the Nanodrop 2000 spectrophotometer (Thermofisher scientific).

3.9 Confirmation of designed recombinant plasmid construct

3.9.1 Polymerase Chain Reaction (PCR)

For the identification and confirmation of the purified recombinant plasmid constructs harboring the synthetic DNA insert (gene) encoding for the hybrid AMP CusF3H+_LL-37_Renalexin and SmbP_LL-37_Renalexin respectively. Conventional colony-based

polymerase chain reaction (PCR) analysis was carried out in a 20 µl reaction volume. For accuracy and specificity of gene amplification, the T7 promoter and T7 terminator sequences that flank the ends of the target gene were employed as primer hybridization sites. A 5'-T7 promoter forward primer (5'-TAATACGACTCACTATAGGG-3') and a 3'-T7 terminator reversed primer (3'-GCTAGTTATTGCTCACGG-5') were used for polymerase chain reaction with the following components DNase-free water, 5 mM dNTPs, 10 ng plasmid DNA template, 0.5 µM primer, 5 U Taq polymerase (Table 3.6, and 3.7). The reaction conditions were carried out as follows, initial denaturation at 95°C for 1 min, denaturation at 95°C for 30 s, primer annealing at 55°C for 45 s, elongation at 72°C for 50 s and final elongations at 72°C for 5 min, 32 reaction cycles were carried out. Samples were stored at 4°C until required for further use.

Table 3. 6: PCR confirmation of pET30a +_CusF3H+_LL-37_Renalexin plasmid construct.

Components	**Reaction volume (20µl)**	**concentration**
DNase-free water	13 µl	12 µl
10 X Buffer	2 µl	1X
dNTPs	1 µl	5 mM
DNA template 1	1 µl	10 ng
T7 Forward primer	1 µl	0.5 µM
T7 Reverse primer	1 µl	0.5 µM
Taq polymerase	1 µl	5 Units

DNA template 1: pET30a+_CusF3H+_LL-37_Renalexin

Table 3. 7: PCR confirmation of pET30a+_SmbP_ LL-37_Renalexin plasmid construct.

Components	Reaction volume (20µl)	Concentration
DNase-free water	13 µl	12 µl
10 X Buffer	2 µl	1X
dNTPs	1 µl	5 Mm
DNA template 2	1 µl	10 ng
T7 Forward primer	1 µl	0.5 µM
T7 Reverse primer	1 µl	0.5 µM
Taq polymerase	1 µl	5 Unit

DNA template 2: pET30a+_SmbP+_LL-37_Renalexin

3.9.2 Visualization of PCR amplicons

The PCR amplicons were viewed on a 1% agarose gel stained with Ethidium bromide (EtBr). Agarose gel was prepared as follows, 0.3 g agarose powder (molecular grade) was dissolved in 30 ml of 1X Tris-acetate−EDTA (TAE) buffer under microwave (RIVAL$_{TM}$ Microwave) heat for 90 s. the dissolved gel was mixed with 5 µl Ethidium bromide (1 µg/ml), appropriately mixed by gentle shaking and subsequently casted into gel casting tray with comb fixed. The gel was allowed to solidify at room temperature for 30 min. Casted agarose gel was then used for electrophoresis analysis of the PCR amplicons under 70 V for 5 min followed by 110 V for 25 min. The stained gel was visualized under UV light (UVP White/UV Transilluminator). A 10 kb DNA molecule (New England Biolabs Inc.) was used as DNA marker for fragment size estimation.

3.9.3 Sequencing of designed plasmid constructs

In our attempt to further confirm the DNA nucleotide accuracy and specificity of the synthetic DNA inserts CusF3H+_LL-37_Renalexin and SmbP_LL-37_Renalexin in the designed recombinant plasmid constructs named above. The Sanger DNA sequencing method was employed and carried out at the DNA synthesis and sequencing laboratory of the Institute of Biotechnology, National Autonomous University of Mexico (UNAM). A 16 µl sample volume consisting of 15 µl of each plasmid construct at a final concentration of 600 ng, and a 1 µl T7 promoter forward primer at 10 µM concentration was prepared in a 1.5 ml Eppendorf tube and transported on ice to the DNA sequencing laboratory at UNAM for Sanger sequencing.

3.10 Small-scale expression of recombinant fusion proteins

For the small-scale expression and analysis of the recombinant fusion proteins CusF3H+_LL-37_Renalexin and SmbP_LL-37_Renalexin, a fresh single colony of transformed *E. coli* BL21(DE3) and *E. coli* SHuffle T7(DE3) competent cells harboring the expression vectors pET30a+_CusF3H+_LL-37_Renalexin and pET30a+_SmbP_LL-37_Renalexin, respectively were inoculated into 4 ml LB/kanamycin (30 µg/ml) medium in a 50 ml test tubes. The cultures were incubated at 37°C with shaking at 220rpm for about 3 – 4 h until an optical cell density (OD_{600nm}) of 0.4 – 0.6 was obtained. Cultures were allowed to cool at room temperature (RT) and peptide expression was induced with Isopropyl-β-D-thiogalactopyranoside (IPTG), 4 µl of 1M IPTG was added per tube at a final concentration of 1mM. For efficient gene induction and peptide expression, induced culture cells were incubated at 25°C, 220 rpm for overnight expression.

Cell pellets were harvested from 2 ml of the overnight cultures by centrifugation at 13,000 rpm for 10 min at 4°C. *E. coli* BL21(DE3) and *E. coli* SHuffle T7(DE3) pellets were resuspended in a 150 µl lysis buffer (50 mM Tris-HCl pH 8.0) and lysed with 150 µl glass beads (0.1 mm) by vortexing on ice for 5 min. The clear supernatant was collected into a new clean 1.5 ml Eppendorf tube as the soluble fraction (SF) of the cell lysate. To obtain the insoluble fraction of the cell pellets that serve as a source of inclusion bodies, the lysed pellets were washed twice in 150 µl distilled water then resuspended in 150 µl of 8 M Urea solution, vortex, and heated at 80°C for 10 min in a water bath. The mixture was then centrifuged, and the supernatant collected as insoluble fraction (IF) of the lysed cells.

3.10.1 Sodium dodecyl sulfate polyacrylamide gel electrophoresis (SDS-PAGE) analysis of small-scale expression.

For SDS–PAGE analysis and characterization of the expressed CusF3H+_LL-37_Renalexin and SmbP_LL-37_Renalexin fusion protein, the soluble and insoluble protein fractions were mixed (5 volume of protein sample: 1 volume of sample buffer) with 6X sample buffer (4 ml of 100% glycerol, 2.4 ml of 1 M Tris buffer at pH 6.8, 0.8 g of SDS, 0.5 ml of β-mercaptoethanol, 4 mg of Bromophenol blue) at a final buffer concentration of 1X. The mixture was incubated at 80°C for 10 min in a water bath to facilitate the complete denaturation of the secondary protein structure into linear polypeptide chain for efficient analysis, characterization, and mobility in the gel. A 15% resolving gel and a 4% stacking gel were prepared with the following compositions, resolving gel (1.825 ml distilled water, 1.25 ml of 1.5 M Tris resolving gel buffer pH 8.8, 1.875 ml of 40% acrylamide/bisacrylamide solution, 50 µl of 10% SDS solution, 5 µl of TEMED, and 40 µl of 10% Ammonium persulfate) and stacking gel (1.6 ml distilled water, 0.62 ml of 0.5 M Tris stacking gel buffer pH 6.8, 0.25 ml of 40%

acrylamide/bisacrylamide solution, 50 µl of 10% SDS solution, 10 µl of TEMED, and 40 µl of 10% Ammonium persulfate). The resolving gel was first cast into a two vertical glass slides and covered with 200 µl Iso-butanol to facilitate the solidification and to prevent air bubbles formation in the gel. After 20 min solidification of the resolving gel, the Iso-butanol was removed, and the gel layer was then rinsed three times with distilled water before the 4% stacking gel was cast with a 15-well comb fixed. A total of 5 µl of prepared protein samples were loaded onto the gel, and a 3 µl of a 120 kDa standard protein (PAGE−MASTER protein standard plus) was employed as the molecular marker for protein size characterization. The gel electrophoresis analysis was run under the following conditions, 80 volts for 10 min followed by 120 volts for 1.3 h. After the gel electrophoresis, the gel was then washed in distilled water for 4 min and subsequently stained in 80 ml SDS staining solution (0.1% Coomassie brilliant blue R250, 50% methanol, 10% glacial acetic acid) for overnight. After overnight staining, the gel was washed twice in distilled water for 5 min and destained for 45min in an 80 ml destaining solution (40% methanol, 10% glacial acetic acid). The stained protein bands in the gel were visualized under white light (UVP White/UV Transilluminator).

3.11 Large-scale expression of recombinant fusion proteins

For the large-scale expression of recombinant fusion proteins CusF3H+_LL-37_Renalexin and SmbP_LL-37_Renalexin, a 5 ml LB/kanamycin (30 µg/ml) broth was inoculated with 5 µl of transformed *E. coli* Bl21(DE3) and *E. coli* SHuffle T7(DE3) competent stock cultures respectively and incubated at 37°C with 220 rpm shaking for overnight. 125 µl overnight cultures were inoculated into 125 ml LB/kanamycin (30 µg/ml) broth in eight 500 ml capacity baffled flasks constituting a total 1-liter (1L)

expression volume. The inoculated culture flasks were incubated at 37°C with 220 rpm shaking for 3 − 4 h approximately until an optical cell density (OD_{600nm}) of 0.4−0.6 was obtained (logarithmic growth phase). Recombinant peptide expression was induced by the addition of 125 µl of 1M IPTG (final concentration of 1mM) per flask. The induced flasks were then incubated at 25°C with 220 rpm shaking for 16 h overnight. For the isolation of expressed recombinant peptide from the periplasmic space of *E. coli* Bl21(DE3) and *E. coli* SHuffle T7(DE3). Cell pellets were collected from the 1-liter overnight cultures into 50ml Eppendorf falcon tubes by centrifugation at 8500 g for 10min at 4°C. Cell pellets were resuspended in a 10ml equilibration buffer (500 mM NaCl, 50 mM Tris-HCl pH 8.0) by vortexing for a few minutes. A single drop of antifoam was added to prevent over viscosity of the suspended cells which may compromise the lysing process. Resuspended cell pellets were mechanically lysed by vortexing with 15 ml of 0.1 mm glass beads for about 15 min on ice with 5 min intermittent cooling which prevents protein degradation. Clear soluble cell lysate was collected as recombinant peptide by centrifugation at 8500 g for 15 min at 4°C and used for peptide purification.

3.12 Purification of recombinant hybrid peptide (Chimeric protein) by Immobilized metal affinity chromatography (IMAC)

For purification of the fusion peptide SmbP_LL-37_Renalexin and CusF3H+_LL-37_Renalexin, the ÄKTA Prime Plus system (GE Healthcare systems) was employed for fast protein liquid chromatography (FPLC) by metal affinity chromatography owing to the strong metal ion affinity of our tag proteins SmbP and CusF3H+ to nickel, copper, and zinc metal ions. A 1 ml HisTrap FF column charged with Ni(II) ions was used to isolate the target recombinant peptide form the pool of cellular proteins present in the soluble lysate collected. The column was equilibrated with 5 column volumes (CV) of

equilibrating buffer (500 mM NaCl, 50 mM Tris-HCl pH 8.0) and was loaded afterward with 45-50 ml of soluble cell lysate (Protein sample) under the conditions of 0.5 MPa pressure and 0.5 ml/min flowrate. After loading the protein sample, the column was washed with 3CV of washing buffer (500 mM NaCl, 2.5 mM Imidazole, 50 mM Tris-HCl pH 8.0); this ensures the removal of untargeted proteins from the column. The recombinant hybrid fusion peptide was eluted from the column by gradient elution with an elution buffer (500 mM NaCl, 200 mM Imidazole, 50 mM Tris-HCl pH 8.0). 40 tubes of elution fractions (1 ml/elution fraction) were collected into a 1.5 ml Eppendorf tube under the conditions of 0.5 ml/min flowrate, 0.5 MPa pressure. 10 µl of each elution fraction was analyzed on a 15% SDS-PAGE and the purity of protein bands was measured by densitometry using ImageJ software (v.2.0). Fractions showing protein bands of target recombinant peptide were pooled together in a 6 cm dialysis membrane and dialyzed against 1X PBS pH 7.2 (10 mM phosphate-buffered saline solution) for an hour with gentle shaking on a magnetic stirrer at room temperature. Subsequently, the dialysis buffer was changed, and the dialysis set up was incubated at 4°C overnight. The concentration of the dialyzed recombinant fusion peptide was measured and quantified by Bradford analysis as described by (Bradford, 1976; Colyer and Walker, 1996; Wingfield, 2007). Briefly, the Bovine Serum Albumin (BSA) as protein standard calibration curve was performed in milligram per milliliter (mg/ml) with concentrations ranging from 1.3 – 0.1 mg/ml. A 10 µl of BSA and the purified recombinant fusion peptide were separately mixed in a 96-well microtiter plate with 200 µl Bradford reagent (50 mg Coomassie brilliant blue G-250, Methanol and 85% Phosphoric acid) and incubated in the dark for 5 – 10 min, absorbance readings were taken at 595 nm. The calibration curve for BSA was established

in Microsoft excel and the concentration of purified recombinant fusion peptide was estimated using the linear equation of the standard BSA calibration curve.

3.13 Enterokinase cleavage and LL-37_Renalexin purification.

For the removal of protein tags SmbP and CusF3H+ from the purified recombinant fusion peptide SmbP_LL-37_Renalexin and CusF3H+_LL-37_Renalexin with enterokinase site between the protein tag and the hybrid LL-37_Renalexin. A 1mg of the purified fusion protein was mixed with 20 Units of enterokinase (5 U/µl) in a 15 ml Eppendorf tube and incubated at room temperature (25°C, RT) for overnight. After the overnight incubation, the enterokinase enzyme (New England Biolabs, USA) was inactivated by 3 h incubation at -20°C. A 10µl of cleavage mixture was analysis on a 18% and 15% Tricine SDS-PAGE. In purifying the released hybrid peptide LL-37_Renalexin from the protein tags, a 1.0 x10 cm chromatographic syringe column was loaded with 1 ml of agarose resins charged with 1 M Ni(II) ion. The column was equilibrated with 10 column volumes (10 CV) of 1X PBS pH 7.2 and the enterokinase cleaved reaction mixture was loaded, mixed with Ni(II) charged agarose resins and incubated at 4°C for 1.5 h allowing for efficient binding of protein tags to the affinity column. After incubation the column flow-through was collected as tagged-free hybrid AMP LL-37_Renalexin and the protein tags were eluted after subsequent incubation of the column with elution buffer (500 mM NaCl, 200 mM Imidazole, 50 mM Tris-HCl pH 8.0). The collected tagged-free hybrid peptide was analyzed on a 15% Tricine SDS-PAGE. The concentration of purified LL-37_Renalexin (tagged-free) was estimated by Bradford analysis and Nanodrop absorbance readings at A_{280nm} (Perez-Perez *et al*., 2021; Santos *et al*., 2019).

3.14 Antimicrobial activity assay of recombinant hybrid peptide LL-37_Renalexin (tag-free)

3.14.1 Culture media

The microbial cultivation of bacteria clinical isolates, as well as inoculum suspension preparations, and antimicrobial activity tests were performed using the following culture media and buffers: (1) Tryptic soy broth (TSB); Tryptone (pancreatic digest of casein) 17.0 g, Soytone (peptic digest of soybean) 3.0 g, Glucose (dextrose) 2.5 g, Sodium chloride 5.0 g, and Dipotassium phosphate 2.5 g pH 7.3. (2) Bacteriological agar, Mueller Hinton Agar (MHA); Beef extract 2.0 g, Acid Hydrolysate of casein 17.5 g, Starch 1.5 g, Agar 17.0 g pH 7.3. (3) Phosphate buffered saline (PBS); Sodium chloride 8 g, Potassium chloride 0.2 g, Sodium phosphate dibasic 1.44 g, Potassium phosphate monobasic 0.245 g pH 7.4.

3.14.2 Inoculum preparation

Single colonies of test bacteria clinical isolates were cultured in 5 ml TSB and incubated at 37°C, 220 rpm for 16 h. 20 µl of overnight culture was inoculated into 5 ml TSB and incubated at 37°C with shaking until an optical cell density (OD_{600nm}) of 0.8 – 1.0 was obtained (mid-logarithmic growth). Cells at log growth phase were serially diluted in 1X PBS buffer and dilution suspensions at 1x 10^5 CFU/ml equivalent to 0.5 McFarland turbidity standard were employed for antimicrobial assay.

3.14.3 Dose-response assay: Minimum inhibitory concentration (MIC) determination

The antimicrobial activity of the hybrid peptide was evaluated against gram-positive and gram-negative bacteria clinical isolates of *Staphylococcus aureus*, *Escherichia coli*, Methicillin-resistant *Staphylococcus aureus*, and *Klebsiella pneumoniae* from UANL

University Hospital. The minimum inhibitory concentrations against the test pathogens were ascertained and estimated in accordance with modification of the National Committee for Clinical Laboratory standards (NCCLS) for broth microdilution method. Briefly, bacteria cell cultures in the mid-log growth phase in TSB were serially diluted in 1x PBS buffer to 1 x 10^5 CFU/ml. A 2-fold broth microdilution assay was performed in a 96-well microtiter plate with a 200 µl assay volume per well composed of 100 µl diluted peptide at concentrations ranging from 0.5 – 33 µM, 80 µl bacteria suspensions and 20 µl TSB broth. The plate was incubated at 37°C for 3 h with shaking. After 3 h incubation, 0.1 ml aliquot was taken per well and a 10-fold dilution made from which a 100 µl aliquot were spread on tryptic soy agar (TSA). Inoculated plates were incubated at 37°C for 20 h and the remaining colony forming units were evaluated, and MICs were calculated as the lowest peptide concentration that obviate visible turbidity using a modified B. Gompertz function for line-of best fit in dose-response analysis (Lambert and Pearson, 2000).

3.14.4 Time-killing assay

The antibacterial killing kinetics of the hybrid peptide was evaluated against two bacterial isolates by ascertaining the time course to kill suspensions of test bacteria isolates of *S. aureus* (gram+), and *E. coli* (gram-) (Kang *et al*., 2019; Klubthawee *et al*., 2020). In brief, bacteria in mid-logarithmic growth phase were incubated as described previously above with the peptide at a concentration approximately 2X MIC in TSB broth. 10 µl aliquot suspensions was taken at every 20 min interval until a period of 3 h incubation was observed. A 10-fold dilution in 1X PBS was made and 0.1 ml aliquots were spread on TSA medium. Inoculated plates were incubated at 37°C for 20 h. Log CFU/ml of test pathogen was plotted against time. Two control samples were made, positive control

(bacterial suspension and kanamycin at the same peptide concentration), and negative control (bacterial suspension and 1X PBS, pH 7.2 buffer). The average of total remaining CFU/ml from each treatment was evaluated and analyzed via one-way analysis of variance (ANOVA). The hybrid peptide with a single disulfide linkage (S-S bond) expressed in *E. coli* SHuffle T7(DE3) showing relatively lower minimum inhibitory concentrations (MICs) was employed for time-killing kinetic assay.

CHAPTER FOUR

4.0 RESULTS

4. 1 Design of hybrid peptide and amino acid sequence of the gene construct

The amino acid sequence of the gene construct designed to encode the novel hybrid antimicrobial peptide LL-37_Renalexin with respective protein tags SmbP and CusF3H+ is depicted below (Figure 4.1). In designing the hybrid peptide with the molecular gene map shown (Figure 4.2A), we employed the mature amino acid sequences that encode for the peptides LL-37 and Renalexin retrieved from the antimicrobial peptide database http://aps.unmc.edu/AP/prediction/ with the accession number AP00310/2K60 and AP00513/P39084 respectively. The amino acid GS (Glycine and Serine) between the peptide LL-37 and Renalexin in the gene construct was employed as a novel simple flexible peptide linker allowing for the construction of the hybrid peptide LL-37_Renalexin. The amino acid sequence DDDDK at the N-terminal of the hybrid peptide serves as enterokinase site that allows for the molecular cleavage of the protein tags SmbP and CusF3H+ yielding a tag-free hybrid AMP LL-37_Renalexin. The biochemical and physicochemical properties of the designed hybrid peptide were analyzed using an online bioinformatics tool http://www.expasy.org/tools/proparameter. The secondary structure (Figure 4.2B) of the peptide was predicted and analyzed with the I-TASSER bioinformatics online tool http://zhanglab.ccmb.med.umich.edy/I-TASSER. The structure predicted and modeled in i-Tasser was confirmed in Phyre2 server (http://www.sbg.bio.ic.ac.uk/phyre2) with 99.9 – 99.3% confidence level under the model template identifier (i.d) c2K6oA (LL-37) and c2fcgF (Renalexin) (Kelley et al., 2016). The target hybrid peptide has the following biochemical properties 59 amino acid length, +9 net charge, pI of 10.3, 44% hydrophobicity, and 56% hydrophilicity, GRAVY index

of 0.00, instability index of 21.3, aliphatic index of 102.37 and a molecular weight 6.740 kDa theoretically predicted in http://www.expasy.org/tools/proparameter. The physicochemical properties of hybrid peptide suggest strong electrostatic cationic polarity, hydropathicity, stability, and good isoelectric potentials which provide theoretical evidence of strong antimicrobial activity of this hybrid peptide at a varying pH range compared to its counterpart singles peptides. Cellular toxicity of the hybrid peptide against healthy human cells was ascertained using ToxIBTL advanced bioinformatic online server (https://server.wei-group.net/ToxIBTL/server.html). ToxIBTL is an online in-silico peptide and protein toxicity prediction tool that operates using evolutionary information and the physicochemical properties of peptide sequence via the integration of bottleneck principle to predict peptide or protein toxicity level. Our in-silico cytotoxicity analysis showed that the hybrid peptide has no toxic effect (zero toxicity) on normal human cells at the niche of infection at a toxicity score of 3.7139784e-05 (0.0000371) which is by far below the standard threshold of 0.5. The entire designed amino acid sequence encoding for the fusion protein SmbP_LL-37_Renalexin peptide has a total of 160 amino acid residues and the CuSF3H+_LL-37_Renalexin has a total of 156 amino acid residues. Inclusive of restriction enzymes, start codons, protein tags, enterokinase, and stop codons amino acid sites.

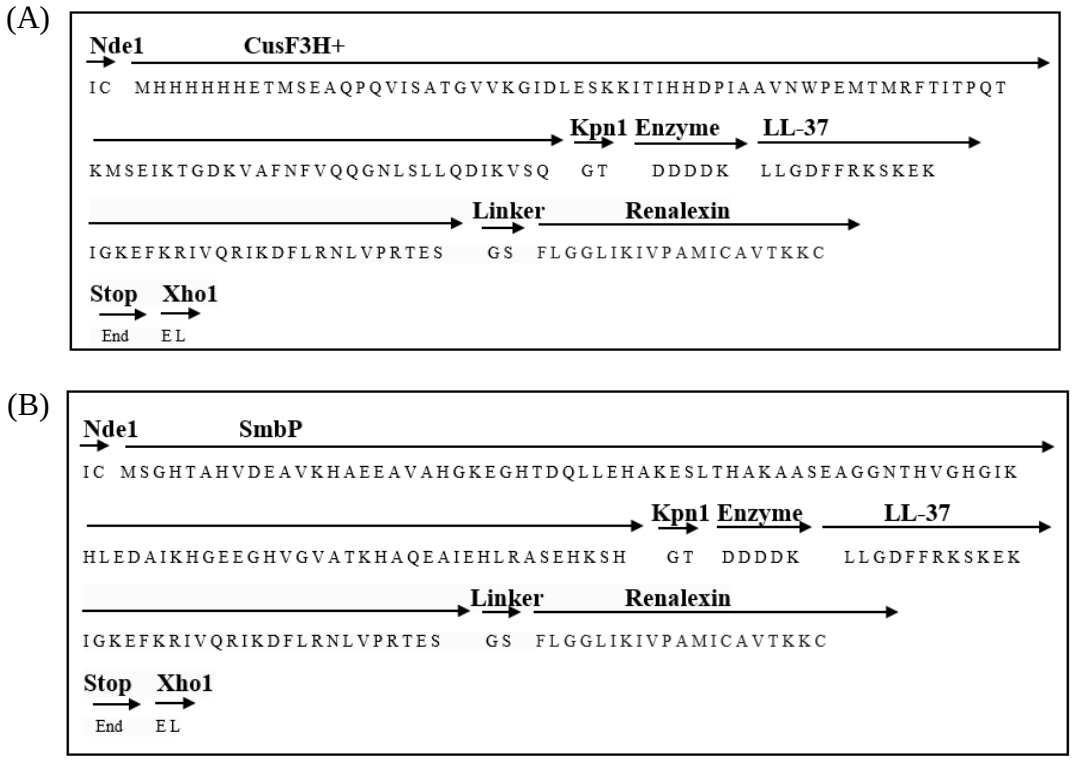

Figure 4. 1: Amino acid sequence flowchart representation of the expression cassette encoding for the hybrid peptide. (A) Expression cassette encoding for CusF3H+_LL-37_Renalexin. (B) Expression cassette encoding for SmbP_LL-37_Renalexin.

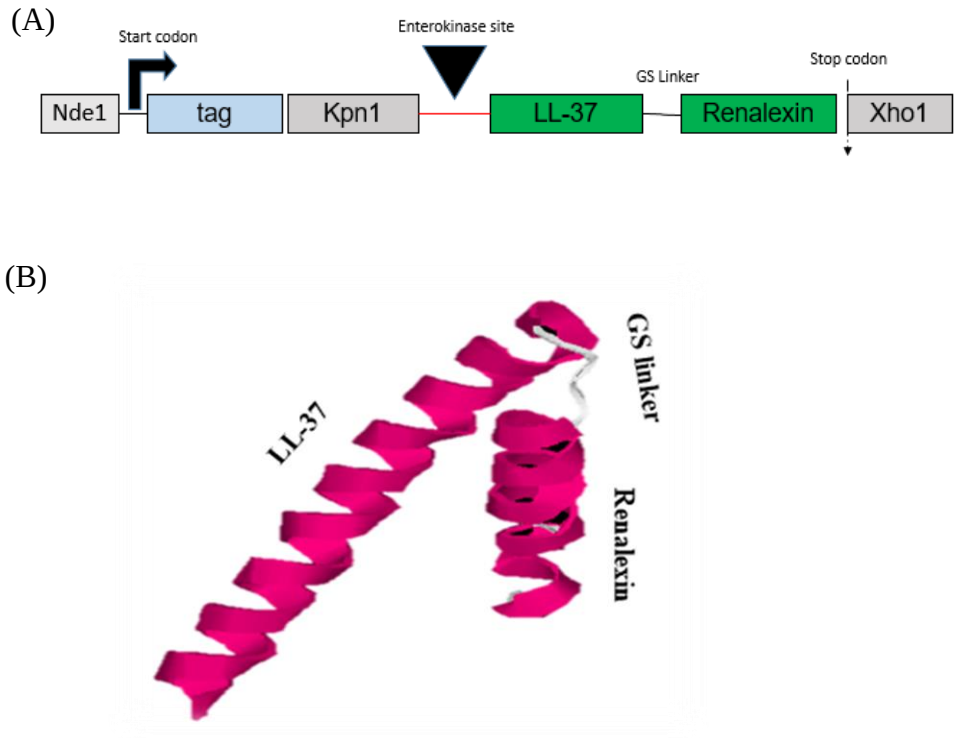

Figure 4. 2: Design of the hybrid antimicrobial peptide LL-37_Renalexin. (A) Representation of expression cassette gene map for LL-37_Renalexin expression in *E. coli*. (B) A 3D Riben molecular secondary structure predicted for the hybrid peptide LL-37_Renalexin showing the components including LL-37 (long peptide on left), the flexible GS peptide linker (midway), and Renalexin (short peptide on far right). The peptide structure was predicted in i-Tasser server and confirmed in Phyre2 server with good positive z-score (1.00) and c-score (-2.09) suggesting an efficient sequence alignment with good, modelled confidence level supporting the predicted structure.

4.2 DNA nucleotide sequence encoding for the hybrid peptide

The synthetic DNA nucleotide sequence of the target gene molecularly cloned into the plasmid expression vector pET30a+ as DNA insert is shown below (Figure 4.3). The DNA (gene) nucleotide sequence was chemically synthesized by GenScript Biotechnology Company, USA. The SmbP construct has about 492 nucleotide base pairs (bp) and the CusF3H+ construct has 480 bp. The complete nucleotide sequences for SmbP_LL-37_Renalexin and CusF3H+_LL-37_Renalexin gene constructs were submitted into NCBI GenBank database with the following accession numbers OR356112 and OR356113, respectively.

(A)

CATATG

ATGCACCACCACCACCACCACGAGACCATGAGCGAGGCCCAGCCCCAGGTGATCAGCG
CCACCGGCGTGGTGAAGGGCATCGACCTGGAGAGCAAGAAGATCACCATCCACCACGA
CCCCATCGCCGCCGTGAACTGGCCCGAGATGACCATGAGGTTCACCATCACCCCCCAGA
CCAAGATGAGCGAGATCAAGACCGGCGACAAGGTGGCCTTCAACTTCGTGCAGCAGGG
CAACCTGAGCCTGCTGCAGGACATCAAGGTGAGCCAGGTACCGACGACGACGATAAAC
TGCTGGGTGATTTCTTTCGTAAAAGCAAAGAGAAAATCGGCAAAGAGTTCAAGCGCATC
GTGCAGCGTATCAAGGACTTCCTGCGTAATCTGGTTCCGCGTACGGAAAGCGGTAGCTT
TTTAGGTGGTCTGATTAAGATCGTGCCGGCAATGATTTGTGCTGTGACCAAAAAGTGC
TAACTCGAG

(B)

CATATG

TCAGGACATACAGCTCACGTAGATGAAGCAGTCAAACACGCTGAAGAAGCGGTGGCCC
ATGGCAAGGAGGGCCACACCGATCAACTGCTGGAACACGCGAAGGAGTCGTTGACCCA
TGCGAAAGCGGCGTCTGAAGCGGGTGGAAACACCCACGTTGGTCACGGCATTAAGCAT
CTCGAGGATGCAATCAAGCACGGCGAAGAGGGTCATGTTGGCGTTGCTACCAAGCACG
CGCAGGAGGCCATTGAACATTTGCGCGCATCCGAGCACAAAAGCCATGGTACCGACGA
CGACGATAAACTGCTGGGTGATTTCTTTCGTAAAAGCAAAGAGAAAATCGGCAAAGAG
TTCAAGCGCATCGTGCAGCGTATCAAGGACTTCCTGCGTAATCTGGTTCCGCGTACGGA
AAGCGGTAGCTTTTTAGGTGGTCTGATTAAGATCGTGCCGGCAATGATTTGTGCTGTGAC
CAAAAAGTGC **TAACTCGAG**

Figure 4. 3: Synthetic DNA nucleotide sequences of the target gene (DNA insert). (A) synthetic DNA nucleotide sequence encoding for CusF3H+_LL-37_Renalexin fusion protein**.** (B) synthetic DNA nucleotide sequence encoding for SmbP_LL-37_Renalexin fusion protein.

4.3 Restriction enzyme digestion of plasmid DNA

Using reliable restriction enzymes *Nde*1 and *Xho*1, the circular plasmid DNAs of pUC57_LL-37_Renalexin, pET30a_SmbP, and pET30a_CusF3H+ were successfully digested into linear DNA molecules with sticky ends that facilitate the molecular ligation reaction, were analyzed on a 1% agarose gel electrophoresis (Figure 4.4). All the target DNA fragments shown in figure 4.4 were cut from the gel using a new scalpel blade for each fragment to avoid DNA fragment contamination. The fragments were purified using a DNA fragment purification kit (*iNtRON* BIOTECHNOLOGY), following the manufacturers protocol with slight modifications, and were quantified using Nanodrop spectroscopy. The purified DNA fragments were stored at 4°C until required for further use.

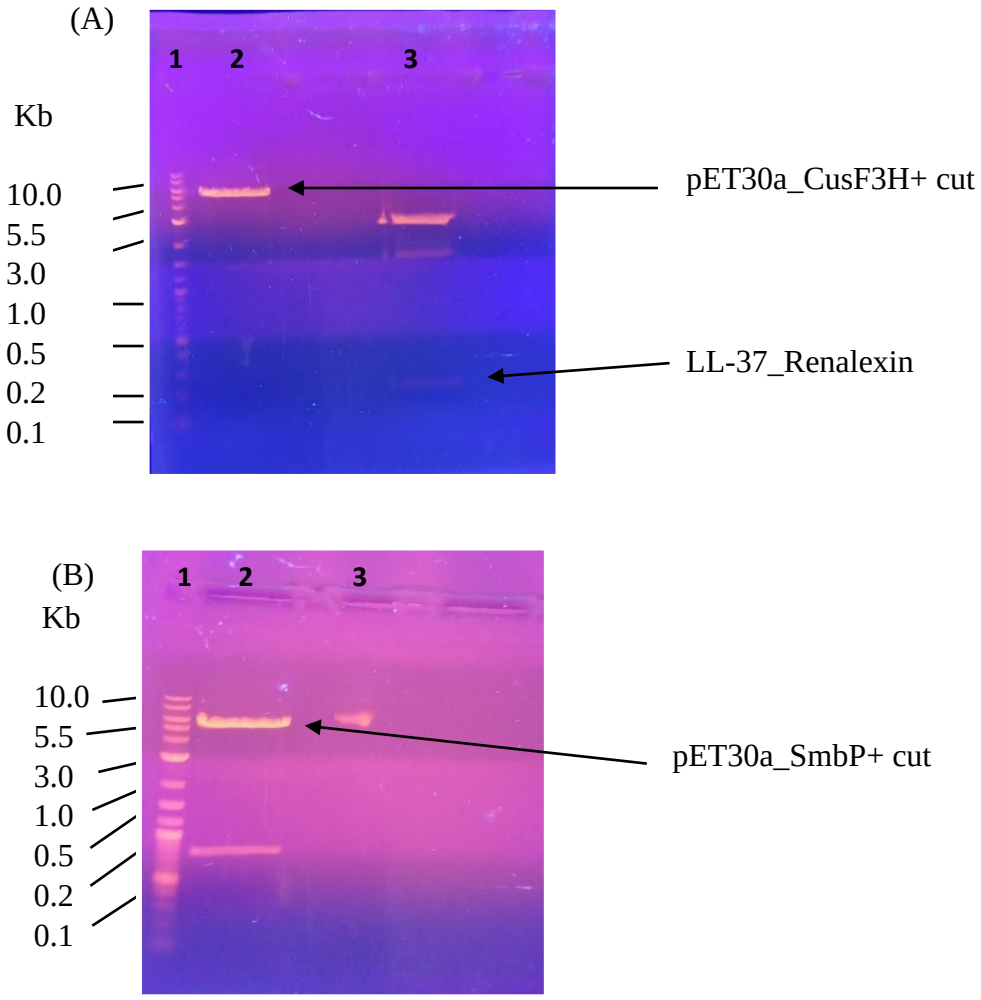

Figure 4. 4: Agarose gel analysis of restriction enzyme digestion of plasmid DNA. (A) 1% Agarose gel analysis of restriction digestion: Lane1; DNA ladder, Lane 2: pET30a_CusF3H+ cut, Lane3; pUC57_SmbP_LL-37_Renalexin cut. (B) 1% Agarose gel analysis of restriction digestion: Lane1; DNA ladder, Lane2; pET30a_SmbP_GFP cut, Lane 3; pET30a_SmbP_GFP uncut.

4.4 In-silico modeling of molecular cloning and the design of recombinant plasmids

An in-silico modeling of the molecular cloning reaction to be performed under wet laboratory conditions was ascertained using SnapGene (www.SnapGene.com), an advance online molecular biology bioinformatics tool to evaluate the efficiency and reliability of the wet laboratory molecular ligation reaction. The schematic flowchart (Figure 4.5) below shows the in-silico modeling of two recombinant plasmid expression vectors.

(A)

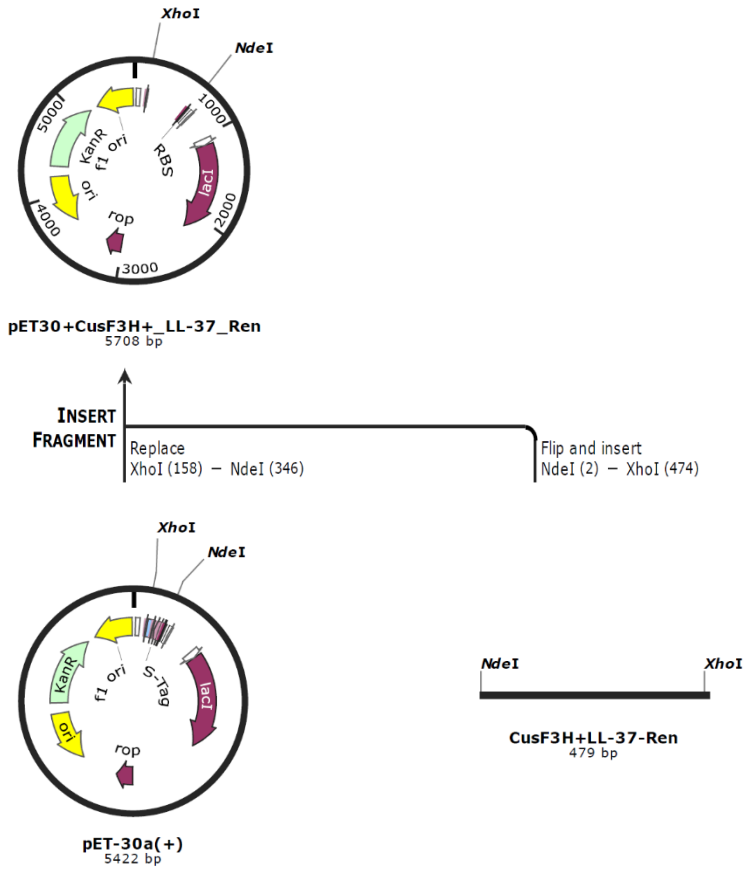

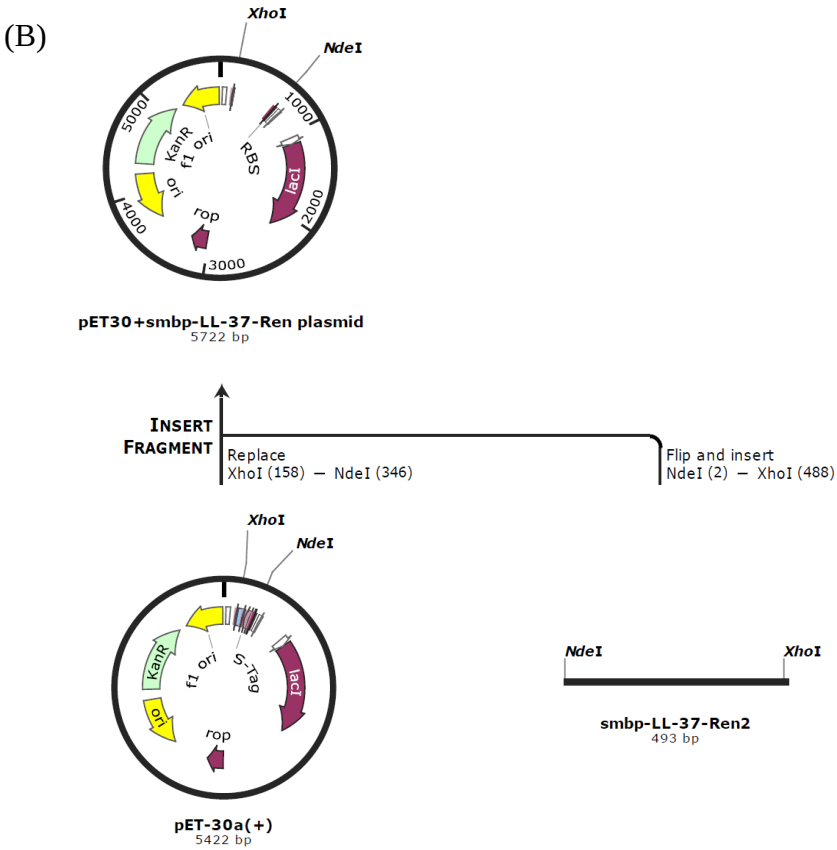

Figure 4. 5: Schematic representation of *in silico* modulation of molecular cloning in SnapGene. (A) *In-silico* modeling of recombinant plasmid construct pET30a_CusF3H+_LL-37_Renalexin. (B) *In-silico* modeling of recombinant plasmid construct pET30a_SmbP_LL-37_Renalexin.

4.5 Plasmid construct confirmation by polymerase chain reaction (PCR)

In evaluating the presence of the target gene that encodes for recombinant fusion proteins CusF3H+_LL-37_Renanlexin and SmbP_LL-37_Renanlexin respectively, in the plasmid constructs designed via molecular ligation, a 20 µl conventional polymerase chain reaction (PCR) was employed using T7 promoter and T7 terminator-specific primers pairs. These

primer pairs anneal strongly to their target sites within which the synthetic DNA insert was cloned at the multiple cloning sites on the plasmid pET30a+ and under the influence T7 promoter. Figure 4.6 depicts the PCR conditions that favor the amplification reaction. PCR amplicons were analyzed on a 1% agarose gel stained with Ethidium bromide (1 μg/ml) and visualized on a UV trans-illuminator (Figure 4.7).

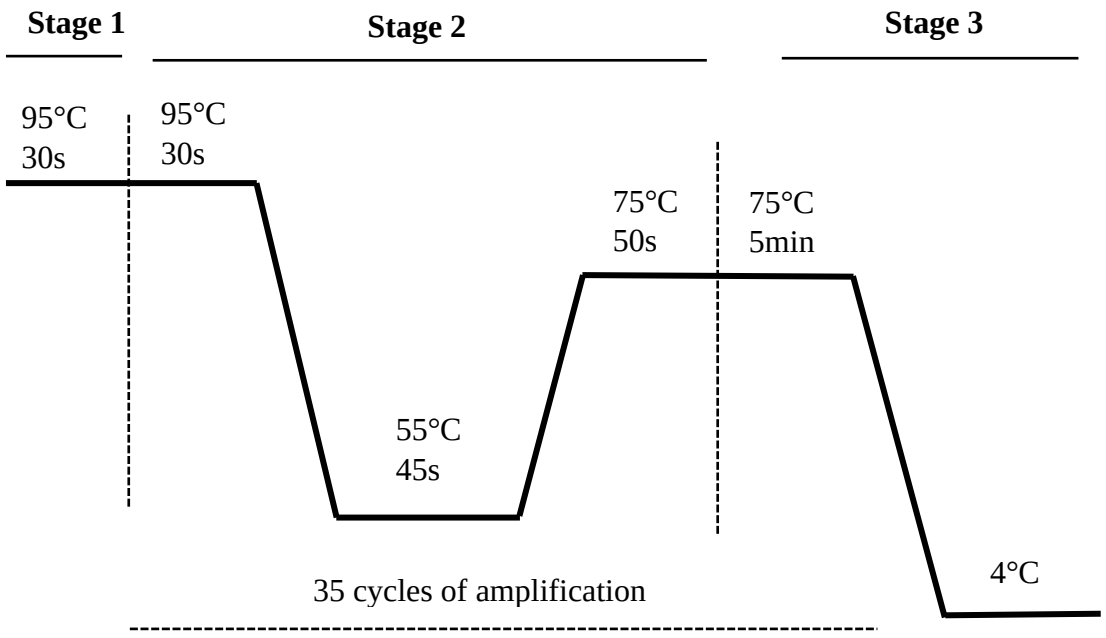

Figure 4. 6: A schematic representation of PCR conditions at various reaction stages. Stage 1: DNA denaturation. Stage 2: Primer annealing and elongation. Stage 3: Final elongation and storage.

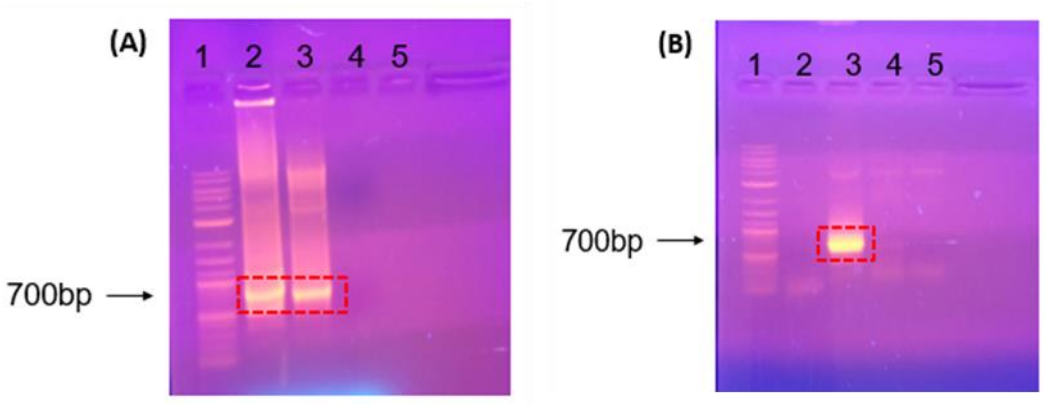

Figure 4. 7: PCR analysis of DNA insert in the designed recombinant plasmid constructs. (A) 1% Agarose gel analysis of CusF3H+_LL-37_Renalexin DNA amplicons: Lane 1; DNA ladder, Lane 2, 3 & 4; PCR amplicons, Lane 5: Negative control (No DNA sample). Amplicons in the red rectangular label indicate the target amplifications. (B) 1% Agarose gel analysis of SmbP_LL-37_Renalexin DNA amplicons: Lane 1; DNA ladder, Lane 2; Negative control (No DNA sample), Lane: 3,4 & 5; PCR amplicons. Amplicons in the red rectangular label indicate the target amplifications.

4.6 Sequence analysis and alignment

The sequence chromatogram and DNA nucleotides generated from the Sanger sequence analyzer were viewed, analyzed, and evaluated using the European Molecular Biology Laboratory online bioinformatics tool (www.ebi.ac.uk/tools/sssEMBOSS.com) for sequence alignment between the synthetic DNA nucleotide sequences and the designed plasmid PCR amplicon sequence. The FinchTV software (www.finchTV.com) tool was used to display sequence chromatogram which shows distinctively clear chromatograms with nicely sharped peaks suggesting a good plasmid constructs purity. Pairwise DNA

sequence alignment analysis (Figure 4.8) was performed using the Needleman−Wunsch algorithm in EMBOSS to assess and evaluate the degree of similarity and identity between the designed plasmid DNA insert and the synthetic DNA construct (Oladipo *et al*., 2023).

(A)

```
# Length: 480
# Identity:     480/480 (100%)
# Similarity:   480/480 (100%)
# Gaps:           0/480 (0.0%)
# Score: 1662
#
#
#=======================================

EMBOSS_001        10 CACCACCACCATCATCATGAAACCATGAGCGAAGCACAACCACAGGTTAT     59
                     ||||||||||||||||||||||||||||||||||||||||||||||||||||
EMBOSS_001        85 CACCACCACCATCATCATGAAACCATGAGCGAAGCACAACCACAGGTTAT    134

EMBOSS_001        60 TAGCGCCACTGGCGTGGTAAAGGGTATCGATCTGGAAAGCAAAAAAATCA    109
                     ||||||||||||||||||||||||||||||||||||||||||||||||||||
EMBOSS_001       135 TAGCGCCACTGGCGTGGTAAAGGGTATCGATCTGGAAAGCAAAAAAATCA    184

EMBOSS_001       110 CCATCCATCACGATCCGATTGCTGCCGTGAACTGGCCGGAGATGACCATG    159
                     ||||||||||||||||||||||||||||||||||||||||||||||||||||
EMBOSS_001       185 CCATCCATCACGATCCGATTGCTGCCGTGAACTGGCCGGAGATGACCATG    234

EMBOSS_001       160 CGCTTTACCATCACCCCGCAGACGAAAATGAGTGAAATTAAAACCGGCGA    209
                     ||||||||||||||||||||||||||||||||||||||||||||||||||||
EMBOSS_001       235 CGCTTTACCATCACCCCGCAGACGAAAATGAGTGAAATTAAAACCGGCGA    284

EMBOSS_001       210 CAAAGTGGCGTTTAATTTTGTCCAGCAGGGCAACCTTTCTTTATTACAGG    259
                     ||||||||||||||||||||||||||||||||||||||||||||||||||||
EMBOSS_001       285 CAAAGTGGCGTTTAATTTTGTCCAGCAGGGCAACCTTTCTTTATTACAGG    334

EMBOSS_001       260 ATATTAAAGTCAGCCAGGGTACCGACGAAAAGGATATACTGCTGATGGAT    309
                     ||||||||||||||||||||||||||||||||||||||||||||||||||||
EMBOSS_001       335 ATATTAAAGAAAGCCAGGGTGCCGACCGGCAGGATCTACAACCGCTTGGT    384
                     ||||||||||||||||||||||||||||||||||||||||||||||||||||
EMBOSS_001       310 ATATTAAAGAAAGCCAGGGTGCCGACCGGCAGGATCTACAACCGCTTGGT    359
```

(B)

```
# Length: 492
# Identity:     492/492 (100%)
# Similarity:   492/492 (100%)
# Gaps:           0/492 (0.0%)
# Score: 1831
#
#
#=======================================

EMBOSS_001         1 CATATGTGAGGACATACAGCTCACGTAGACGAAGCAGTGAAGCACGCTGA     50
                     ||||||||||||||||||||||||||||||||||||||||||||||||||||
EMBOSS_001        31 CATATGTGAGGACATACAGCTCACGTGGACGAAGCAGTGAAGCACGCTGA     80

EMBOSS_001        51 AGAAGCGGTGGCCCATGGCAAAGAAGGCCATACCGATCAATTACTGGAAC    100
                     ||||||||||||||||||||||||||||||||||||||||||||||||||||
EMBOSS_001        81 GGAAGCGGTGGCCCATGGTAAAGAAGGCCATACCGATCAATTACTGGAAC    130

EMBOSS_001       101 ATGCGAAGGAATCTCTGACACATGCGAAAGCTGCGACTGAAGCAGGTGGA    150
                     ||||||||||||||||||||||||||||||||||||||||||||||||||||
EMBOSS_001       131 ATGCGAAGGAATCTCTGACACATGCGAAAGCTGCGACTGAAGCAGGTGGA    180

EMBOSS_001       151 AACACGCATGTTGGTCACGGAATCAAACATCTCGAAGATGCAATCAAGCA    200
                     ||||||||||||||||||||||||||||||||||||||||||||||||||||
EMBOSS_001       181 AACACGCATGTTGGTCACGGAATCAAACATCTCGAAGATGCAATCAAGCA    230

EMBOSS_001       201 CGGCGAAGAGGGTCATGTCGGTGTTGCTACCAAGCATGCGCAAGAGGCTA    250
                     ||||||||||||||||||||||||||||||||||||||||||||||||||||
EMBOSS_001       231 CGGCGAAGAAGGTCATGTCGGTGTTGCTACCAAGCATGCGCAAGAGGCTA    280

EMBOSS_001       251 TCGAGCATTTGCGTGCATCCGAACATAAATGGCACGGTACCGTCGACGTT    300
                     ||||||||||||||||||||||||||||||||||||||||||||||||||||
EMBOSS_001       281 TCGAGCATTTGCGTGCATCCGAACATAAATGGCACGGTACCGTGGACGTT    330

EMBOSS_001       301 GAGCTAAACTGCTCGGAAATGTTCAATCGTAAACGCCTACACAAGCTTGG    347
                     ||||||||||||||||||||||||||||||||||||||||||||||||||||
EMBOSS_001       331 GAGCTAAACTGCTCGGAAATGTTCAATCGTAAACGCCTACACGAGCTTGG    377
```

Figure 4. 8: DNA nucleotide sequence alignment using the Needleman−Wunsch algorithm for pairwise analysis between the synthetic DNA and designed plasmid DNA insert (amplicon). (A) Sequence nucleotide alignment for CusF3H+_LL-37_Renalexin DNA amplicon. (B) Sequence nucleotide alignment for SmbP_LL-37_Renalexin DNA amplicon.

4.7 Small-scale expression of the hybrid AMP: LL-37_Renalexin

In evaluating the expression of the hybrid chimeric peptides CusF3H+_LL-37_Renalexin and SmbP_LL-37_Renalexin (17 kDa) in *E. coli* BL21(DE3) and *E. coli* SHuffle T7(DE3), soluble cell lysates were prepared by lysing cell pellets collected from 2 ml overnight cultures in a 150 µl lysing buffer (50 mM Tris-HCl pH 8.0). 5µl of each soluble lysate was treated with 6X sample buffer (final concentration of 1X) and analyzed on a 15% Sodium Dodecyl Sulfate Polyacrylamide gel electrophoresis (SDS-PAGE) (Figure 4.9). To access the cytoplasmic expression of the target fusion proteins in *E. coli* BL21(DE3) and SHuffle T7(DE3) transformed cells, both soluble and insoluble cell lysate fractions were made and analyzed to ascertain the presence of inclusion bodies in the insoluble lysate fraction that may indicate the production of the target peptides as misfolded protein. Two *E. coli* BL21(DE3) and SHuffle T7(DE3) control samples were made. Transformed cells without IPTG induction and untransformed cells.

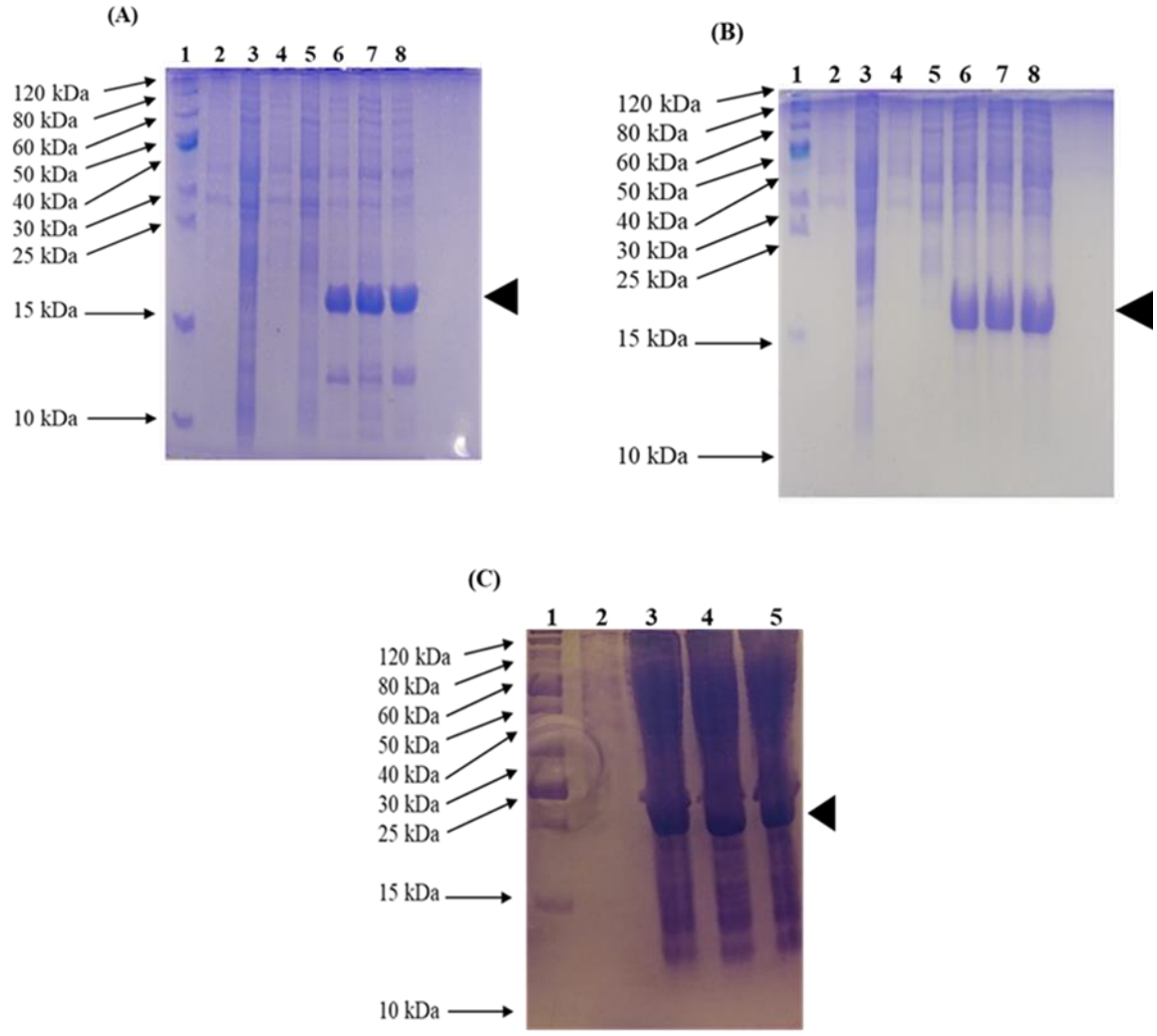

Figure 4. 9: Small-scale expression of recombinant fusion peptides in *E. coli*. (A) 15% SDS-PAGE analysis of CusF3H+_LL-37_Renalexin expressed in *E. coli* BL21(DE3): Lane 1: Protein ladder, Lanes 2, 3: soluble (SF) and insoluble (IF) fractions of untransformed control cells, Lanes 4, 5: SF and IF of uninduced transformed cells, Lane 6, 7, and 8: SF of induced transformed cells. (B) 15% SDS PAGE analysis of SmbP_LL-37_Renalexin expressed in *E. coli* BL21(DE3): Lane 1: Protein ladder, Lanes 2, 3: SF and IF of untransformed control cells, Lanes 4, 5: SF and IF of uninduced transformed cells, Lane 6, 7, and 8: SF of induced transformed cells. (C) 15% SDS-PAGE analysis of

CusF3H+_LL-37_Renalexin expressed in *E. coli* SHuffle T7(DE3): Lane 1: Protein ladder, Lanes 2: soluble fraction of uninduced transformed cells (control), Lane 3, 4, and 5: SF of induced transformed cells.

4.8 Large-scale expression of the hybrid AMP: LL-37_Renalexin

For evaluation of the level of expression and IMAC purification of the recombinant fusion proteins (chimeric) CusF3H+_LL-37_Renalexin (Figure 4.10) and SmbP_LL-37_Renalexin (Figure 4.11) expressed in *E. coli* BL21(DE3) and *E. coli* SHuffle T7(DE3), respectively. From a 1 L expression volume, cell pellets were collected from 1 mM IPTG induced overnight cultures and lysed by mechanical vortexing on ice with 0.1 mm glass beads. After cell lysis, clear soluble lysate was collected and employed as protein source for the immobilized metal affinity chromatography.

For purification of fusion protein SmbP_LL-37_Renalexin and CusF3H+_LL-37_Renalexin, the ÄKTA Prime Plus system (GE Healthcare Systems) was employed for fast protein liquid chromatography (FPLC) by metal affinity chromatography. A 1 ml HisTrap FF column charged with Ni(II) was used to isolate the target recombinant peptide form the pool of cellular proteins present in the soluble lysate fractions collected. Analysis of IMAC purification fractions of the recombinant fusion protein on a 15% SDS PAGE showed evidence of target peptide in the elution fractions (200 mM imidazole) without any trace of peptide indications in the column flow-through. This result showing the presence of the target recombinant fusion peptides in the elution fractions on the gel confirms the high affinity of CusF3H+ and SmbP to agarose-resin Ni(II) charged column that facilitates the binding of the target proteins unto the column whiles the untargeted cellular proteins exit the column as flow-through (Montfort-Gardeazabal *et al*., 2021;

Perez-Perez *et al*., 2021; Vargas-Cortez *et al*., 2017). The purity level of protein bands in the elution fractions was evaluated by densitometry in ImageJ.

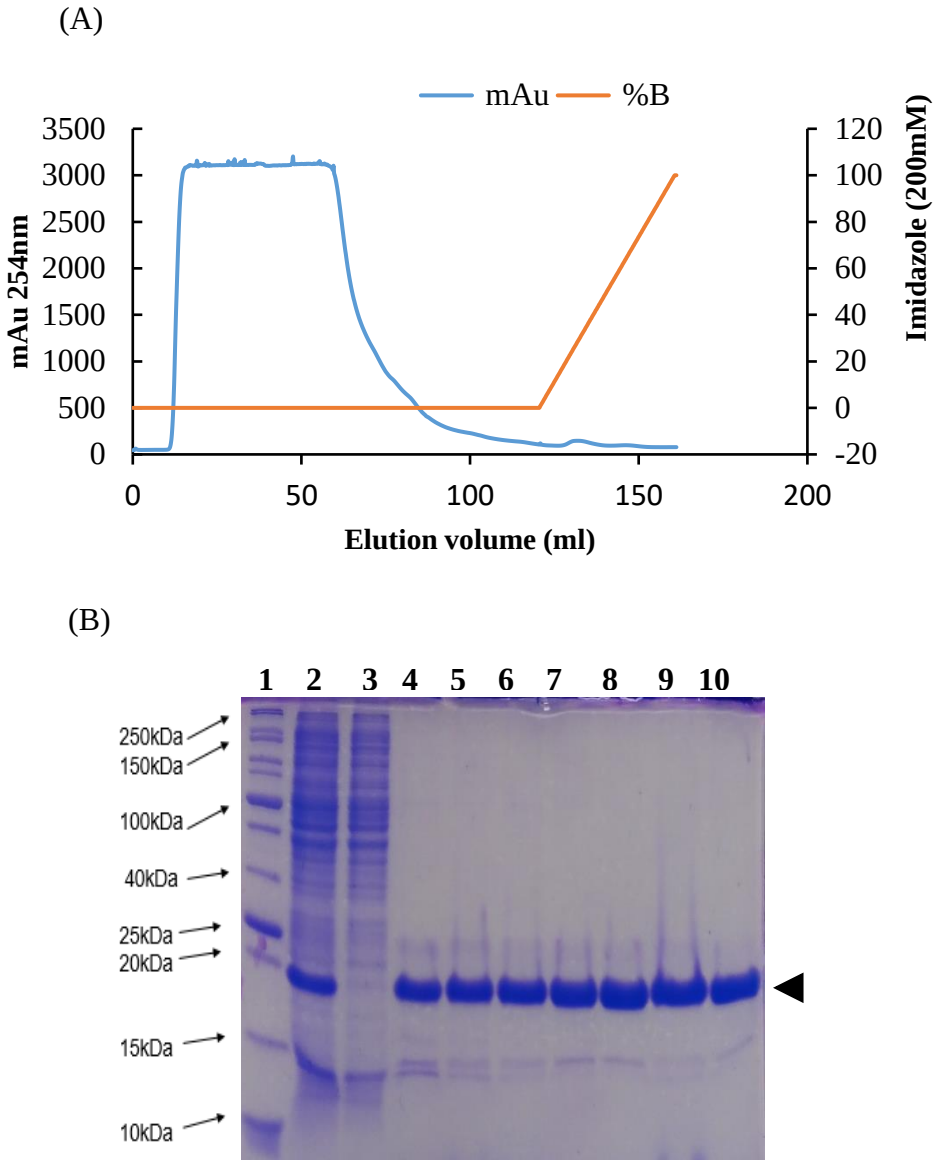

Figure 4. 10: IMAC purification of CusF3H+_LL-37_Renalexin (17 kDa) expressed in *E. coli* SHuffle T7(DE3). (A) IMAC Chromatogram of the purification using the ÄKTA Prime Plus System with 1 ml His-Trap FF column. The column was equilibrated with 500 mM NaCl, 50 mM Tris-HCl pH 8.0 and washed with 500 mM NaCl, 2.5 mM Imidazole,

50 mM Tris-HCl pH 8.0. Gradient elution was performed with 500 mM NaCl, and 200 mM Imidazole, 50 mM Tris-HCl pH 8.0. (B) 15% SDS PAGE analysis of the eluted fractions, Lane 1: protein marker, Lane 2: cell lysate, Lane 3: column flow-through, Lane 4 – 10: elution fractions.

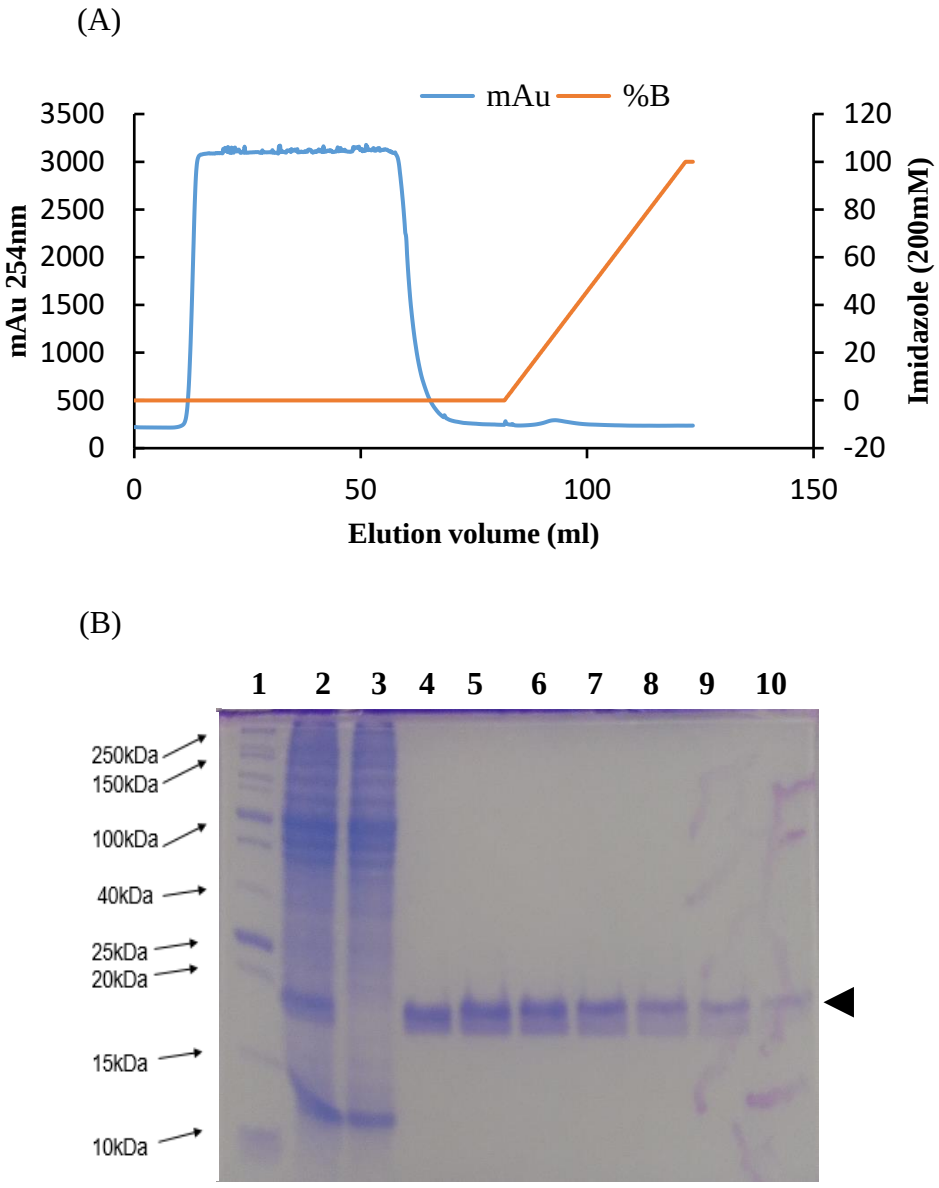

Figure 4. 11: IMAC purification of SmbP_LL-37_Renalexin (17 kDa) expressed in *E. coli* BL21(DE3). (A) IMAC Chromatogram of the purification using the ÄKTA Prime

Plus System with 1 ml His-Trap FF column. The column was equilibrated with 500 mM NaCl, 50 mM Tris-HCl pH 8.0 and washed with 500 mM NaCl, 2.5 mM Imidazole, 50 mM Tris-HCl pH 8.0. Gradient elution was performed with 500 mM NaCl, and 200 mM Imidazole, 50 mM Tris-HCl pH 8.0. (B) 15% SDS-PAGE analysis of the eluted fractions, Lane 1: protein marker, Lane 2: cell lysate, Lane 3: column flow-through, Lane 4 – 10: elution fractions.

4.9 Bradford analysis and protein quantification

The BSA standard protein at concentrations ranging from 1.3 – 0.1 mg/ml was used to establish a calibration curve by plotting the concentrations against the average of three absorbance readings obtained at 595 nm. The calibration equation and correlation co-efficient were calculated in Microsoft Excel (Colyer and Walker, 1996). The calibration curve (Figure 4.12A) with good correlation (r^2 = 0.978) was employed to estimate the concentration of recombinant fusion protein CusF3H+_LL-37_Renalexin and the calibration curve (Figure 4.12 B) with good correlation (r^2 = 0.991) was used in the case of recombinant fusion protein SmbP_LL-37_Renalexin. The degree of correlation obtained was significant and reliable for estimating and quantifying recombinant protein concentrations. Our Bradford quantification analysis using the respective calibration equations indicated a peptide concentration of 3.136 mg/L for CusF3H+_LL-37_Renalexin and 2.16 mg/L for tag-free LL-37_Renalexin (with disulfide bond) produced in *E. coli* SHuffle T7(DE3). In the case of peptide SmbP_LL-37_Renalexin and tag-free LL-37_Renalexin (without disulfide bond) produced in *E. coli* BL21(DE3), we had 1.523 mg/L and 0.72 mg/L, respectively.

(A)

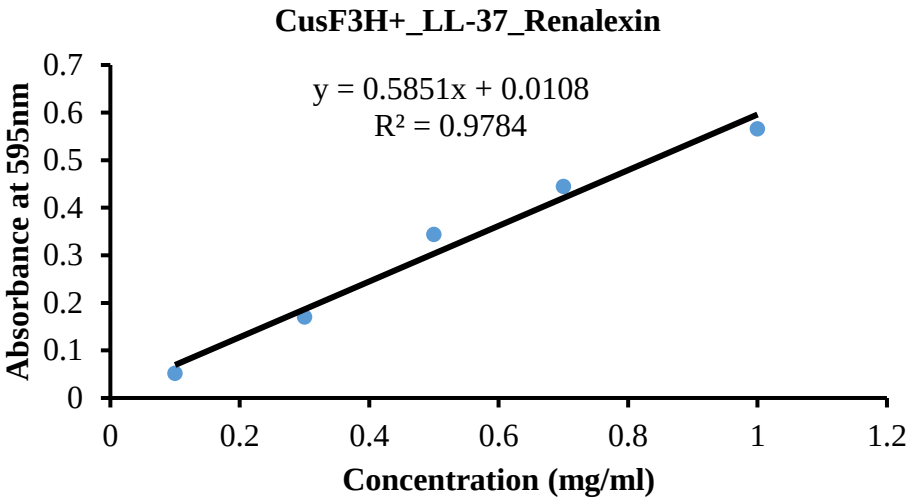

(B)

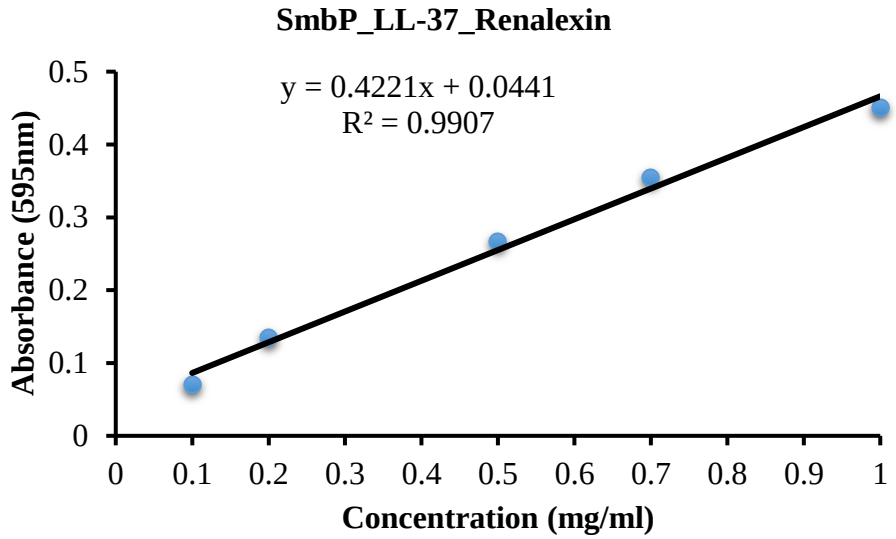

Figure 4. 12: Bovine Serum Albumin (BSA) standard calibration curve and protein quantification by Bradford analysis. (A) Calibration standard curve for recombinant fusion protein CusF3H+_LL-37_Renalexin (with disulfide bond) expressed in *E. coli* SHuffle T7(DE3). (B) Calibration standard curve for the peptide SmbP_LL-37_Renalexin (without disulfide bond) expressed in *E. coli* BL21(DE3).

4.10 Enterokinase cleavage and purification recombinant LL-37_Renalexin

In evaluating the bioactivity of the hybrid peptide, enzymatic removal of carrier proteins is crucial as this may compromise the degree of antibacterial effect of the target hybrid peptide. The purified recombinant fusion proteins have an enterokinase site (DDDDK) between the target hybrid peptide LL-37_Renalexin and the carrier protein. Selective removal of the carrier proteins CusF3H+ and SmbP respectively from the purified fusion protein (chimeric peptide) was performed by enterokinase cleavage reaction as described by the supplier. A 3 ml reaction volume was carried out composed of 1 mg of the chimeric protein and 20 U of the enterokinase enzyme (5 U/µl) and incubated under the conditions of 25°C for 16 h, followed by enzyme inactivation at -20°C incubation for 3 h. Electrophoretic analysis of inactivated enterokinase cleavage mixture revealed three protein bands of approximate molecular size 18 kDa (uncleaved fusion peptide), 13 kDa (CusF3H+ or SmbP), and 10 kDa (LL-37_Renalexin, tag-free) on Tricine SDS-PAGE (Figure 4.13). The uncleaved fusion peptide detected was due to an incomplete enzymatic cleavage reaction suggesting inefficient enzymatic release of the protein tags from the recombinant fusion peptide, with a release yield of 50 – 70% (tag-free LL-37_Renalexin). Finally, the tag-free LL-37_Renalexin was purified via a one-step IMAC purification using agarose-resin Ni(II) charged syringe column unto which the uncleaved fusion peptide and the carrier proteins CusF3H+ and SmbP remains bounded allowing for the elution of the target hybrid peptide LL-37_Renalexin as column flowthrough. A 2.16 mg/L for tag-free LL-37_Renalexin with disulfide bond expressed in SHuffle T7(DE3) and 0.72 mg/L without disulfide bond expressed in BL21(DE3) were obtained after Bradford and Nanodrop spectrometry (A280nm) quantification analysis.

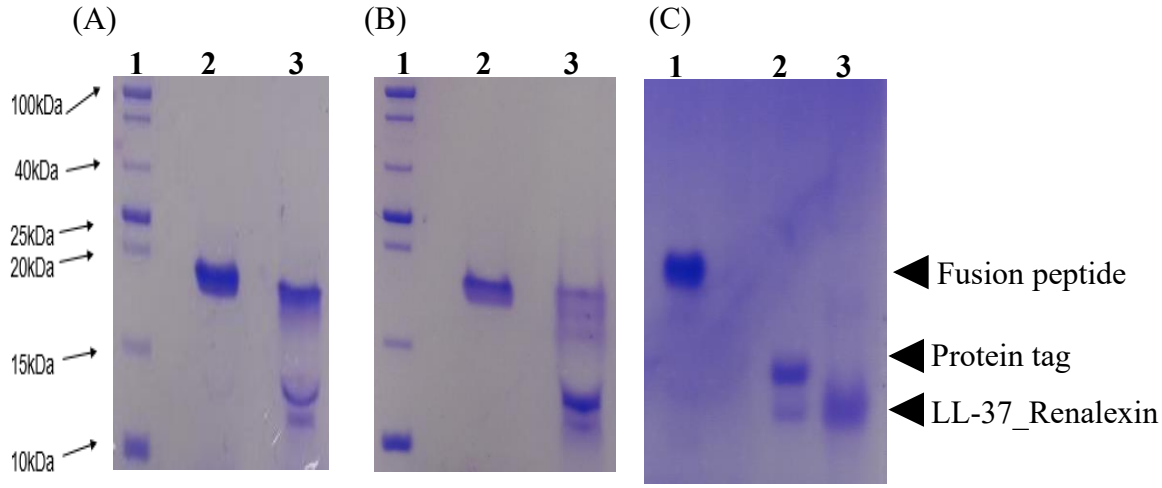

Figure 4. 13: Enterokinase cleavage, tag removal, and second IMAC purification of tag-free LL-37_Renalexin analyzed on Tricine SDS-PAGE. (A) 18% Tricine gel, Lane 1: Protein ladder, Lane 2: CusF3H+_LL-37_Renalexin (uncut) expressed in *E. coli* SHuffle T7(DE3), Lane 3: cut CusF3H+_LL-37_Renalexin (enterokinase mix). (B) 18% Tricine gel, Lane 1: Protein ladder, Lane 2: SmbP_LL-37_Renalexin (uncut) expressed in *E. coli* BL21(DE3), Lane 3: cut SmbP_LL-37_Renalexin (enterokinase mix). (C) 15% Tricine gel, Lane 1: Fusion peptide CusF3H+_LL-37_Renalexin (uncut), Lane 2: Enerokinase mix (Protein tag and tag-free LL-37_Renalexin), Lane 3: second IMAC purified hybrid peptide LL-37_Renlexin (tag-free).

4.11 Antimicrobial activity and minimum inhibition concentration (MIC) determination

The antimicrobial potency of the purified hybrid peptide against clinical isolates of *Staphylococcus aureus, Escherichia coli,* Methicillin-resistant *Staphylococcus aureus* (MRSA), and *klebsiella pneumoniae* was evaluated, and the minimum inhibitory concentrations (MICs) determined via the broth microdilution and colony-forming assay

method as described by NCCLSI (Lacy *et al*., 2004). Data on remaining colony-forming units (CFU/ml) of test pathogens after overnight culture with the peptide was taken by manually counting of colonies on each replica plates and analyzed statistically. The MIC, defined as the minimum peptide concentration that prevented visible turbidity in the test pathogen, was calculated using a modified Benjamin Gompertz sigmoid function (Lambert and Pearson, 2000) from the plot of peptide concentrations and remaining CFU/ml (dose-response plot). The dose-response plots (Figure 4.14) show the antibacterial activity of the hybrid AMP LL-37_Renalexin at MIC levels of 10 – 27 µM, much lower than reported MICs of single peptides LL-37 and Renalexin (50 – 100 µM) (Aleinein *et al*., 2013; Kang *et al*., 2019; 2000; Perez-Perez *et al*., 2021). Interestingly, we evaluated the bioactivity of the hybrid peptide without disulfide-linkage expressed in *E. coli* BL21(DE3), the results (Table 4.1) suggested no significant difference in the MICs compared to the hybrid peptide with disulfide-linkage expressed in *E. coli* SHuffle T7(DE3). (Cheng *et al*., 2021; Dürr *et al*., 2006; Kang *et al*., 2019; Wei, 2016; Seyedjavadi *et al*., 2021b). The dose-response antimicrobial activity results indicated that the test bacterial pathogens were sensitive to the recombinant hybrid peptide at active peptide concentrations as low as 10 µM and 33 µM.

Table 4. 1: MICs of LL-37_Renalexin expressed in BL21(DE3) and SHuffle T7(DE3) E. coli strains.

	MICs: LL-37_Renalexin (µM)	
Pathogens	*E. coli* BL21(DE3)	*E. coli* SHuffle T7(DE3)
Staphylococcus aureus	20.1	18.2
Escherichia coli	21.4	19.7
MRSA	N/A	17.5
Klebsiella pneumoniae	N/A	27.8

N/A: Not Analyzed (peptide expressed in *E. coli* SHuffle T7(DE3) was used for subsequent bioactivity).

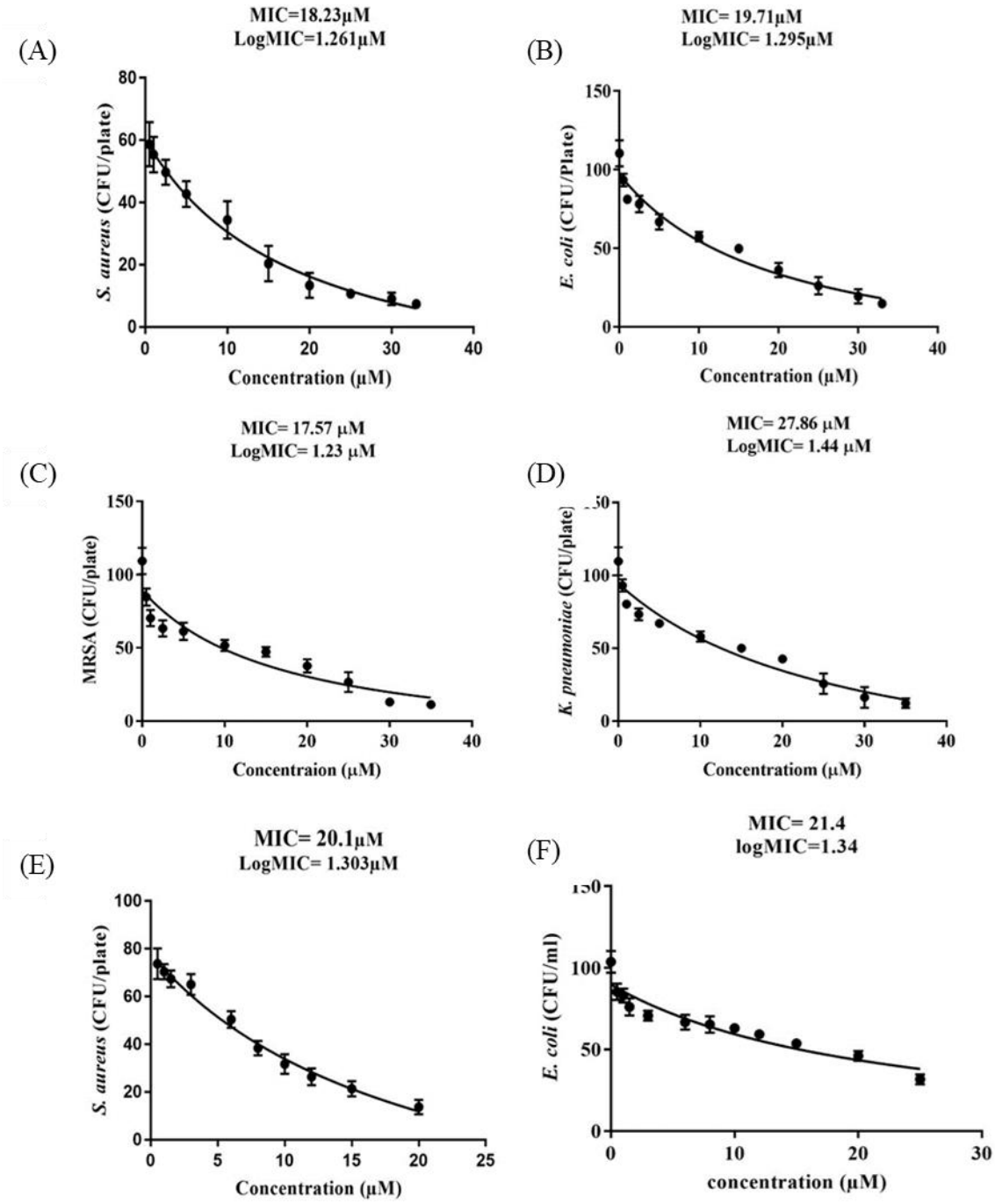

Figure 4. 14: Antimicrobial activity of purified recombinant hybrid AMP LL-37_Renalexin (tag-free) against $1x10^5$ CFU/ml of bacteria pathogens. (A) Dose-response activity of LL-37_Renalexin expressed in *E. coli* SHuffle T7(DE3) against CFU/ml of *S. aureus*. (B) Dose-response activity of LL-37_Renalexin expressed in *E. coli* SHuffle T7(DE3) against CFU/ml of *E. coli*. (C) Dose-response activity of LL-37_Renalexin expressed in *E. coli* SHuffle T7(DE3) against CFU/ml of MRSA. (D) Dose-response activity of LL-37_Renalexin expressed in *E. coli* SHuffle T7(DE3) against CFU/ml of *K. pneumoniae*. (E) Dose-response activity of LL-37_Renalexin expressed in *E. coli* BL21(DE3) against CFU/ml of *S. aureus*. (F) Dose-response activity of LL-37_Renalexin expressed in *E. coli* BL21(DE3) against CFU/ml of *E. coli*. The data points represent the mean remaining CFU/ml of the test pathogen from three replica plates, and the error bar represents the standard deviation of the mean. Statistical analysis was performed using Gompertz sigmoid function for non-linear regression between the peptide concentration and the CFU/ml of test pathogen.

4.12 Time-kill kinetics analysis

In evaluating bacteria killing kinetics of the peptide against the test pathogens with respect to time. Time-kill assay was performed by assessing the CFU/ml from bacteria suspensions treated with approximately 2X MICs of the peptide. The time-kill kinetic assay (Figure 4.15) disclosed that the hybrid peptide shows a multifunctional antibacterial activity within one and a half hours via membrane integrity disruption and membrane traversing, demonstrating a strong but relatively slow antibacterial potency against all investigated gram-positive and gram-negative bacterial pathogens as compared to the classical antibiotic kanamycin that exhibited its antibacterial activity within less than an

hour. We observed that the antibacterial activity of the hybrid peptide in comparison to the known antibiotic kanamycin analyzed against total remaining CFU/ml showed a significant difference at p values < 0.05 (Figure 4.16), with the hybrid peptide showing relatively similar antibacterial actions as exhibited by kanamycin (Aleinein *et al*., 2013; Hanafiah *et al*., 2020; Montfort-Gardeazabal *et al*., 2021; Perez-Perez *et al*., 2021).

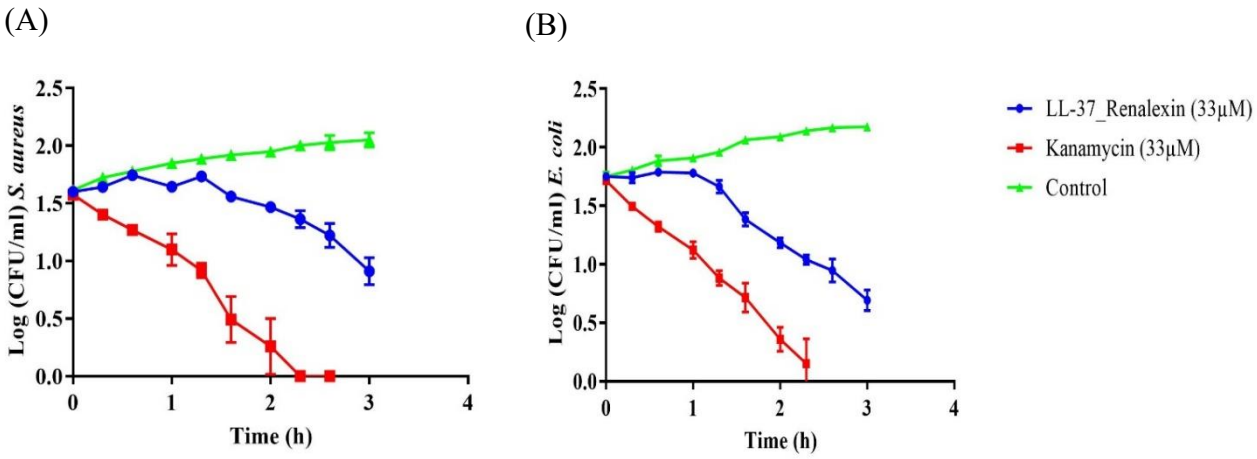

Figure 4. 15: Time-killing kinetics of LL-37_Renalexin expressed in *E. coli* SHuffle T7(DE3), tag-free at 2X MIC against the log $1x10^5$ CFU/ml of the test pathogens within 3 h time interval of treatment. (A) Time-kill assay of the hybrid peptide against *S. aureus*. (B) Time-kill assay of the hybrid peptide against *E. coli*. A 1X PBS buffer (pH 7.2) and suspensions of bacteria inoculum were used as the negative control. Antibiotic kanamycin was employed as positive control. The data points represent the mean of log remaining CFU/ml of the test pathogens from three replica plates, and the error bars represent the standard deviation (SD) of the mean CFUs.

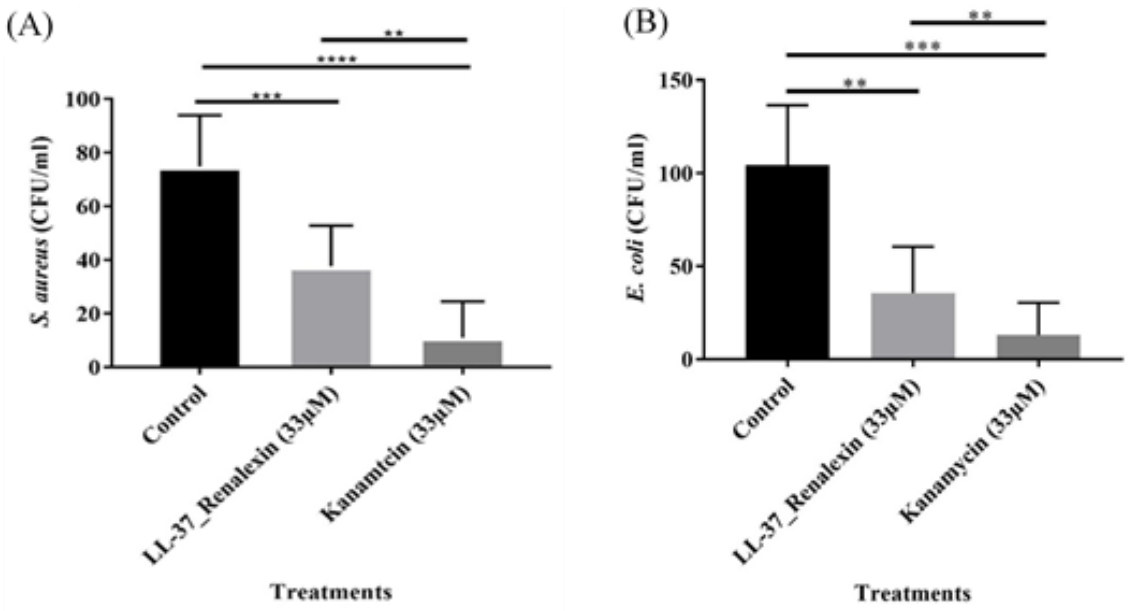

Figure 4. 16: Antimicrobial activity of the hybrid peptide LL-37_Renalexin expressed in *E. coli* SHuffle T7(DE3), tag-free against $1x10^5$ CFU/ml of test pathogens analyzed by one-way analysis of variance (ANOVA). (A) Antibacterial activity against the CFU/ml of *S. aureus*. (B) Antibacterial activity against the CFU/ml of *E. coli*. A 1X PBS buffer (pH 7.2) and suspension of bacteria inoculum were used as negative control. The bars represent the mean remaining CFU/ml of the test pathogens from three replica plates and the error bars represent the standard deviation (SD) of the means. Asterisks indicate the statistical significance difference (all P values < 0.05) between the peptide, the negative control and kanamycin (positive control).

CHAPTER FIVE

DISCUSSION

Antimicrobial peptides (AMPs) as drug candidates are being considered the new hope for the biomedical and pharmaceutical industries in conjunction with their multifunctional antibacterial pharmacological actions against infectious agents (Montfort-Gardeazabal *et al*., 2021; Moretta *et al*., 2021; Nuti *et al*., 2017). The production of AMPs as therapeutic peptides via the applications of recombinant DNA technology (rDNA) and the use of cost-effective microbial expression systems has facilitated the large-scale acquisition of bioactive AMPs, enhancing clinical and research applications (Akhtar *et al*., 2012; Dar *et al*., 2017). In addition to the successful application of rDNA, the efficient, fast, and easy growth of microbial expression hosts like *E. coli* BL21(DE3) and *E. coli* SHuffle T7(DE3) has allowed for commercial production of bioactive cationic AMPs independent of posttranslational modifications (Aleinein *et al*., 2013; Klubthawee *et al*., 2020; Montfort-Gardeazabal *et al*., 2021). Novel AMPs like Brevinin-2R, Renalexin, Cecropin A, and LL-37 as single peptides have been produced as recombinant protein-based drug candidates in microbial systems and have shown a promising antimicrobial effect (Aleinein *et al*., 2013; Chhetri *et al*., 2015; Zhang *et al*., 2018). The thriving commercial production of AMPs in *E. coli* largely depends on the design and use of protein tags, including but not limited to poly-Histidine, maltose binding protein (MBP), thioredoxin protein (THX), and Glutathione S-transferase (GST) that allows for the expression of recombinant proteins as fusion proteins in benign forms (Afzal *et al*., 2021; El-Gayar, 2015;Gddoa Al-sahlany *et al*., 2020; Mo *et al*., 2018; Riguero *et al*., 2020). Recently, our newly designed small metal-binding proteins SmbP and CusF3H+ have been extensively exploited as protein tags which aided in the production and purification of AMPs like LL-37 and Bin1b, and

green fluorescence protein (GFP) in different *E. coli* strains (Montfort-Gardeazabal et al., 2021; Perez-Perez et al., 2021; Vargas-Cortez et al., 2016, 2017). Our previous study has unraveled the capabilities of these protein tags that facilitate the secretion, folding, and purification of expressed recombinant LL-33 and Bin1b as single peptides with intact bioactivity at purity above 80% (Montfort-Gardeazabal *et al*., 2021; Perez-Perez *et al*., 2021; Santos *et al*., 2019). Peptide hybridization has been considered an advanced technique for the design of novel AMPs having reliable peptide stability, long half-life with intact therapeutic activity with hybrid peptides like Cecropin A_Thanatin, and Indolicidin_Renalexin showing broad-spectrum antimicrobial activity against multi-drug resistant bacterial pathogens (Seyedjavadi *et al*., 2021b; Wade *et al*., 2019).

The broad-spectrum antibacterial activity of LL-37 as a single peptide although at a higher peptide concentration has led us to design a recombinant hybrid peptide production strategy via the application of GS flexible peptide linker and a carrier proteins CusF3H+ and SmbP. The simple GS peptide linker enhances the expression of the hybrid peptide LL-37_Renalexin and maintains the spatial configuration within the hybrid peptide with intact and advanced bioactivity. This data strongly suggests that the GS peptide linker can be employed as a reliable simple flexible linker for the design and expression of recombinant therapeutic peptides as compared to the RGGPDGSGPDESGPDE flexible linker employed in the design of hybrid and dimeric peptide with primary structural modifications (Klubthawee *et al*., 2020; Seyedjavadi *et al*., 2021b).

In this study, we have efficiently employed the mature amino acids of LL-37 and Renalexin for the design of a novel hybrid peptide LL-37_Renalexin. We reliably cloned synthetic DNA that encodes for the target peptide into pET30α+ under the T7 promoter

and terminator regions and obtained a successful expression in *E. coli* BL21(DE3) and *E. coli* SHuffle T7(DE3) under the condition of 25°C, for 16 h with 1 mM IPTG. In other studies, the microbial strains, induction and temperature conditions demonstrated profound effect on the expression of both single, hybrid and dimeric peptides with inclusion bodies indications (Chhetri *et al*., 2015; Montfort-Gardeazabal *et al*., 2021; Shang *et al*., 2020; Seyedjavadi *et al*., 2021b; Wade *et al*., 2019; Xu *et al*., 2014). The expression condition and peptide isolation protocols observed in this study, made it possible for efficient production coupled with a 4-fold higher cytoplasmic yield.

Recombinant fusion peptides CusF3H+_LL-37_Renalexin and SmbP_LL-37_Renalexin expression level and its presence in soluble cell lysate provides an evidential advantage of protein tag CusF3H+ and SmbP over others like glutathione S-transferase, maltose binding protein, amyloid-β peptide, and thioredoxin tag (Aleinein *et al*., 2013; Chhetri *et al*., 2015; Zhang *et al*., 2018) yielding up to 95% peptide purity which matched the purity standard of commercially available synthetic therapeutic peptides. In this present study, Bradford quantification of purified and PBS-dialyzed elution fractions revealed a total recombinant peptide yield of 1.5 – 3.1 mg/L fusion proteins SmbP_LL-37_Renalexin and CusF3H+_LL-37_Renalexin expressed in BL21(DE3) and SHuffle T7(DE3), respectively. We observed a 2-fold higher peptide yield in *E. coli* SHuffle T7(DE3) for both SmbP and CusF3H+ tagged fusion proteins than in *E. coli* BL21(DE3), providing relevant supportive data on the usage of *E. coli* SHuffle T7(DE3) as microbial host for the production of either single or hybrid recombinant hybrid peptides with or without disulfide bonds (Montfort-Gardeazabal *et al*., 2021). Our result showed a higher cytoplasmic expression level of the recombinant hybrid peptide as soluble protein than reported from

other studies, 0.9 mg/L by (Seyedjavadi *et al*., 2021), 0.9 mg/L by (Clement *et al*., 2015), and 0.3 mg/L by (Cheng *et al*., 2021).

We employed the restriction enzyme enterokinase for selective cleavage of protein tags CusF3H+ and SmbP from the purified fusion peptides due to the presence of enterokinase site between the hybrid peptide and the protein tag. Analysis of inactivated enterokinase cleavage mixture revealed three protein bands of approximate molecular size of 18 kDa (uncleaved fusion peptide), 13 kDa (CusF3H+ or SmbP), and 10 kDa (LL-37_Renalexin, tag-free) on Tricine SDS-PAGE with tag-free recombinant hybrid peptide showing slightly higher band size than the theoretically expected size (6.740 kDa). This result can be attributed to inefficient enterokinase cleavage observed, associated with the presence of phenylalanine, leucine, and isoleucine residues and heptapeptide motif (Rana box) in Renalexin that forms a cyclic disulfide bond aiding a molecular structural loop formation folded unto the N-terminal that is known to influence enzymatic cleavage and peptide reduction. Also, the high hydrophobicity of the peptide which prevents complete reduction with SDS and mercaptoethanol reagents, and the peptide molecular folding in aqueous systems all of which influence poor peptide mobility. These findings agrees with previous studies reported where the single peptides LL-37 and Renalexin show higher protein band sizes than the theoretically determined sizes (Aleinein *et al*., 2013; Perez-Perez *et al*., 2021; Ishvaanjil *et al*., 2016). A 0.7 – 2.1 mg/L LL-37_Renalexin (tag-free) peptide was obtained upon spectroscopic and Bradford quantification of the second IMAC purification elution fractions (Montfort-Gardeazabal *et al*., 2021; Perez-Perez *et al*., 2021; Vargas-Cortez *et al*., 2017).

The relatively slow induction of antibacterial activity of LL-37_Renalexin compared to the well-known antibiotic kanamycin we observed in the time-killing kinetic assay results can be related to the high hydrophobicity of the hybrid peptide which may cause partial exposure of hydrophilic regions to bacterial membrane (Wei and Zhang, 2022) coupled with the presence of monovalent Na(I) and K(I) cations in the assay medium that is known to cause shielding effects between the cationic peptides and anionic bacterial membrane surface hence, the delay in eliciting antibacterial activity in the case of the hybrid peptide as compared to kanamycin (Huan *et al*., 2020; Nuti *et al*., 2017). Our findings show that the hybrid peptide LL-37_Renalexin with 44% hydrophobicity and 56% hydrophilicity elicited near microbicidal activity against all tested pathogens with above 85% reduction in bacteria colony-forming units at 33 μM peptide concentration. The decrease in CFU/ml observed suggests a bactericidal activity since the level of reduction (R_L) in CFU/ml is more significant than 3 times the logarithm CFU/ml of bacteria (Klubthawee *et al*., 2020; Zhang *et al*., 2018). All *S. aureus*, *E. coli*, MRSA, and *K. pneumoniae* clinical isolates showed 85% sensitivity at 33 μM as minimum peptide bactericidal concentration with about 25% increment in sensitivity indicative of higher antibacterial potency of this novel hybrid peptide compared to its counterpart single peptide LL-37 as reported from our previous study with 64% sensitivity against *E. coli* and 69% against *S. aureus* (Perez-Perez *et al*., 2021). We envisioned that the hybrid peptide's antimicrobial effects are brought about through its ability to disrupt cell membranes, thanks to its pronounced cationic polarity which enables it to create a strong electrostatic bond with the negatively charged bacteria membrane. Additionally, it is thought that the hybrid peptide's V-shaped structure, made possible by the presence of the GS flexible linker, allows it to effectively

engage with bacterial chromosomal DNA. This interaction can lead to the formation of DNA supercoils, ultimately hindering DNA replication and transcription (Q. Y. Zhang et al., 2021).

CHAPTER SIX

6.0 CONCLUSION AND RECOMMENDATIONS

6.1 Conclusion

- Recently, antimicrobial peptides represented one of the most reliable and promising future peptide-based antimicrobial therapeutic agents for combating clinical infection and multi-drug resistant bacterial pathogens that serve global public health peril.
- In this study, we have designed, produced, and purified a novel multifunctional recombinant hybrid peptide LL-37_Renalexin for the first time via the application of newly designed flexible GS peptide linker and a characterized carrier proteins SmbP and CusF3H+.
- The small metal binding protein tags SmbP and CusF3H+ provide an evidential advantage in cytoplasmic secretion, production, and purification of the novel hybrid AMP LL-37_Renalexin with intact biochemical properties and can be applied as a new avenue to produce recombinant peptides and proteins.
- The purified tag-free hybrid peptide LL-37_Renalexin exhibited above 85% reduction in bacteria CFU/ml against both *S. aureus*, *E. coli*, MRSA, and *K. pneumoniae* clinical isolates at lower minimum inhibitory concentration levels of 10 – 33 µM as compared to its counterpart single AMPs LL-37 and Renalexin of 50 – 100 µM reported (Aleinein *et al*., 2013; Kang *et al*., 2019; Perez-Perez *et al*., 2021), making it a competitive antimicrobial agent.
- The recombinant DNA strategies used in the design, production, and purification of recombinant fusion proteins provide a reliable platform and protocol for

expression and purification of therapeutic recombinant proteins in *E. coli* BL21(DE3) and *E. coli* SHuffle T7(DE3) as microbial expression hosts.

6.2 Recommendations

- Evaluate the antimicrobial potency of the hybrid peptide against bacterial pathogens at varying salt concentrations (salt stability of the peptide).
- Evaluate the antimicrobial potency of the hybrid peptide against bacterial pathogens after exposure to varying heat levels (thermal stability of the peptide).
- Evaluate the mechanisms of bacterial membrane disruption upon treatment with the hybrid peptide via advanced microscopy.

  Evaluate the antimicrobial efficacy of the hybrid peptide in combination therapy with known clinically prescribed antibiotics.

CHAPTER SEVEN

LABORATORY SAFETY AND WASTE MANAGEMENT

Standard laboratory safety measures including but not limited to the handling of both pathogenic and non-pathogenic bacterial isolates, recombinant plasmid, carcinogenic reagents like Ethidium bromide, acrylamide and corrosive chemicals like Hydrochloric acid were strictly observed. The disposal of chemicals, media, cultures, and buffers used in this project were managed in accordance with the guidelines rules described by the department of environmental safety of the Faculty of Chemical Sciences (FCQ) of the Autonomous University of Nuevo Leon (UANL). The waste generated and their respective waste collectors is tabulated below.

Table 7. 1: Laboratory waste generated and their respective waste collectors.

Collector	**Waste generated**
Collector A (Buffer and saline solutions, acids and organic bases, pH 6-8)	Tris-acetate-EDTA, Tris-Hydrochloric acid, Acetic acid, Methanol, Iso-butanol, Tris-Glycine Sodium Dodecyl Sulfate (Tris-SDS), tricine buffer (Tricine, Tris-HCl, SDS), Equilibrating buffer (Tris-HCl, NaCl), Elution buffer (Tris-HCl, NaCl, Imidazole), Phosphate Buffered Saline (PBS solution) and Fast protein liquid chromatography (FPLC) waste solutions.

Collector G (Solid organic blends)	Agarose (molecular biology and bacteriology grade), polyacrylamide/Bisacrylamide
Colorants and dyes	Coomassie brilliant blue G250/R250, Bromophenol blue.
Collector I	Hand gloves (Nitril and non-nitril)
Biohazard rubber bag	Inoculated cultured plates, plastic inoculation loops, cotton swabs, tissue paper, microplates.

REFERENCES

1. Adamíková, J., Antošová, M., & Polakovič, M. (2019). Chromatographic purification of recombinant human erythropoietin. *Biotechnology Letters, 41*(4–5), 483–493. https://doi.org/10.1007/s10529-019-02656-8
2. Akhtar, M. S., Imran, M. B., Nadeem, M. A., & Shahid, A. (2012). Antimicrobial peptides as infection imaging agents: Better than radiolabeled antibiotics. *International Journal of Peptides, 2012*. https://doi.org/10.1155/2012/965238
3. Aleinein, R. A., Hamoud, R., Schäfer, H., & Wink, M. (2013). Molecular cloning and expression of ranalexin, a bioactive antimicrobial peptide from *Rana catesbeiana* in *Escherichia coli* and assessments of its biological activities. *Applied Microbiology and Biotechnology*, *97*(8), 3535–3543. https://doi.org/10.1007/s00253-012-4441-1
4. Amábile-cuevas, C. F. (2020). Antibiotic usage and resistance in Mexico : an update after a decade of change. https://doi.org/10.3855/jidc.13467
5. Bolívar Parra, L., Giraldo Hincapié, P. A., & Montoya Campuzano, O. I. (2020). Antimicrobial activity of a synthetic bacteriocin found in the genome of *lactobacillus* casei on the microbiota of antioquian soft cheese (Quesito antioqueÑo). *Vitae*, *27*(1), 1–9. https://doi.org/10.17533/udea.vitae.v27n1a02
6. Cheng, J., Ahmat, M., Guo, H., Wei, X., Zhang, L., Cheng, Q., & Zhang, J. (2021). Expression , Purification and Characterization of a Novel Hybrid. *Molecules*, *26*, 7142.
7. Chhetri, G., Kalita, P., & Tripathi, T. (2015). An efficient protocol to enhance

recombinant protein expression using ethanol in *Escherichia coli*. *MethodsX*, *2*, 385–391. https://doi.org/10.1016/j.mex.2015.09.005

8. Collins, T., Azevedo-Silva, J., da Costa, A., Branca, F., Machado, R., & Casal, M. (2013). Batch production of a silk-elastin-like protein in *E. coli* BL21(DE3): Key parameters for optimisation. *Microbial Cell Factories*, *12*(1), 1–16. https://doi.org/10.1186/1475-2859-12-21
9. Colyer, J., & Walker, J. M. (1996). Protein Handbook *Edited by* (Issue January).
10. Dar, M. A., Ali, A., Dar, P. A., Dar, T. A., Ayaz, A., & Tajamul Mumtaz, P. (2017). Antimicrobial Peptides: Classification, action and therapeutic potential. *International Journal of Research Available*, *04*(17), 2437–2442. https://edupediapublications.org/journals
11. David, I. W. F., & Karl, S. (n.d.). Antimicrobial Resistance in the 21st Century.
12. De J. Sosa, A., Byarugaba, D. K., Amabile-Cuevas, C. F., Hsueh, P. R., Kariuki, S., & Okeke, I. N. (2010). Antimicrobial resistance in developing countries. In Antimicrobial Resistance in Developing Countries (Issue August). https://doi.org/10.1007/978-0-387-89370-9
13. Deng, T., Ge, H., He, H., Liu, Y., Zhai, C., Feng, L., & Yi, L. (2017). The heterologous expression strategies of antimicrobial peptides in microbial systems. *Protein Expression and Purification*, *140*, 52–59. https://doi.org/10.1016/j.pep.2017.08.003
14. Dürr, U. H. N., Sudheendra, U. S., & Ramamoorthy, A. (2006). LL-37 , the only human member of the cathelicidin family of antimicrobial peptides. *1758*, 1408–1425. https://doi.org/10.1016/j.bbamem.2006.03.030
15. El-Gayar, K. E. (2015). Principles of recombinant protein production, extraction

and purification from bacterial strains. *International Journal of Microbiology and Allied Sciences*, *2*(2), 18–33.

16. Erdem Büyükkiraz, M., & Kesmen, Z. (2022). Antimicrobial peptides (AMPs): A promising class of antimicrobial compounds. *Journal of Applied Microbiology*, *132*(3), 1573–1596. https://doi.org/10.1111/jam.15314
17. Fazaeli, A., Golestani, A., Lakzaei, M., Rasi Varaei, S. S., & Aminian, M. (2018). Expression optimization of recombinant cholesterol oxidase in *Escherichia coli* and its purification and characterization. *AMB Express*, *8*(1). https://doi.org/10.1186/s13568-018-0711-3
18. Gan, B. H., Gaynord, J., Rowe, S. M., Deingruber, T., & Spring, D. R. (2021). The multifaceted nature of antimicrobial peptides: Current synthetic chemistry approaches and future directions. *Chemical Society Reviews*, *50*(13), 7820–7880. https://doi.org/10.1039/d0cs00729c
19. Garza-González, E., Morfín-Otero, R., Mendoza-Olazarán, S., Bocanegra-Ibarias, P., Flores-Treviño, S., Rodríguez-Noriega, E., Ponce-de-León, A., Sanchez-Francia, D., Franco-Cendejas, R., Arroyo-Escalante, S., Velázquez-Acosta, C., Rojas-Larios, F., Quintanilla, L. J., Maldonado-Anicacio, J. Y., Martínez-Miranda, R., Ostos-Cantú, H. L., Gomez-Choel, A., Jaime-Sanchez, J. L., Avilés-Benítez, L. K., … Camacho-Ortiz, A. (2019). A snapshot of antimicrobial resistance in Mexico. Results from 47 centers from 20 states during a six-month period. *PLoS ONE*, *14*(3), 1–13. https://doi.org/10.1371/journal.pone.0209865
20. Gddoa Al-sahlany, S. T., Altemimi, A. B., Abd Al-Manhel, A. J., Niamah, A. K., Lakhssassi, N., & Ibrahim, S. A. (2020). Purification of Bioactive Peptide with

Antimicrobial Properties Produced by *Saccharomyces cerevisiae*. *Foods*, *9*(3), 1–11. https://doi.org/10.3390/foods9030324

21. Gomez-Lugo, J. J., Santos, B. D., Perez-Perez, D. A., Montfort-Gardeazabal, J. M., McEvoy, M. M., and X. Z. (2014). Protein Downstream Processing. *Molecular Biotechnology*, *1129*, 435–441.
22. Hanafiah, M., Helmi, T. Z., Sutriana, A., Priyowidodo, D., & Fihiruddin, F. (2020). Cloning and expression of *Toxoplasma gondii* GRA-4 recombinant protein as a toxoplasmosis diagnostic kit candidate. *Veterinary World*, *13*(10), 2085–2091. https://doi.org/10.14202/vetworld.2020.2085-2091
23. Huan, Y., Kong, Q., Mou, H., & Yi, H. (2020). Antimicrobial Peptides: Classification, Design, Application and Research Progress in Multiple Fields. *Frontiers in Microbiology*, *11*(October), 1–21. https://doi.org/10.3389/fmicb.2020.582779
24. Jindal, H. M., Le, C. F., Yusof, M. Y. M., Velayuthan, R. D., Lee, V. S., Zain, S. M., Isa, D. M., & Sekaran, S. D. (2015). Antimicrobial activity of novel synthetic peptides derived from indolicidin and ranalexin against *Streptococcus pneumoniae*. *PLoS ONE*, *10*(6), 1–23. https://doi.org/10.1371/journal.pone.0128532
25. Jit, M., Hui, D., Ng, L., Luangasanatip, N., Sandmann, F., Atkins, K. E., Robotham, J. V, & Pouwels, K. B. (2020). Quantifying the economic cost of antibiotic resistance and the impact of related interventions : rapid methodological review , conceptual framework and recommendations for future studies. 1–14.
26. Kang, J., Dietz, M. J., & Li, B. (2019). Antimicrobial peptide LL-37 is

bactericidal against *Staphylococcus aureus* biofilms. *PLoS ONE*, *14*(6), 1–13. https://doi.org/10.1371/journal.pone.0216676

27. Kaprou, G. D., Bergšpica, I., Alexa, E. A., Alvarez-Ordóñez, A., & Prieto, M. (2021). Rapid methods for antimicrobial resistance diagnostics. *Antibiotics*, *10*(2), 1–30. https://doi.org/10.3390/antibiotics10020209
28. Kelley, L. A., Mezulis, S., Yates, C. M., Wass, M. N., & Sternberg, M. J. (2016). Trabajo práctico N^{o} 13 . Varianzas en función de variable independiente categórica. *Nature Protocols*, *10*(6), 845–858. https://doi.org/10.1038/nprot.2015-053
29. Kesidis, A., Depping, P., Lodé, A., Vaitsopoulou, A., Bill, R. M., Goddard, A. D., & Rothnie, A. J. (2020). Expression of eukaryotic membrane proteins in eukaryotic and prokaryotic hosts. *Methods*, *180*, 3–18. https://doi.org/10.1016/j.ymeth.2020.06.006
30. Klubthawee, N., Adisakwattana, P., Hanpithakpong, W., Somsri, S., & Aunpad, R. (2020). A novel, rationally designed, hybrid antimicrobial peptide, inspired by cathelicidin and aurein, exhibits membrane-active mechanisms against *Pseudomonas aeruginosa*. *Scientific Reports*, *10*(1), 1–17. https://doi.org/10.1038/s41598-020-65688-5
31. Kravchenko, S. V., Domnin, P. A., Grishin, S. Y., Panfilov, A. V., Azev, V. N., Mustaeva, L. G., Gorbunova, E. Y., Kobyakova, M. I., Surin, A. K., Glyakina, A. V., Fadeev, R. S., Ermolaeva, S. A., & Galzitskaya, O. V. (2022). Multiple Antimicrobial Effects of Hybrid Peptides Synthesized Based on the Sequence of Ribosomal S1 Protein from *Staphylococcus aureus*. *International Journal of Molecular Sciences*, *23*(1). https://doi.org/10.3390/ijms23010524

32. Kruchinin, A., & Bolshakova, E. (2022). Hybrid Strategy of Bioinformatics Modeling (in silico): Biologically Active Peptides of Milk Protein. *Food Processing: Techniques and Technology*, *April*, 46–57. https://doi.org/10.21603/2074-9414-2022-1-46-57

33. Lacy, M. K., Klutman, N. E., Horvat, R. T., & Zapantis, A. (2004). Antibiograms: New NCCLS guidelines, development, and clinical application. *Hospital Pharmacy*, *39*(6), 542–553. https://doi.org/10.1177/001857870403900608

34. Lambert, R. J. W., & Pearson, J. (2000). Susceptibility testing : accurate and reproducible minimum inhibitory concentration (MIC) and non-inhibitory concentration (NIC) values. *Mic*, 784–790.

35. Lee, S. B., Li, B., Jin, S., & Daniell, H. (2011). Expression and characterization of antimicrobial peptides Retrocyclin-101 and Protegrin-1 in chloroplasts to control viral and bacterial infections. *Plant Biotechnology Journal*, *9*(1), 100–115. https://doi.org/10.1111/j.1467-7652.2010.00538.x

36. Leite, M. L., Sampaio, K. B., & Costa, F. F. (2019). Molecular farming of antimicrobial peptides : available platforms and strategies for improving protein biosynthesis using modified virus vectors. *91*, 1–23. https://doi.org/10.1590/0001-3765201820180124.Abstract

37. Li, R. F., Lu, Y. L., Lu, Y. B., Zhang, H. R., Huang, L., Yin, Y., Zhang, L., Liu, S., Lu, Z., & Sun, Y. (2015). Antiproliferative effect and characterization of a novel antifungal peptide derived from human chromogranin a. *Experimental and Therapeutic Medicine*, *10*(6), 2289–2294. https://doi.org/10.3892/etm.2015.2838

38. Liscano, Y., Oñate-Garzón, J., & Ocampo-Ibáñez, I. D. (2020). In silico

discovery of antimicrobial peptides as an alternative to control Sars-cov-2. *Molecules*, *25*(23). https://doi.org/10.3390/molecules25235535

39. *Literature MsR*. (n.d.).
40. Llanes, J. M., Varon, J., Félix, J. S. V., & González-Ibarra, F. P. (2012). Antimicrobial resistance of *Escherichia coli* in Mexico: How serious is the problem? *Journal of Infection in Developing Countries*, *6*(2), 126–131. https://doi.org/10.3855/jidc.1525
41. Madom, T., Amritha, S., Mahajan, S., Subramaniam, K., Chandramohan, Y., & Id, A. D. (2020). Cloning , expression and purification of recombinant dermatopontin in *Escherichia coli*. 1–14. https://doi.org/10.1371/journal.pone.0242798
42. Malmsten, M. (2014). Antimicrobial peptides. *Upsala Journal of Medical Sciences*, *119*(2), 199–204. https://doi.org/10.3109/03009734.2014.899278
43. Mesa-Pereira, B., Rea, M. C., Cotter, P. D., Hill, C., & Ross, R. P. (2018). Heterologous expression of biopreservative bacteriocins with a view to low cost production. *Frontiers in Microbiology*, *9*, 1–15. https://doi.org/10.3389/fmicb.2018.01654
44. Mo, Q., Fu, A., Lin, Z., Wang, W., Gong, L., & Li, W. (2018). Expression and purification of antimicrobial peptide AP2 using SUMO fusion partner technology in *Escherichia coli*. *Letters in Applied Microbiology*, *67*(6), 606–613. https://doi.org/10.1111/lam.13079
45. Mohammed, A., & Yousuf, F. (2018). Expression of Recombinant Protein in *Escherichia coli*. *January*. https://doi.org/10.13140/RG.2.2.15148.16000
46. Mohan, R. (2016). in Silico Docking Studies of Staphylococcus Aureus Virulent

Proteins With Antimicrobial Peptides. *February 2012*.

47. Montfort-Gardeazabal, J. M., Balderas-Renteria, I., Casillas-Vega, N. G., & Zarate, X. (2021). Expression and purification of the antimicrobial peptide Bin1b in *Escherichia coli* tagged with the fusion proteins CusF3H+ and SmbP. *Protein Expression and Purification*, *178*(October 2020), 105784. https://doi.org/10.1016/j.pep.2020.105784
48. Moretta, A., Scieuzo, C., Petrone, A. M., Salvia, R., Manniello, M. D., Franco, A., Lucchetti, D., Vassallo, A., Vogel, H., Sgambato, A., & Falabella, P. (2021). Antimicrobial Peptides: A New Hope in Biomedical and Pharmaceutical Fields. *Frontiers in Cellular and Infection Microbiology*, *11*(June), 1–26. https://doi.org/10.3389/fcimb.2021.668632
49. Moulahoum, H., Ghorbani Zamani, F., Timur, S., & Zihnioglu, F. (2020). Metal Binding Antimicrobial Peptides in Nanoparticle Bio-functionalization: New Heights in Drug Delivery and Therapy. *Probiotics and Antimicrobial Proteins*, *12*(1), 48–63. https://doi.org/10.1007/s12602-019-09546-5
50. Mukherjee, R., Priyadarshini, A., Pati Pandey, R., & Samuel Raj, V. (2021). Antimicrobial Resistance in *Staphylococcus aureus* . *March*. https://doi.org/10.5772/intechopen.96888
51. Nooranian, S., Oskuee, R. K., & Jalili, A. (2021). Antimicrobial Peptides, a Pool for Novel Cell Penetrating Peptides Development and Vice Versa. *International Journal of Peptide Research and Therapeutics*, *27*(2), 1205–1220. https://doi.org/10.1007/s10989-021-10161-8
52. Nuti, R., Goud, N. S., Saraswati, A. P., Alvala, R., & Alvala, M. (2017). Antimicrobial Peptides: A Promising Therapeutic Strategy in Tackling

Antimicrobial Resistance. *Current Medicinal Chemistry*, *24*(38), 4303–4314. https://doi.org/10.2174/0929867324666170815102441

53. Oladipo, E. K., Oluwasegun, J. A., Owoeye, V. O., Oladunni, T. D., Olasinde, O. T., & Onyeaka, H. (2023). Immunoinformatics aided design of a peptide-based kit for detecting *Escherichia coli* O157 : H7 from food sources. *May*, 1–12. https://doi.org/10.1111/jfs.13073
54. Ołdak, A., & Zielińska, D. (2017). Bakteriocyny bakterii fermentacji mlekowej jako alternatywa antybiotyków Bacteriocins from lactic acid bacteria as an alternative to antibiotics. 328–338.
55. Pasupuleti, M., Schmidtchen, A., & Malmsten, M. (2011). Antimicrobial peptides : key components of the innate immune system. January, 1–29. https://doi.org/10.3109/07388551.2011.594423
56. Perez-Perez, D. A., Villanueva-Ramirez, T. de J., Hernandez-Pedraza, A. E., Casillas-Vega, N. G., Gonzalez-Barranco, P., & Zarate, X. (2021). The small metal-binding protein smbp simplifies the recombinant expression and purification of the antimicrobial peptide LL-37. *Antibiotics*, *10*(10). https://doi.org/10.3390/antibiotics10101271
57. Peters, B. M., Shirtliff, M. E., & Jabra-Rizk, M. A. (2010). Antimicrobial peptides: Primeval molecules or future drugs? *PLoS Pathogens*, *6*(10), 4–7. https://doi.org/10.1371/journal.ppat.1001067
58. Protein, E. (2016). Expression of Recombinant Hybrid Peptide Gaegurin4 and LL37 using Fusion Expression of Recombinant Hybrid Peptide Gaegurin4 and LL37 using Fusion Protein in *E . coli*. *February*, 4–6. https://doi.org/10.4014/kjmb.1203.03004

59. Purification, I., & Characterization, A. (2020). Expression of Hybrid Peptide EF-1 in *Pichia pastoris* , Its Purification, and Antimicrobial Characterization. 1–11.

60. Reinhardt, A., & Neundorf, I. (2016). Design and Application of Antimicrobial Peptide Conjugates. https://doi.org/10.3390/ijms17050701.

61. Riguero, V., Clifford, R., Dawley, M., Dickson, M., Gastfriend, B., Thompson, C., Wang, S. C., & O'Connor, E. (2020). Immobilized metal affinity chromatography optimization for poly-histidine tagged proteins. *Journal of Chromatography A*, *1629*, 461505. https://doi.org/10.1016/j.chroma.2020.461505

62. Rodríguez-Rojas, A., Baeder, D. Y., Johnston, P., Regoes, R. R., & Rolff, J. (2021). Bacteria primed by antimicrobial peptides develop tolerance and persist. *PLoS Pathogens*, *17*(3), 1–30. https://doi.org/10.1371/JOURNAL.PPAT.1009443

63. Rosano, G. L., & Ceccarelli, E. A. (2014). Recombinant protein expression in microbial systems. *Frontiers in Microbiology*, *5*(JULY), 2013–2015. https://doi.org/10.3389/fmicb.2014.00341

64. Santos, B. D., Morones-Ramirez, J. R., Balderas-Renteria, I., Casillas-Vega, N. G., Galbraith, D. W., & Zarate, X. (2019). Optimizing Periplasmic Expression in Escherichia coli for the Production of Recombinant Proteins Tagged with the Small Metal-Binding Protein SmbP. *Molecular Biotechnology*, *61*(6), 451–460. https://doi.org/10.1007/s12033-019-00176-4

65. Scott, M. G., Davidson, D. J., Gold, M. R., Bowdish, D., & Hancock, R. E. W. (2002). The Human Antimicrobial Peptide LL-37 Is a Multifunctional Modulator of Innate Immune Responses. *The Journal of Immunology*, *169*(7), 3883–3891.

https://doi.org/10.4049/jimmunol.169.7.3883

66. Seyedjavadi, S. S., Khani, S., Amani, J., Halabian, R., Goudarzi, M., Hosseini, H. M., Eslamifar, A., Shams-Ghahfarokhi, M., Imani Fooladi, A. A., & Razzaghi-Abyaneh, M. (2021a). Design, Dimerization, and Recombinant Production of MCh-AMP1–Derived Peptide in *Escherichia coli* and Evaluation of Its Antifungal Activity and Cytotoxicity. *Frontiers in Fungal Biology*, *2*(April), 1–11. https://doi.org/10.3389/ffunb.2021.638595
67. Seyedjavadi, S. S., Khani, S., Amani, J., Halabian, R., Goudarzi, M., Hosseini, H. M., Eslamifar, A., Shams-Ghahfarokhi, M., Imani Fooladi, A. A., & Razzaghi-Abyaneh, M. (2021b). Design, Dimerization, and Recombinant Production of MCh-AMP1–Derived Peptide in *Escherichia coli* and Evaluation of Its Antifungal Activity and Cytotoxicity. *Frontiers in Fungal Biology*, *2*(April). https://doi.org/10.3389/ffunb.2021.638595
68. Shang, L., Li, J., Song, C., Nina, Z., Li, Q., Chou, S., Wang, Z., & Shan, A. (2020). Hybrid Antimicrobial Peptide Targeting *Staphylococcus aureus* and Displaying Anti-infective Activity in a Murine Model. *Frontiers in Microbiology*, *11*(September), 1–13. https://doi.org/10.3389/fmicb.2020.01767
69. Soares, A., Gomes, L. C., Monteiro, G. A., & Mergulhão, F. J. (2021). The influence of nutrient medium composition on *Escherichia coli* biofilm development and heterologous protein expression. *Applied Sciences (Switzerland)*, *11*(18). https://doi.org/10.3390/app11188667
70. Soltani, S., Hammami, R., Cotter, P. D., Rebuffat, S., Biron, E., Drider, D., Said, B., & Fliss, I. (2021). Bacteriocins as a new generation of antimicrobials : toxicity aspects and regulations. *March 2020*, 1–24.

https://doi.org/10.1093/femsre/fuaa039

71. Sriram, A., Kalanxhi, E., Kapoor, G., Craig, J., Ruchita Balasubramanian, S. B., Criscuolo, N., Hamilton, A., Klein, E., Tseng, K., Boeckel, T. Van, & Laxminarayan, R. (2021). The State of the World's Antibiotics in 2021: A Global Analysis of Antimicrobial Resistance and Its Drivers. *The Center for Disease Dynamics, Economics & Policy*, 1–115. https://cddep.org/blog/posts/the-state-of-the-worlds-antibiotics-report-in-2021/
72. Vargas-Cortez, T., Morones-Ramirez, J. R., Balderas-Renteria, I., & Zarate, X. (2016). Expression and purification of recombinant proteins in *Escherichia coli* tagged with a small metal-binding protein from Nitrosomonas europaea. *Protein Expression and Purification*, *118*, 49–54. https://doi.org/10.1016/j.pep.2015.10.009
73. Vargas-Cortez, T., Morones-Ramirez, J. R., Balderas-Renteria, I., & Zarate, X. (2017). Production of recombinant proteins in *Escherichia coli* tagged with the fusion protein CusF3H+. *Protein Expression and Purification*, *132*, 44–49. https://doi.org/10.1016/j.pep.2017.01.006
74. Wade, H. M., Darling, L. E. O., & Elmore, D. E. (2019). Hybrids made from antimicrobial peptides with different mechanisms of action show enhanced membrane permeabilization. *Biochimica et Biophysica Acta - Biomembranes*, *1861*(10), 182980. https://doi.org/10.1016/j.bbamem.2019.05.002
75. Wang, G., Li, X., & Wang, Z. (2016). APD3: The antimicrobial peptide database as a tool for research and education. *Nucleic Acids Research*, *44*(D1), D1087–D1093. https://doi.org/10.1093/nar/gkv1278
76. Wei, D., & Zhang, X. (2022). Biosafety and Health Biosynthesis , bioactivity ,

biotoxicity and applications of antimicrobial peptides for human health. *Biosafety and Health*, *4*(2), 118–134. https://doi.org/10.1016/j.bsheal.2022.02.003

77. Wingfield, P. T. (2007). Purification of Recombinant Proteins. *Current Protocols in Protein Science*, *47*(1). https://doi.org/10.1002/0471140864.ps0600s47
78. Xu, W., Zhu, X., Tan, T., Li, W., & Shan, A. (2014). Design of embedded-hybrid antimicrobial peptides with enhanced cell selectivity and anti-biofilm activity. *PLoS ONE*, *9*(6). https://doi.org/10.1371/journal.pone.0098935
79. Zhang, C., & Yang, M. (2022). Antimicrobial Peptides: From Design to Clinical Application. *Antibiotics*, *11*(3), 1–19. https://doi.org/10.3390/antibiotics11030349
80. Zhang, M., Shan, Y., Gao, H., Wang, B., Liu, X., Dong, Y., Liu, X., Yao, N., Zhou, Y., Li, X., & Li, H. (2018). Expression of a recombinant hybrid antimicrobial peptide magainin II-cecropin B in the mycelium of the medicinal fungus *Cordyceps militaris* and its validation in mice. *Microbial Cell Factories*, *17*(1), 1–14. https://doi.org/10.1186/s12934-018-0865-3
81. Zhang, Q. Y., Yan, Z. Bin, Meng, Y. M., Hong, X. Y., Shao, G., Ma, J. J., Cheng, X. R., Liu, J., Kang, J., & Fu, C. Y. (2021). Antimicrobial peptides: mechanism of action, activity and clinical potential. In *Military Medical Research* (Vol. 8, Issue 1). https://doi.org/10.1186/s40779-021-00343-2

Appendix

LB broth medium

15.5 g of LB media (0.5g/L NaCl, 10g/L Tryptone, and 5g/L yeast extract) and 9.5g NaCl was weighed and dissolved in 800 ml distilled water. The mixture was mixed by stirring on a heating mantel without heat. Afterward, the volume was adjusted to 1L. Sterilization in autoclave was carried out at 121°C, 15psi, for 15 min. Stored at 4°C to prevent contamination.

LB agar medium

1.5g of LB media (0.5g/L NaCl, 10g/L Tryptone, and 5g/L yeast extract), 2.0 g agar and 0.95g NaCl was weighed and dissolved in 80 ml distilled water. The mixture was mixed by stirring on a heating mantel without heat. Afterward, the volume was adjusted to 100ml. Sterilization in autoclave was carried out at 121°C, 15psi, for 15 min. Stored at 4°C to prevent contamination.

Tryptic soy broth medium

2g of tryptic soy broth (TSB) medium (17g/L casein digest peptone, 3g/L papaic digest of soybean meal, 2.5g/L Disodium Phosphate, 2.5g/L Dextrose, 5.0g/L Sodium Chloride) was dissolved in 80 ml distilled water and mixed thoroughly by stirring on heating mantel without heat, the mixture volume adjusted to 100ml. Sterilization in autoclave was carried out at 121°C, 15psi, for 15 min. Stored at 4°C to prevent contamination.

Tryptic soy broth medium

2g of tryptic soy broth (TSB) medium (17g/L casein digest peptone, 3g/L papaic digest of soybean meal, 2.5g/L Disodium Phosphate, 2.5g/L Dextrose, 5.0g/L Sodium Chloride), and 2.0g agar was dissolved in 80 ml distilled water and mixed thoroughly by stirring on

heating mantel without heat, the mixture volume adjusted to 100ml. Sterilization in autoclave was carried out at 121°C, 15psi, for 15 min. Stored at 4°C to prevent contamination.

Mueller Hinton agar

2.1g of Mueller Hinton medium (2.0g/L Beef extract, 17.5g/L Acid Hydrolysate of casein, 1.5g/L Starch), and 1.5g agar was dissolved in 80 ml distilled water and mixed thoroughly by stirring on heating mantel without heat, the mixture volume adjusted to 100ml. Sterilization in autoclave was carried out at 121°C, 15psi, for 15 min. Stored at 4°C to prevent contamination.

Mueller Hinton broth

2.1g of Mueller Hinton medium (2.0g/L Beef extract, 17.5g/L Acid Hydrolysate of casein, 1.5g/L Starch) was dissolved in 80 ml distilled water and mixed thoroughly by stirring on heating mantel without heat, the mixture volume adjusted to 100ml. Sterilization in autoclave was carried out at 121°C, 15psi, for 15 min. Stored at 4°C to prevent contamination.

Equilibration buffer (50 mM Tris–HCl, 500 mM NaCl)

Weigh 6.06 g Tris-HCl, 29.22 g NaCl, and dissolve in 900ml sterilized distilled water, adjust pH with 12N HCl until pH of 8.0 is obtained, make up volume to 1 L with distilled water. Store at 4°C.

Elution buffer (50 mM Tris–HCl, 500 mM NaCl, 200 mM imidazole)

Weigh 6.06 g Tris base, 29.22 g NaCl, and 13.61 g imidazole, dissolve them in 900ml distilled water, adjust pH with 12N HCl, until pH of 8.0 is obtained. Make up volume to 1 L with distilled water. Store at 4°C.

Kanamycin (1000X) of 30mg/ml

0.3 g of kanamycin sulfate salt weighed and dissolved in 10 mL of sterilized MQ water. The mixture was stirred to completely dissolve the salt. Filter through a 0.22μm membrane pore and distributed into 1.5ml Eppendorf tubes. Store in aliquots at -20°C.

Lysis buffer (50 mM Tris–HCl)

0.61 g of Tris base was weighed and dissolve in 80 ml of distilled water, adjust pH with 12N HCl until pH of 8.0 is obtained, and make up to 100 mL with distilled water.

1M IPTG solution

Dissolve 2.38 g of Isopropyl β-D-1-thiogalactopyranoside in 8 mL of sterilized distilled water and allow to dissolve completely, top up the volume to 10ml. Filter through a 0.22-μm membrane. Store in aliquots at -20°C.

Sample buffer (4X)

Mix 4 mL of 100% glycerol, 2.4 mL of 1 M Tris-HCl buffer pH: 6.8, 0.8 g of SDS, 4 mg of bromophenol blue, 0.5 mL of beta-mercaptoethanol, and 3.1 mL of sterilized distilled water, total volume of 10ml. Store in aliquot at -20°C.

8M urea solution (50 mM Tris–HCl, 8 M urea)

Weigh 96.1 g of urea and 1.21 g Tris base, dissolve in 180 ml water, adjust pH with 12N HCl until pH of 8.0 is obtained and make up to 200 ml with distilled water.

Modified Gompertz function

M=logMIC - 1/Slope

Y= Bottom + Span*exp (-1*exp (Slope*(X-M))

Y= Functional area

X= log concentration of the antimicrobial agent

M= log concentration of the inflexion point